INTEGRATED HYDROLOGICAL MODEL FOR THE ASSESSMENT OF GROUNDWATER RESOURCES IN ŚWIDNICA AREA (POLAND)

HEZRON PHILIPO TIMOTHY

March, 2015

SUPERVISORS:

1st Dr. Maciek Lubczynski
2nd Dr. Zoltán Vekerdy

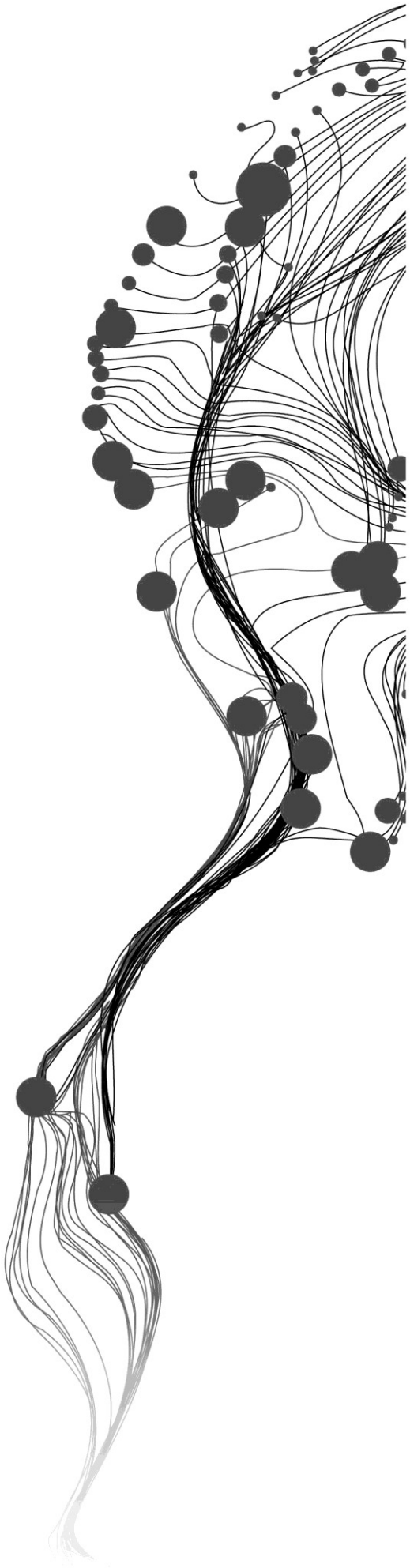

INTEGRATED HYDROLOGICAL MODEL FOR THE ASSESSMENT OF GROUNDWATER RESOURCES IN ŚWIDNICA AREA

HEZRON PHILIPO TIMOTHY
Enschede, The Netherlands, March, 2015

Thesis submitted to the Faculty of Geo-Information Science and Earth Observation of the University of Twente in partial fulfilment of the requirements for the degree of Master of Science in Geo-information Science and Earth Observation.
Specialization: Water Resources and Environmental Management

THESIS ASSESSMENT BOARD:
Dr. Ir. C. van der Tol (Chair)
Dr. P. Gurwin (External Examiner, University of Wroclaw)
Dr. M.W. Lubczynski
Dr. Z. Vekerdy

DISCLAIMER

This document describes work undertaken as part of a programme of study at the Faculty of Geo-Information Science and Earth Observation of the University of Twente. All views and opinions expressed therein remain the sole responsibility of the author, and do not necessarily represent those of the Faculty.

ABSTRACT

In this study, the integrated hydrological model was used to investigate groundwater resources in the Świdnica area (Poland). The previously done, but modified steady-state standalone 3D model from Groundwater Modelling System (GMS) by Gurwin and Lubczynski (2004) was used as starting point for this study. The model was imported into MODFLOW-NWT under ModelMuse environment and run first in steady-state and then in transient states. The simulation period for the model was three hydrological years. The main objective of the study was to evaluate sustainability of groundwater resources in Świdnica area by calibrating transient integrated hydrological model of the study area and analysing its water balance.

The water balance of the steady-state model showed that gross groundwater recharge was 62% of precipitation followed by stream leakage which accounted for about 17.8 %. The lateral inflow and reservoir leakage accounted for about 6 and 1.8 %, respectively. The outflow components were dominated by GW-ET which accounted for 32 % of precipitation followed 19.7 % stream leakage. The surface leakage accounted for about 14.6 % of precipitation. Well abstraction, lateral outflow and reservoir leakage accounted for about 1.3, 2 and 0.1 %, respectively.

The transient model results showed that gross groundwater recharge was 49.9 % of precipitation followed by stream leakage which accounted for about 17.2 %. The lateral inflow and reservoir leakage accounted to about 6 and 3 %, respectively. The outflow components were dominated by surface leakage which accounted to 31 % of precipitation, lateral outflow 21.2 %, followed 20.5 % stream leakage. The GW-ET, well abstraction and reservoir leakage accounted for about 1.3, 1.2 and 0.3 %, respectively. The change in groundwater storage was about 0.8 % of precipitation. It was observed that in the years analysed the net recharge in Świdnica area was largely positive reflecting good groundwater potential of the investigated area.

The spatial variability of ground water fluxes in the study area indicated even distribution. Groundwater recharge was almost uniform over the entire modelled area. The surface leakage was highly concentrated at the middle part of the study area towards the SW boundary with a minimum and maximum of 1.29 and 34 mm d^{-1}, respectively. The temporal variability of fluxes indicated the gross groundwater recharge varied between 0.37 and 8.63 mm d^{-1} and net recharge varied between -0.11 and 6.83 mm d^{-1}. GW-ET had a maximum value of 1.69 mm d^{-1}.

The transient integrated hydrological model led to the better solution of the assessment of groundwater resources in the study area. This model was the appropriate method for analysing water balance of the multi-aquifer systems in Świdnica area.

Key words: Integrated hydrological model; Assessment of groundwater resources.

ACKNOWLEDGEMENTS

I would like to thank the Netherlands Fellowship Programme (NFP) and my employer, the Ministry of Water in the United Republic of Tanzania, for giving me the opportunity to study at the Faculty of Geo-information science and Earth observation (ITC), University of Twente - Netherlands.

I would like to thank the administration from Wroclaw University (Poland) for supporting me toward obtaining the research datasets. In addition, I would like to give a special thanks to Dr. Jacek Gurwin who kindly arranged for field work in Świdnica study area.

I would like to thank Dr. Maciek Lubczynski and Dr. Zoltán Vekerdy for the technical support and guidance towards my research work.

I would like to thank Mr. Amr EL Zehairy for the technical support towards my research work..

I would like to thank Mr. Richard Winston from USGS for the technical support about MODFLOW-NWT under ModelMuse environment.

I would like to thank all staff from WREM at ITC to enable me to achieve my goal.

Finally, special thanks to my parents and my wife for encouraging me throughout my MSc study period.

TABLE OF CONTENTS

1. INTRODUCTION 1
1.1. Introduction 1
1.2. Problem definition 1
1.3. Research objectives and questions 1
1.3.1. Main research objective 1
1.3.2. Specific objectives 1
1.3.3. Main research question 1
1.3.4. Specific questions 2
1.4. Study area 2
1.4.1. Location 2
1.4.2. Climate 3
1.4.3. Topography 4
1.4.4. Land use 4
1.4.5. Hydrology 5
1.4.6. Geology 9
1.4.7. Hydrogeology 9
2. RESEARCH METHOD 12
2.1. Introduction 12
2.2. Reconnaissance survey and data collection 13
2.3. Literature review 13
2.4. Data processing 14
2.4.1. Precipitation and potential evapotranspiration (PET) 14
2.4.2. Water level fluctuations for the two piezometers 15
2.4.3. Fault groundwater inflow at the SW model boundary 15
2.4.4. Lake Mietkowskie water level fluctuations and river gauge discharges 15
2.5. Conceptual model 16
2.5.1. Hydrostratigraphical units 16
2.5.2. Flow pattern, distribution and flow rate 16
2.5.3. Preliminary groundwater balance 16
2.5.4. Model boundaries 16
2.6. Numerical model 17
2.6.1. General concept 17
2.6.2. Software selection 17
2.6.3. Grid design 18
2.6.4. Schematic model setting 18
2.6.5. Driving forces 19
2.6.6. System parameterization 20
2.6.7. Boundary conditions 20
2.6.8. State variables for model calibration 23
2.6.9. Time descretisaton and initial condition 23
2.6.10. Numerical model calibration 23
3. RESULTS AND DISCUSSION 27
3.1. Data processing calculation results 27
3.1.1. Potential evapotranspiration (PET) 27

3.1.2. Precipitation and infiltration rate....28
3.2. Steady state model results....30
3.2.1. Calibrated parameters results....30
3.2.2. Head distributions....31
3.2.3. Calibrated piezometric heads....32
3.2.4. Calibrated Lake Mietkowskie water level fluctuations....32
3.2.5. Calibrated river discharges....32
3.2.6. Water balance for the steady-state model calibration....33
3.2.7. Comparison of this research and the previous study model results....36
3.3. Transient model results....38
3.3.1. Calibrated parameters results....38
3.3.2. Head distributions....39
3.3.3. Calibrated piezometric heads....41
3.3.4. Calibrated lake stages....43
3.3.5. Calibrated river gauge discharges....44
3.3.6. Water balance for the transient model calibration....50
3.3.7. Spatial variability of surface and ground water fluxes....53
3.3.8. Temporal variability of surface and ground water fluxes....54
3.3.9. Quantification of surface and ground water fluxes for the steady-state and the transient model calibration....56
3.3.10. `Comparison of steady-state and transient IHM calibration results....58
3.3.11. Sensitivity analysis for the transient model....58
4. CONCLUSIONS AND RECOMMENDATIONS....63
4.1. Conclusions....63
4.2. Recommendations....64

LIST OF FIGURES

Figure 1-1. Study area adapted from Gurwin and Lubczynski (2004) 2
Figure 1-2. Precipitation from Pszenno station 3
Figure 1-3. PET for the study area 3
Figure 1-4. Topography 4
Figure 1-5. Land use in the study area 5
Figure 1-6. Pelczanica river gauge discharges (Figure 1-1) 6
Figure 1-7. Pilawa river gauge discharges (Figure 1-1 6
Figure 1-8. Bystrzyca L. river gauge discharges (Figure 1-1) 7
Figure 1-9. Bystrzyca K. river gauge discharges (Figure 1-1) 7
Figure 1-10. Strzegomka river gauge discharges (Figure 1-1) 8
Figure 1-11. Water level fluctuation of Lake Mietkowskie (Figure 1-1) 8
Figure 1-12. Hydrogeological cross-section (source: Gurwin and Lubczynski (2004)) 9
Figure 1-13. Measured piezometric heads of Studnia I/710-2 for Quaternary aquifer 10
Figure 1-14. . Measured piezometric heads of Studnia I/710-3 for Tertiary aquifer 10
Figure 1-15. Steady-state head distributions for the Quaternary ((a) and (b)) and Tertiary (c) aquifers (source: (Gurwin and Lubczynski, 2004)) 11
Figure 2-1.Research method 12
Figure 2-2.Summary of all datasets for the research 13
Figure 2-3. Aquifer systems (source: Kovalevsky, Kruseman, and Rushton (2004)) 16
Figure 2-4. MODFLOW-NWT model structure 18
Figure 2-5. Schematic diagram of the model setup in Świdnica study area after Zehairy (2014) 19
Figure 2-6. Boundary conditions unconfined Quaternary aquifer 22
Figure 2-7. Boundary condition for Confined Tertiary aquifer 22
Figure 3-1. Correlation between ADAS and CLIMVIS- Legnica stations (min, max and mean) temps. 27
Figure 3-2. Correlation between reference evapotranspiration (ET_o) from FAO and Hargreaves equations 28
Figure 3-3. Final PET calculated after ET_o gaps filled 28
Figure 3-4. Statistical results of (a) fraction of land use class area in percentage and (b) vegetation area in percentage 29
Figure 3-5. The relationships between infiltration rate and prevailing precipitation in Swidnica area 29
Figure 3-6. Calibrated parameters results for the steady-state model calibration 30
Figure 3-7. Head distributions in meter above mean sea level for (a) Quaternary and (b) Tertiary aquifers 31
Figure 3-8. Comparison of observed and simulated river discharges 33
Figure 3-9. Steady-state groundwater budget for the Quaternary and Tertiary aquifers 34
Figure 3-10. Schematic diagram of the steady-state groundwater budget for the entire aquifer systems 35
Figure 3-11. Calibrated parameters for the transient model 39
Figure 3-12. Head distributions in meter above mean sea level for the (a) Quaternary and (b) Tertiary aquifers taken at the last simulation period on 30th Sept, 2003 40
Figure 3-13. Observed against simulated head for the two piezometers 41
Figure 3-14. Time series for the comparison of observed and simulated heads for Studnia I/710-2 in Quaternary aquifer 42
Figure 3-15. Time series for the comparison of observed and simulated heads for Studnia I/710-3 in the Tertiary aquifer 42

Figure 3-16. The comparison of observed and simulated lake stages....43
Figure 3-17. Time series for the comparison of observed and simulated lake stages....43
Figure 3-18. Comparison of the reservoir leakages and net leakage from groundwater balance results....44
Figure 3-20. Time series for the comparison of observed and simulated river gauge discharges - Pelczarna....45
Figure 3-19. The discrepancy for the comparison of observed and simulated river gauge discharges - Pelczarna....45
Figure 3-21. The discrepancy for the comparison of observed and simulated river gauge discharges - Pilawa....46
Figure 3-22. Time series for the comparison of observed and simulated river gauge discharges - Pilawa...46
Figure 3-23. The discrepancy for the comparison of observed and simulated river gauge discharges - Bystrzyca L.....47
Figure 3-24. Time series for the comparison of observed and simulated river gauge discharges - Bystrzyca L.....47
Figure 3-25. The discrepancy for the comparison of observed and simulated river gauge discharges - Bystrzyca K.....48
Figure 3-26. Time series for the comparison of observed and simulated river gauge discharges - Bystrzyca K....48
Figure 3-27. The discrepancy for the comparison of observed and simulated river gauge discharges- Strzegomka....49
Figure 3-28. Time series for the comparison of observed and simulated river gauge discharges-Strzegomka....49
Figure 3-29. Schematic diagram of the three years average of groundwater balance for the Quaternary and Tertiary aquifers in the transient model....51
Figure 3-30. Schematic diagram of the three years average of groundwater balance for the entire aquifer systems in the transient model....52
Figure 3-31.UZF recharge (gross GW recharge)....54
Figure 3-32. Groundwater - ET....54
Figure 3-33.Surface leakage (groundwater exfiltration)....54
Figure 3-34. Daily variability of different groundwater balance components over the 3 years (1096 days) MODFLOW-NWT simulation period retrieved under the use of UZF package....55
Figure 3-35. More clarification of Figure 3 34....55
Figure 3-36. Effect of changing HK parameter....59
Figure 3-37. Effect of changing VK parameter....59
Figure 3-38. Effect of changing Sy parameter....59
Figure 3-39. Effect of changing VKCB parameter....60
Figure 3-40. Effect of changing Ss parameter....60
Figure 3-41. General effect of calibrated parameters....60
Figure 3-42. Effect of changing HK parameter....61
Figure 3-43. Effect of changing VK parameter....61
Figure 3-44. Effect of changing Sy parameter....62
Figure 3-45. General effect of changing calibrated parameters on river discharges....62
Figure 3-46. Effect of changing river inflow....62

LIST OF TABLES

Table 3-1. Statistical results of fraction of land use classes and vegetation areas in percentages 29
Table 3-2.Comparison of observed and simulated heads 32
Table 3-3. Comparison of observed and simulated lake stage 32
Table 3-4. Comparison of observed and simulated river discharge 32
Table 3-5. Steady-state groundwater budget in the Quaternary and Tertiary aquifers 34
Table 3-6. Steady-state groundwater budget for the entire aquifer systems 35
Table 3-7. Comparison of this research and the previous study by Gurwin and Lubczynski (2004) 37
Table 3-8. Calibrated piezometric head errors 41
Table 3-9. Calibrated lake stage errors 43
Table 3-10. Comparison of observed and simulated river gauge discharges 44
Table 3-11. Three years average of groundwater budget for the Quaternary and Tertiary aquifers in the transient model 50
Table 3-12. Three years average of groundwater balance of the entire aquifer systems for the transient model 52
Table 3-13. Quantification of surface and ground water fluxes for the transient model calibration 56
Table 3-14. Comparison of the surface and ground water fluxes for the steady-state and the average of the transient model in Table 3-15 56
Table 3-15. The yearly variability of driving forces and different groundwater balance components over the 3 years (1096 days) MODFLOW-NWT simulation period 57
Table 3-16. Effect of changing HK parameter 59
Table 3-17. Effect of changing VK parameter 59
Table 3-18. Effect of changing Sy parameter 59
Table 3-19. Effect of changing VKCB parameter 60
Table 3-20. Effect of changing Ss parameter 60
Table 3-21. General effect of calibrated parameters 60
Table 3-22. Effect of changing HK parameter 61
Table 3-23. Effect of changing VK parameter 61
Table 3-24. Effect of changing Sy parameter 62
Table 3-25. General effect of changing calibrated parameters on river discharges 62

LIST OF ABBREVIATIONS

3D	The three Dimensional
ADAS	Automatic Data Acquisitions System
CLIMVIS	The Climate Visualization System
DEM	Digital Elevation System
ETo	Reference evapotranspiration
FAO	Food and Agriculture
GMS	Groundwater Modelling System
HOB	Head Observation Package of MODFLOW
IHM	Integrated Hydrological Model
ILWIS	Integrated Land and Water Information System
NWT	Newtonian
PET	Potential Evapotranspiration
RES	Reservoir Package of MODFLOW
SFR2	Streamflow-Routing Package 2 of MODFLOW
SRTM	Shuttle Radar Topographic Mission
UZF1	Unsaturated-Zone Flow Package of MODFLOW
ZONEBUDGET	Zone Budget program

1. INTRODUCTION

1.1. Introduction

Subsurface water is a general term of all waters below the earth's surface; it includes water in unsaturated and saturated zones. The subsurface water is a part of the hydrological cycle. Groundwater is a portion of subsurface water and defined as all water found in the saturated zone, where it occupies all or part of the void space in the soil or geological units. In addition, the study of groundwater is known as Hydrogeology. Recently, over exploitation and unreasonable utilization of groundwater resources has caused serious problems such as declining water level, groundwater pollution, water resources depletion, land subsidence, etc, which have seriously restricted the sustainable development of society, economy and the construction of ecological environment. Groundwater resources management requires assessments, which in turn needs models so as to promote its sustainable use for today's water needs and to protect the resources for the future.

Normally, groundwater models are used to represent the natural groundwater flow in a given environment. The models can be used to simulate and predict the aquifer conditions. The uses of groundwater models may include: (1) study of surface and groundwater interactions (Anderson and Woessner, 1992), (2) study of the effects of groundwater abstraction and predict the future of the aquifer systems (Wikipedia, 2014). These are often named as groundwater simulation models; (3) quality (chemical) aspects of the groundwater; such models try to predict the fate and movement of the chemical in nature. Thus, groundwater models are potential to answer the specific questions or facilitate to achieve the specific objectives.

1.2. Problem definition

Groundwater continues to be the main sources of domestic water supply in Świdnica area (Gurwin, 2010). Due to the intensive groundwater abstraction in the study area, it accelerated to the declines of water table and river discharges. In addition, the decline is exacerbated by the number and spatial distribution of boreholes. The presence of groundwater intakes such as Bokserska and Pszenno at well fields interferes with the hydrological systems in the study area. Nevertheless, no reliable modelling solutions integrating surface with groundwater fluxes have been proposed to account for the transient system responses to abstractions to ensure sustainable groundwater resources management. Presently, there is only steady-state standalone 3D model which does not describe the dynamics of the hydrological system (Gurwin and Lubczynski, 2004).

1.3. Research objectives and questions

1.3.1. Main research objective

To evaluate sustainability of groundwater resources in Świdnica study area.

1.3.2. Specific objectives

1) To calibrate a transient integrated hydrological model.
2) To analyse the water balance of the study area.

1.3.3. Main research question

What are the effects of groundwater abstractions on the aquifer systems and river discharges?

1.3.4. Specific questions

1) What is spatio-temporal variability of groundwater fluxes
2) What are the effects of groundwater abstractions upon the water balance of the catchment?

1.4. Study area

1.4.1. Location

The study area is approximately 614.05 km² and belongs to the Sudety Foreland (Gurwin and Lubczynski, 2004) The area is bounded by Polish coordinates; X= 3,587,730.0 from west, X= 3,621,780.0 from east and Y= 5,655,210.0 from north, Y= 5,628,650.0 from south (Figure 1-1)

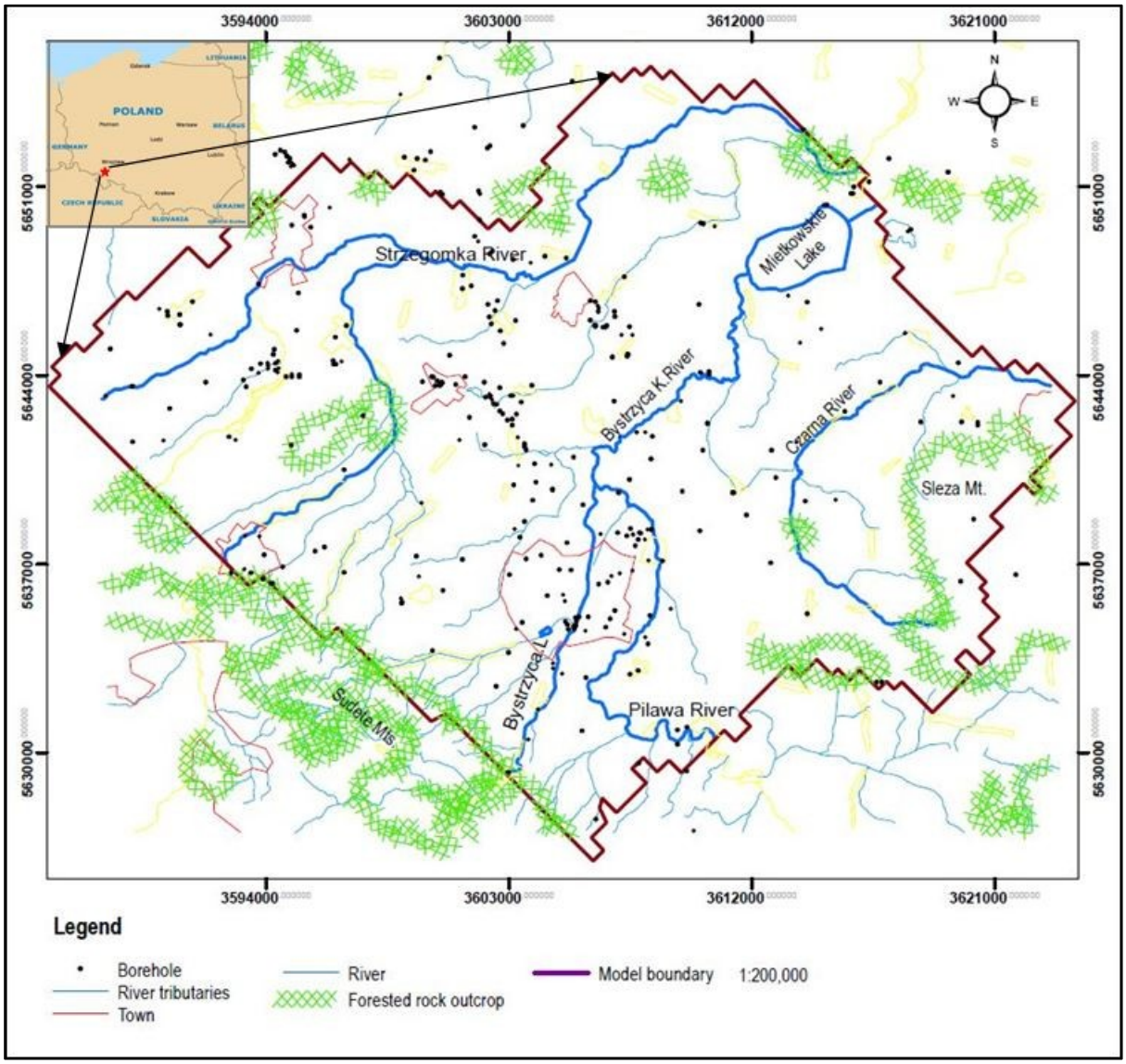

Figure 1-1. Study area adapted from Gurwin and Lubczynski (2004)

1.4.2. Climate

1.4.2.1. Precipitation

The hydrological cycle is mostly controlled by driving forces such as precipitation and evapotranspiration. In addition, topography plays a big role in the formation of precipitation (Brutsaert, 2005). The amount of precipitation increases with an increase of altitude. In Świdnica area, the smallest rainfall is in the lowland surface while the largest is within the Strzegomka Hills, Sleza Mountain and Sudety Mountains (Figure 1-1). There were daily rainfall records from Pszenno ground gauge station (Figure 1-2) with a complete data for the study period (01/10/2000 to 30/09/2003).

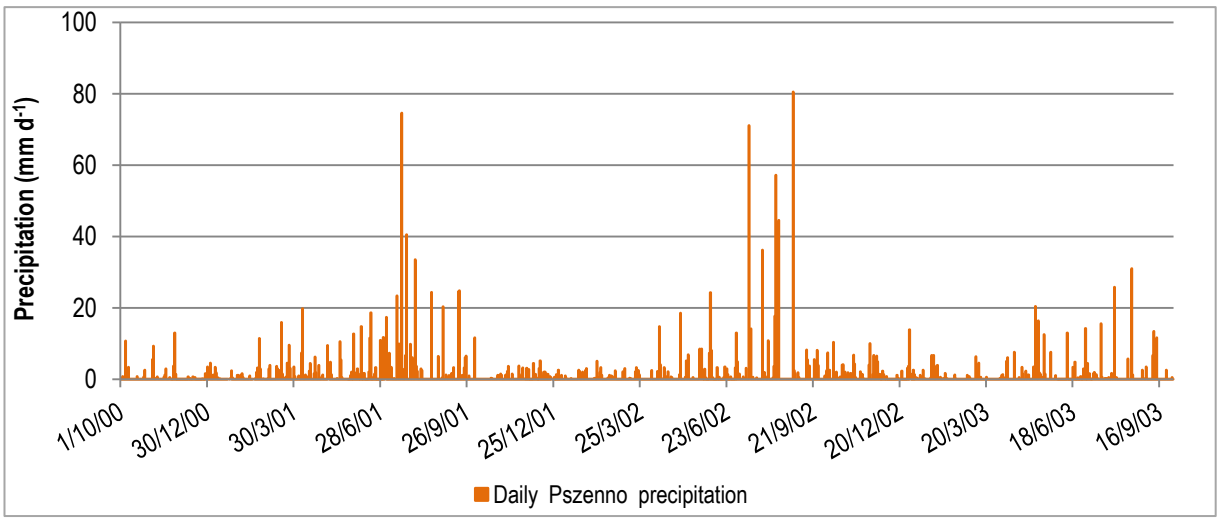

Figure 1-2. Precipitation from Pszenno station

1.4.2.2. Potential evapotranspiration (PET)

The PET was calculated using the main original Penman-Monteith equation (Allen et al., 1998).The standard climatic data from 03/04/2002 to 22/12/2002 used to prepare reference evapotranspiration (ETo) and finally to compute for potential evapotranspiration (Figure 1-3).

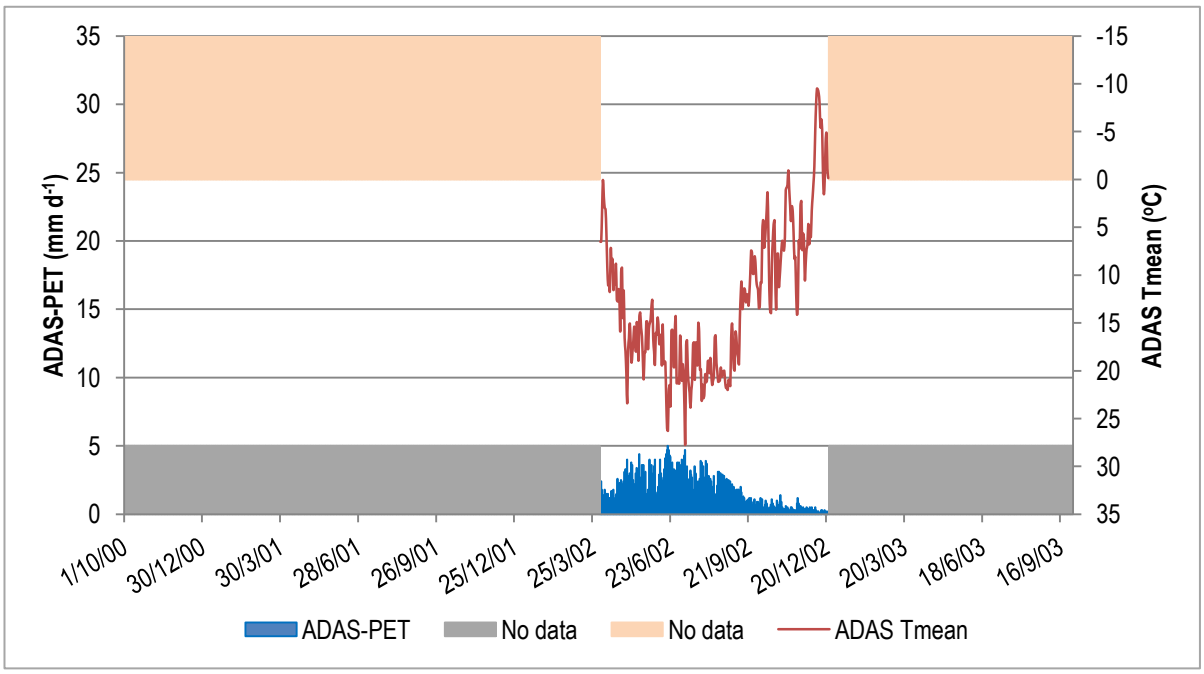

Figure 1-3. PET for the study area

1.4.3. Topography

The study area is mostly characterized by hilly topography and low surface areas. The digital elevation model (DEM) data were downloaded from Shuttle Radar Topographic Mission (SRTM) with 90 m resolution, which covered the whole Świdnica area (Figure 1-4). The elevation from SW to NE is ranging between 450 m to 170 m a. m. s. l at the surrounding area of Lake Mietkowskie.

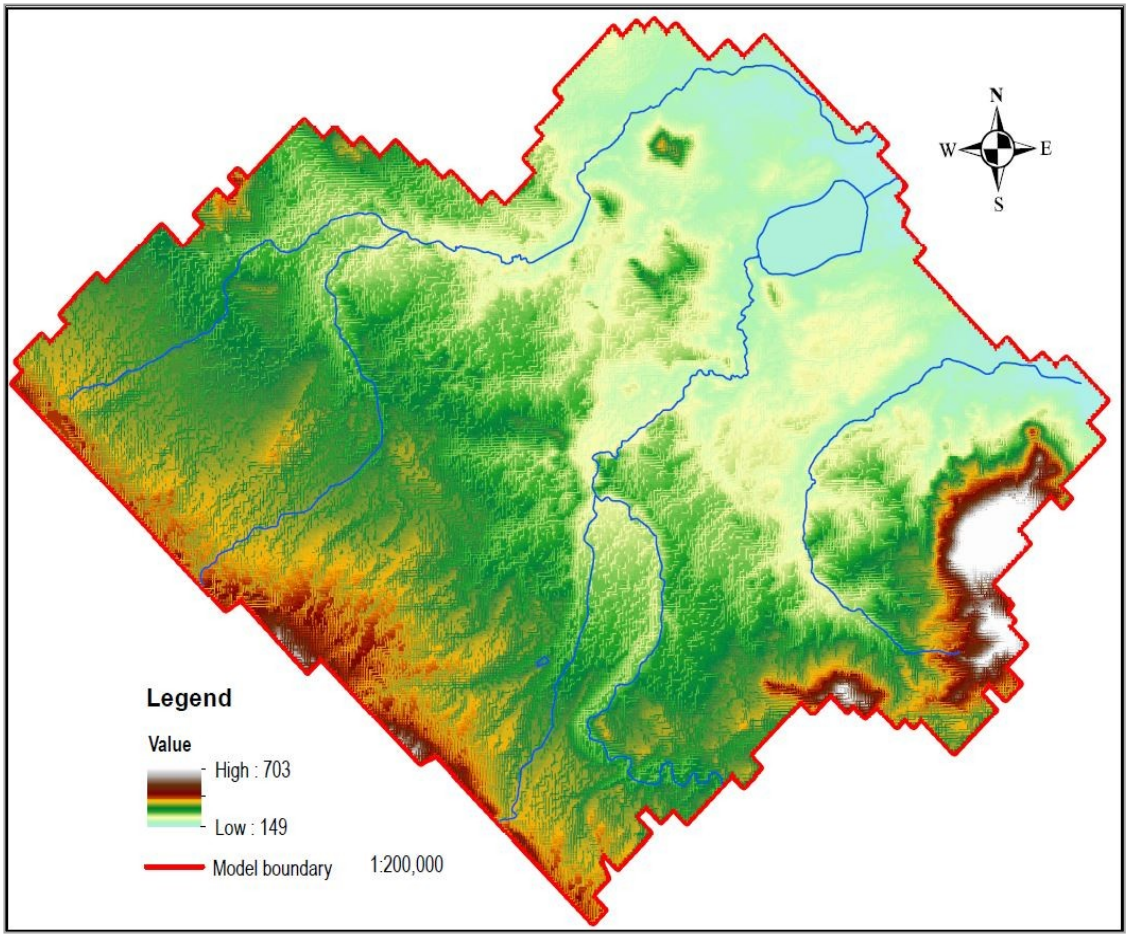

Figure 1-4. Topography

1.4.4. Land use

Land use is defined as the use of land in a given environment. This could involve the management and modification of the natural environment into such as agriculture, managed forest, settlements, artificial water storages, etc. Świdnica area is possessing different types of land use, but in this research land use was classified into the extensive and intensive use of the environment. The extensive land use considered agriculture farmland which is a larger part of the study area (Figure 1-5). The intensive land use, which includes; lake, forest and Town, this nature of categorizing land use was also applied by Łowicki (2008).

Vegetation cover is defined as all natural and artificial plants that grown in a certain environment. They can be presented on the map as indices of greenness. The vegetation covers in Świdnica area were divided into two parts, namely: 1) agriculture farmland - vegetation species which include wheat and grasslands and 2) forest (Figure 1-5).

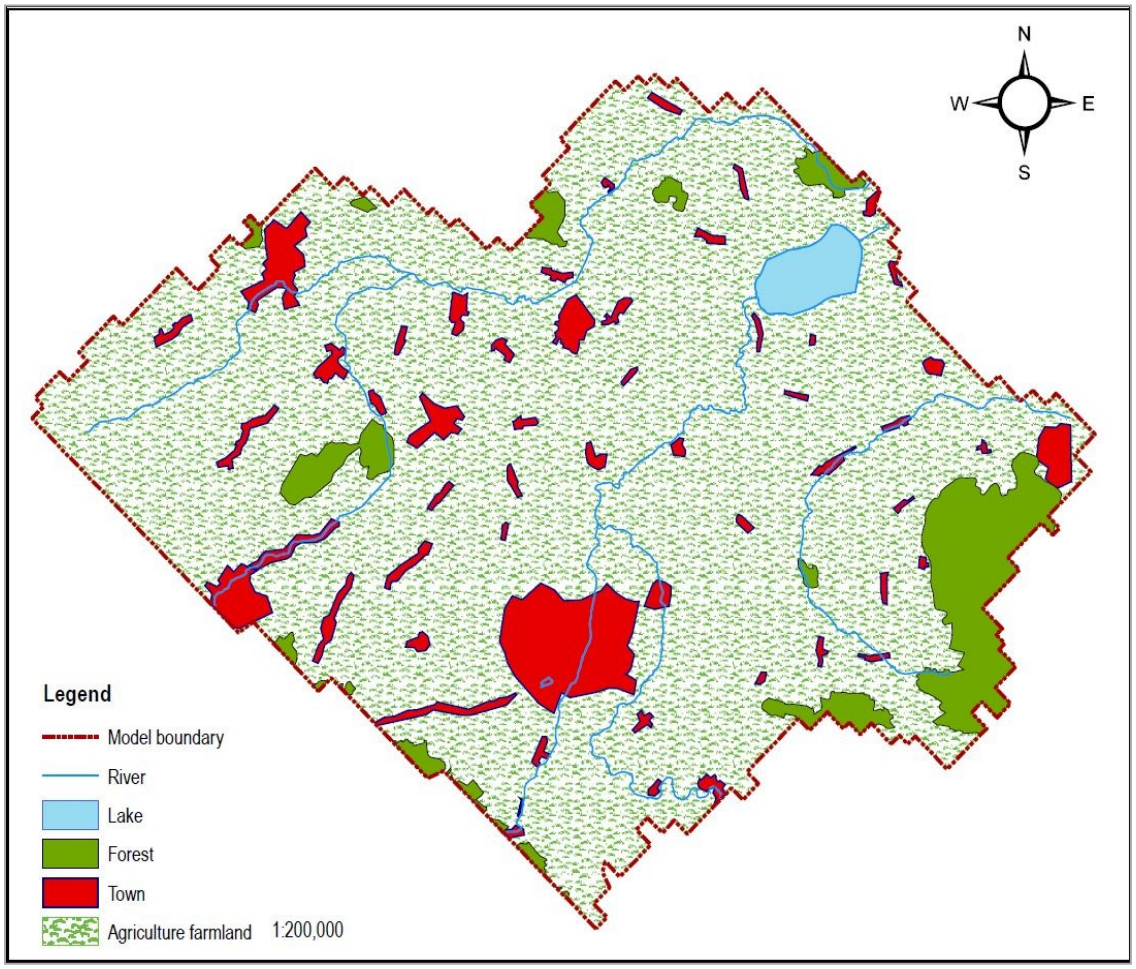

Figure 1-5. Land use in the study area

1.4.5. Hydrology

The study area is located within the Odra River Watershed and includes three river catchments; Bystrzyca, Strzegomka and Czarna with associated streams. Bystrzyca and Strzegomka rivers originate from Sudety Mountains while Czarna river originates from Sleza Mountain. The main rivers are supplied by the small inlets and streams which flow all the time (Figure 1-1). Their outflows are contributed from the water table and surface runoff formed by rainfall (precipitation) and melting snow. There were five daily river gauge discharges with data recorded from 01/12/2000 to 30/09/2003, the missing data are indicated by shading in Figure 1-6 to Figure 1-10.

Lake Mietkowskie is an artificial reservoir which acts as a flood control structure in the lower surface area (NE), because it collects all runoff from Bystrzyca river. There is an earthen dam with piezometers at a specific interval of 100 m which enables to determine dam seepage as well as groundwater recharges (Figure 1-1). The daily water level fluctuations of Mietkowskie Lake were obtained for the period of 01/10/2000 to 30/09/2003 (Figure 1-11).

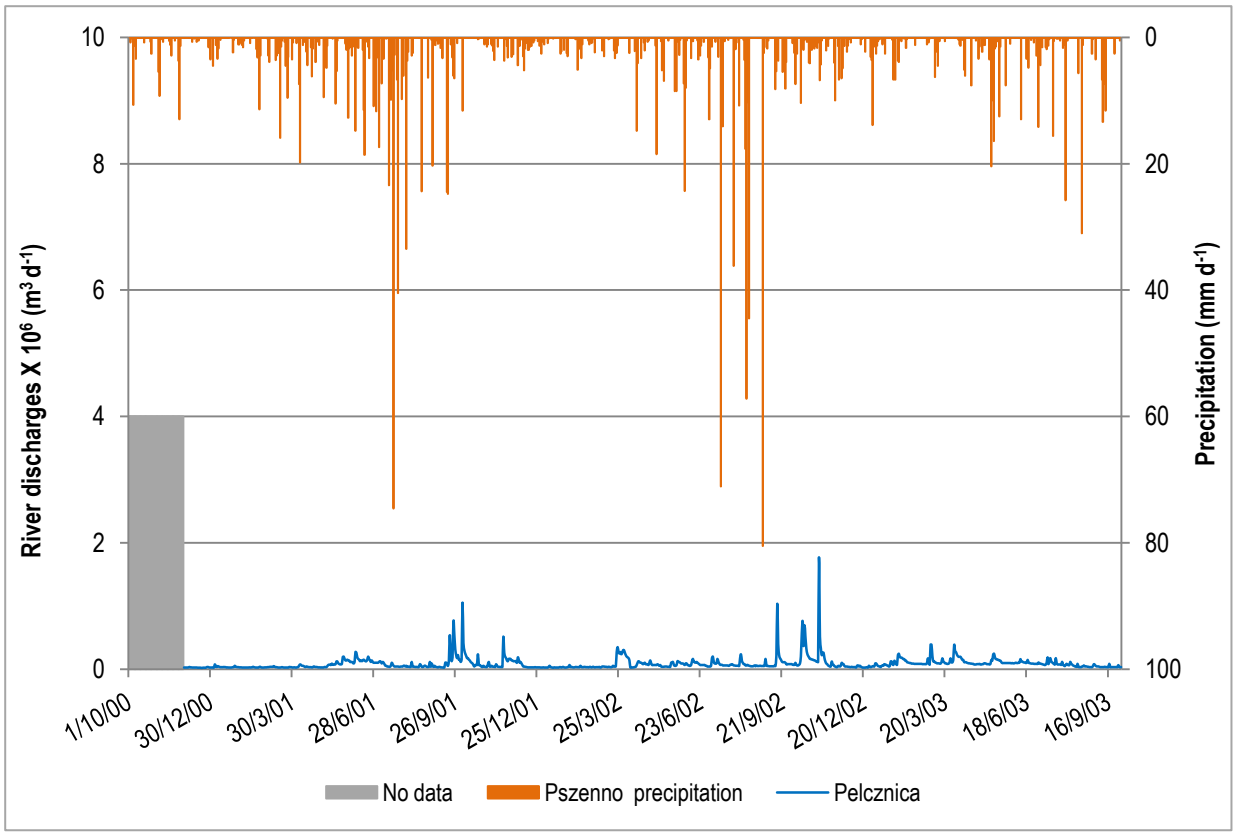

Figure 1-6. Pelczanica river gauge discharges (Figure 1-1)

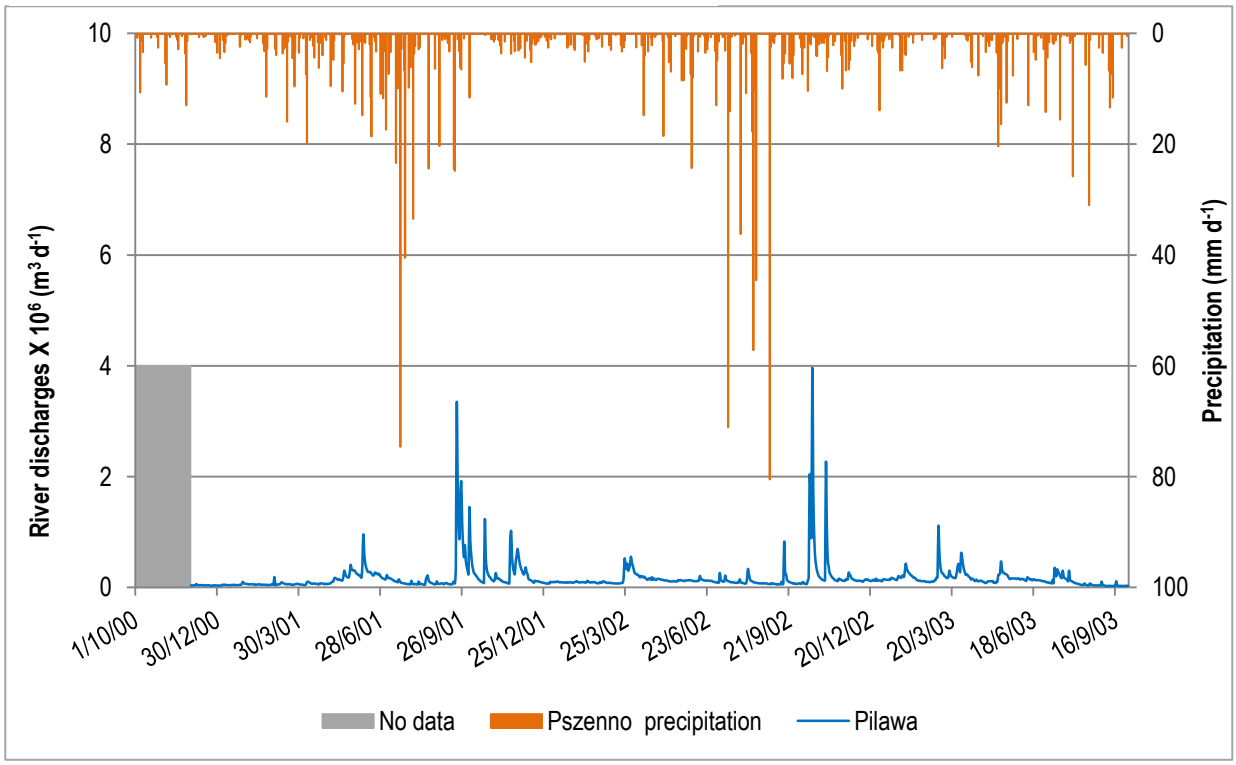

Figure 1-7. Pilawa river gauge discharges (Figure 1-1

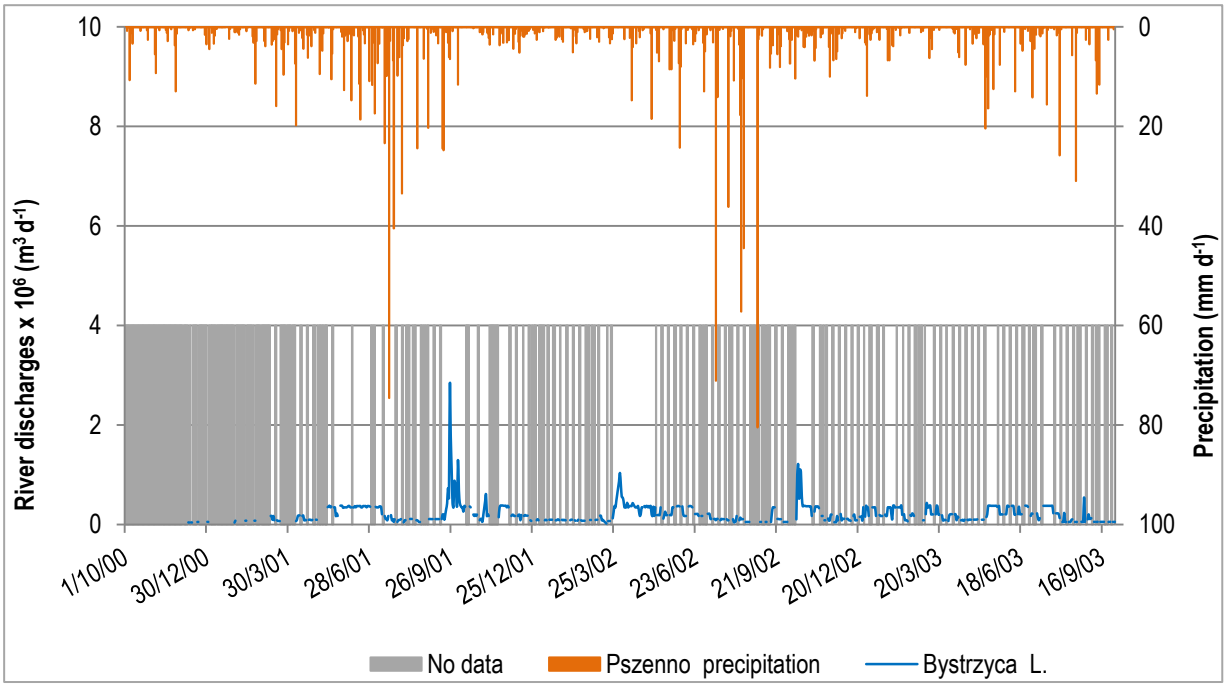

Figure 1-8. Bystrzyca L. river gauge discharges (Figure 1-1)

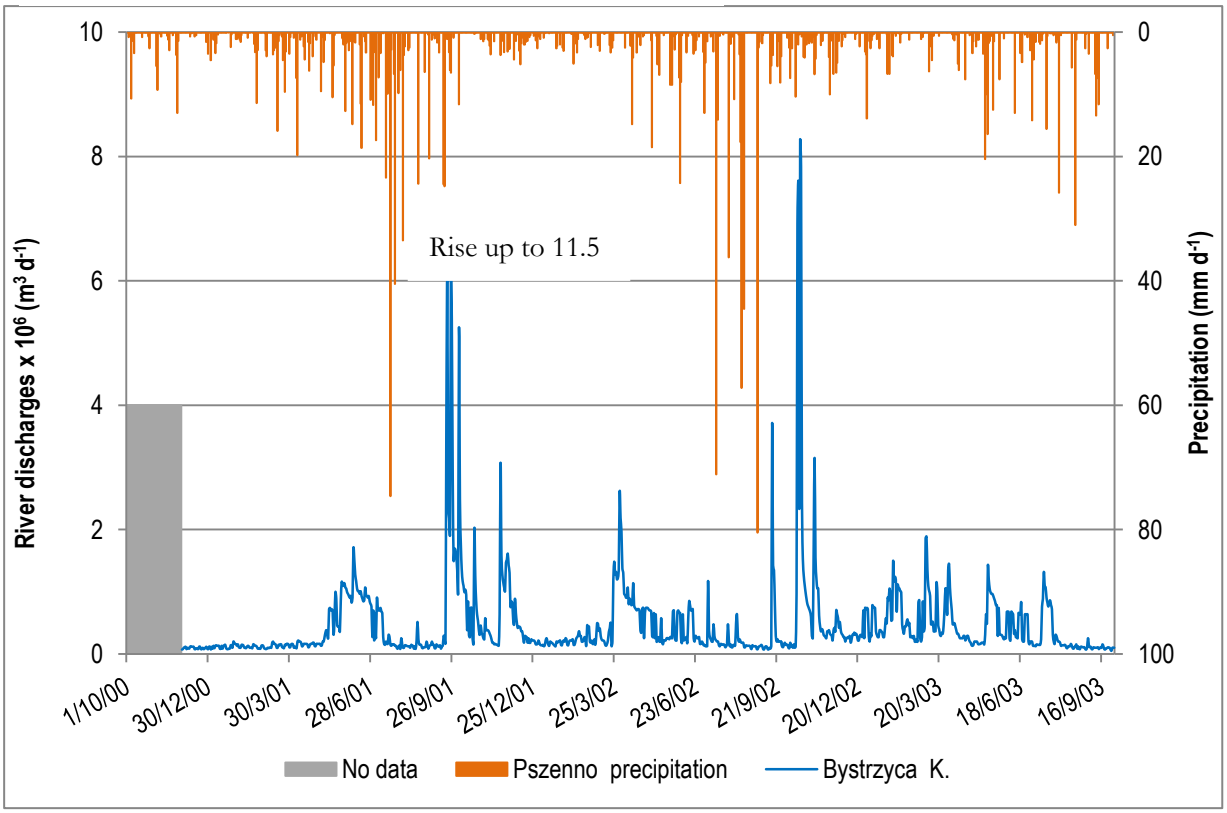

Figure 1-9. Bystrzyca K. river gauge discharges (Figure 1-1)

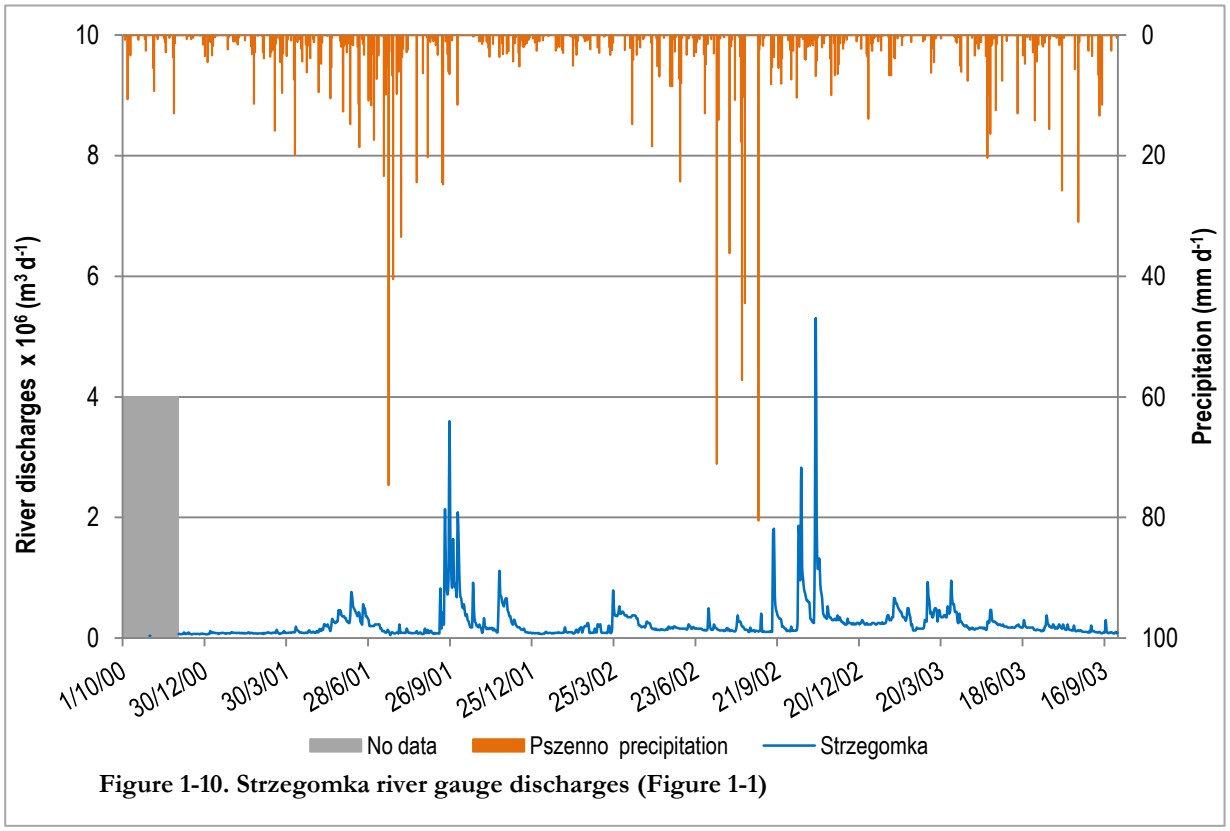

Figure 1-10. Strzegomka river gauge discharges (Figure 1-1)

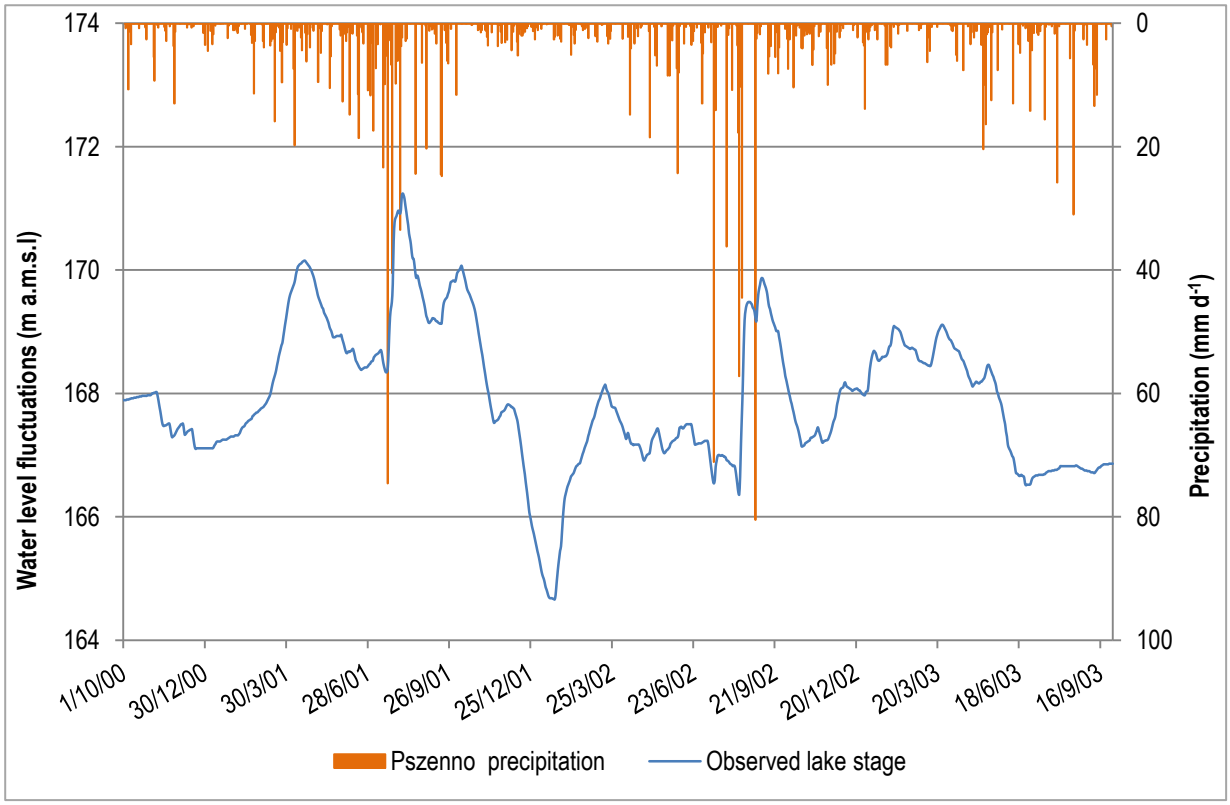

Figure 1-11. Water level fluctuation of Lake Mietkowskie (Figure 1-1)

1.4.6. Geology

The study area is lithologically described by two major rock formations (Gurwin and Lubczynski, 2004), namely: 1) Cainozoic unconsolidated sediments, mainly; sands, gravels, clays and tills; 2) Palaeozoic crystalline bedrocks which are composed of epimetamorphic and granitic rock types (Figure 1-12).

Stratigraphic is defined as the branch of geology, which classify rock layers. It addresses the study of sedimentary and volcanic rocks layered in a particular environment. In Świdnica area, Gurwin and Lubczynski (2004) described the sequence of layers which is comprised of sands and gravels as an aquifer layer, clay materials as the aquitard layer and crystalline rocks as an outcrop or bedrocks (Figure 1-12).

The tectonic process is the movement of rock mass as a result of plate movement, which causes rocks to be moved away from where they were formed. It plays a big role in a rock cycle, because the movements can produce fault/joint in the rocks. In the study area, aquifer systems are bounded in SW by the fault zone trending along the NW to SE (Gurwin and Lubczynski, 2004) (Figure 1-12).

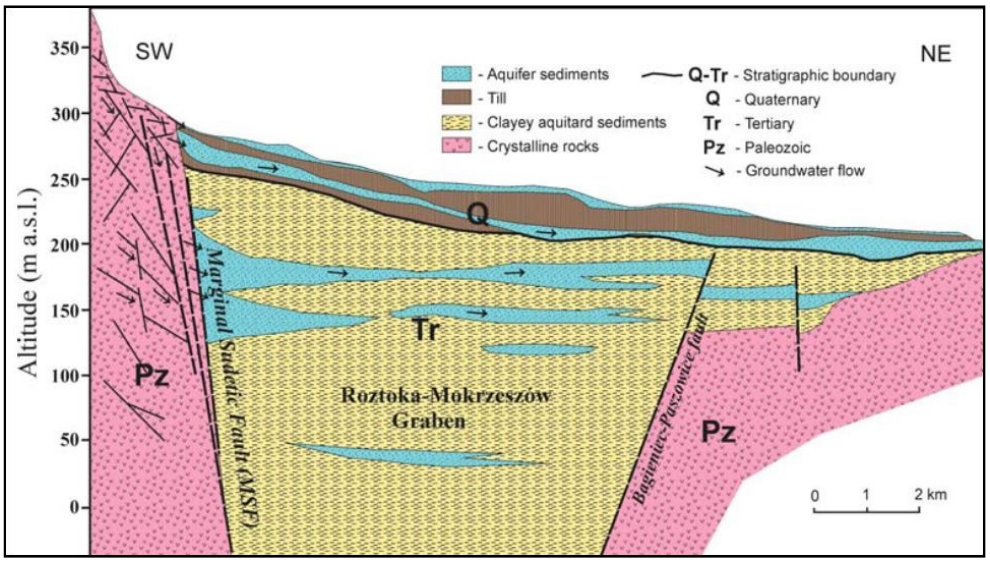

Figure 1-12. Hydrogeological cross-section (source: Gurwin and Lubczynski (2004))

1.4.7. Hydrogeology

Due to better protection of aquifer systems in the area, Świdnica Municipality is dealing with two main well fields namely: Pszenno and Bokserska. The boreholes in these fields are in Tertiary aquifer thickness. The groundwater well abstractions were obtained from Gurwin and Lubczynski (2004) study case. They described the yield of groundwater supply from Pszenno well field (8000 $m^3 d^{-1}$) which consists of 5 wells in use and Bokserska well field (6500 $m^3 d^{-1}$) which consists of 9 wells in use.

Borehole Bank Hydro data were obtained from Wroclaw University. Some of the boreholes are drilled up to Quaternary and others to Tertiary aquifers. Just to demonstrate the few borehole distributions were indicated (Figure 1-1). To ensure groundwater resources management, Automatic Data Acquisition System (ADAS) have two piezometers for groundwater monitoring (one in Quaternary and another in Tertiary aquifer).The available daily water level fluctuations data of two piezometers were obtained for the period of 02/10/2000 to 24/03/2003 (Figure 1-13 and Figure 1-14).

Gurwin and Lubczynski (2004) determined the flow into aquifer systems along the fault zone in the SW of the study area, they used a natural model to quantify the discharge values in both aquifers.

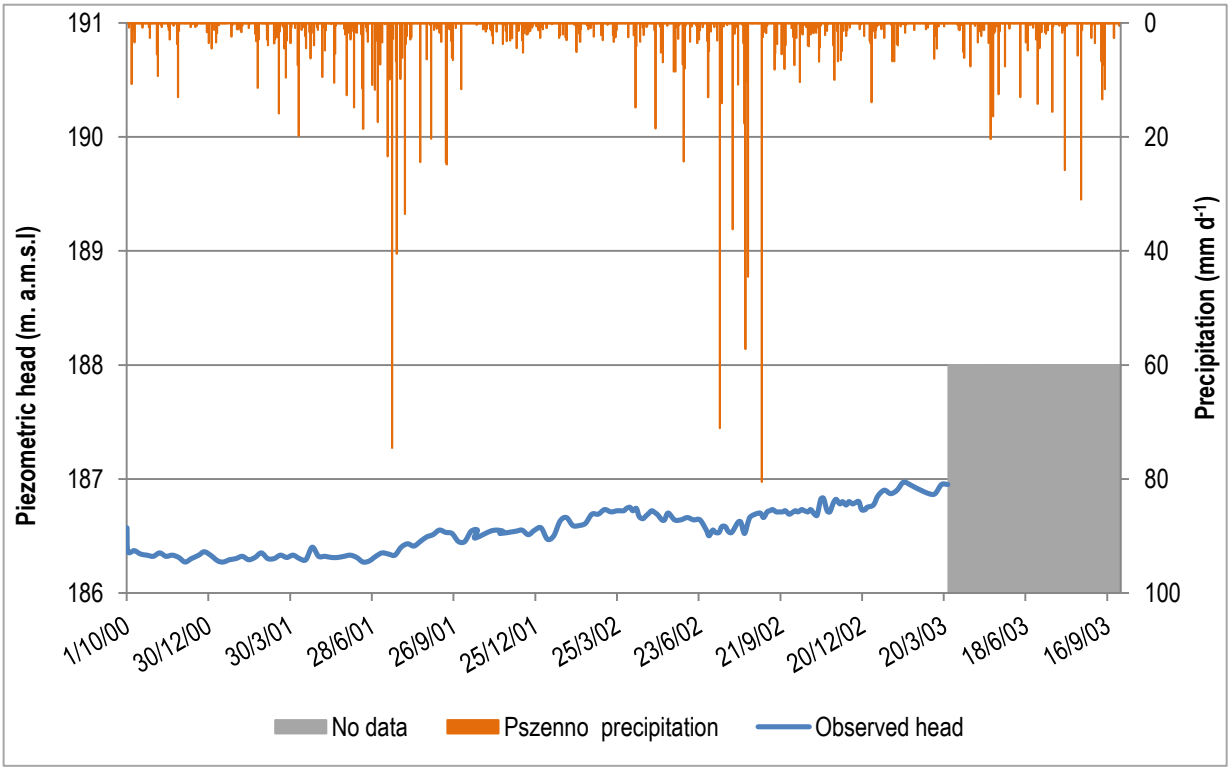

Figure 1-13. Measured piezometric heads of Studnia I/710-2 for Quaternary aquifer

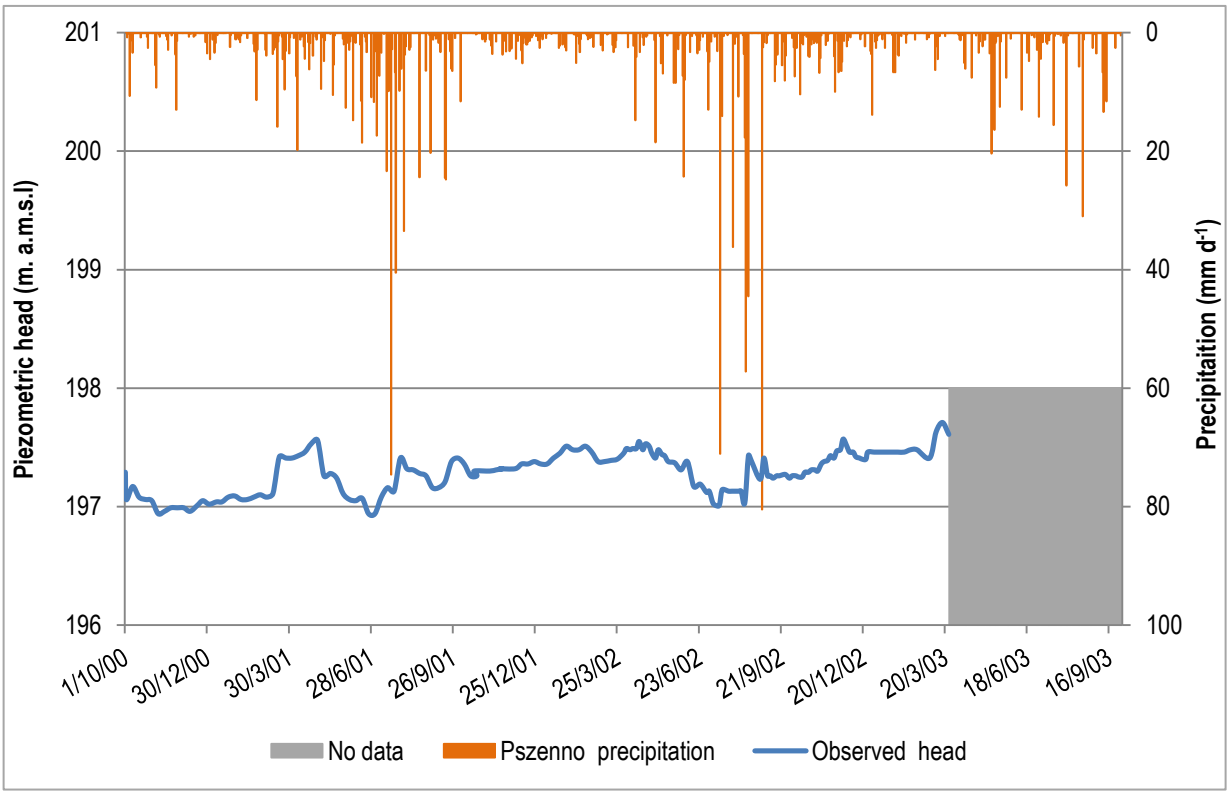

Figure 1-14. . Measured piezometric heads of Studnia I/710-3 for Tertiary aquifer

1.4.7.1. Head distributions from the previous steady-state model in Świdnica area

The head distributions and groundwater flow directions were indicated by Gurwin and Lubczynski (2004). In their model set up, they had three aquifers, where (a) and (b) are the Quaternary aquifers and (c) Tertiary aquifer (Figure 1-15). Thus, the legend of Quaternary and Tertiary aquifers indicated that; number 1 was head contour, arrows numbered 2 and 3 in Figure 1-15 (a) and (b), respectively were the groundwater flow directions. The number 3 and 6 in Figure 1-15 (a), (b) and (c) were rivers or streams and also number 5 in Figure 1-15 (b) and (c) was calibrated point (Gurwin and Lubczynski, 2004).

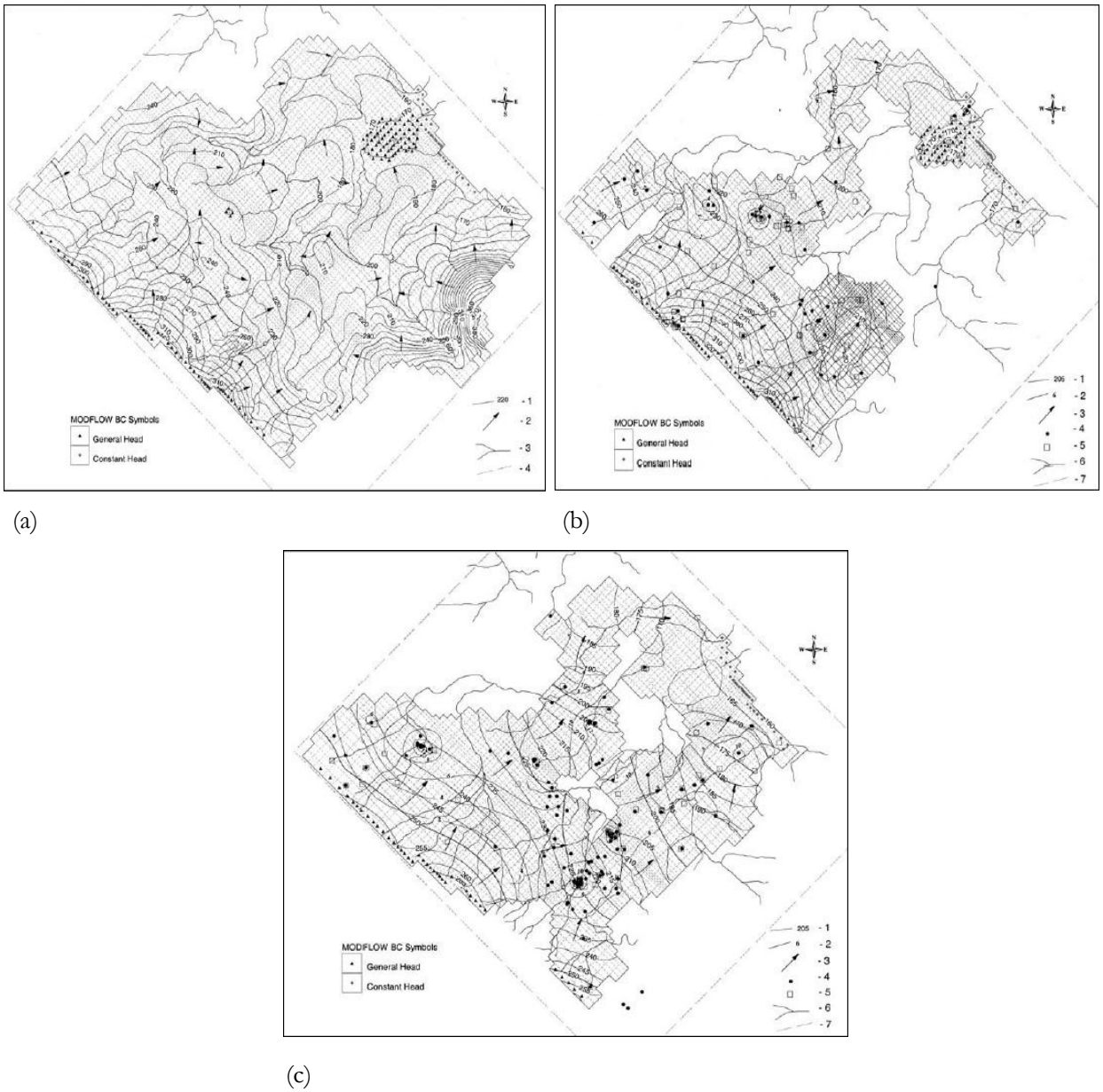

(a) (b)

(c)

Figure 1-15. Steady-state head distributions for the Quaternary ((a) and (b)) and Tertiary (c) aquifers (source: (Gurwin and Lubczynski, 2004))

2. RESEARCH METHOD

2.1. Introduction

The research method was adhered to these working contents (Figure 2-1).

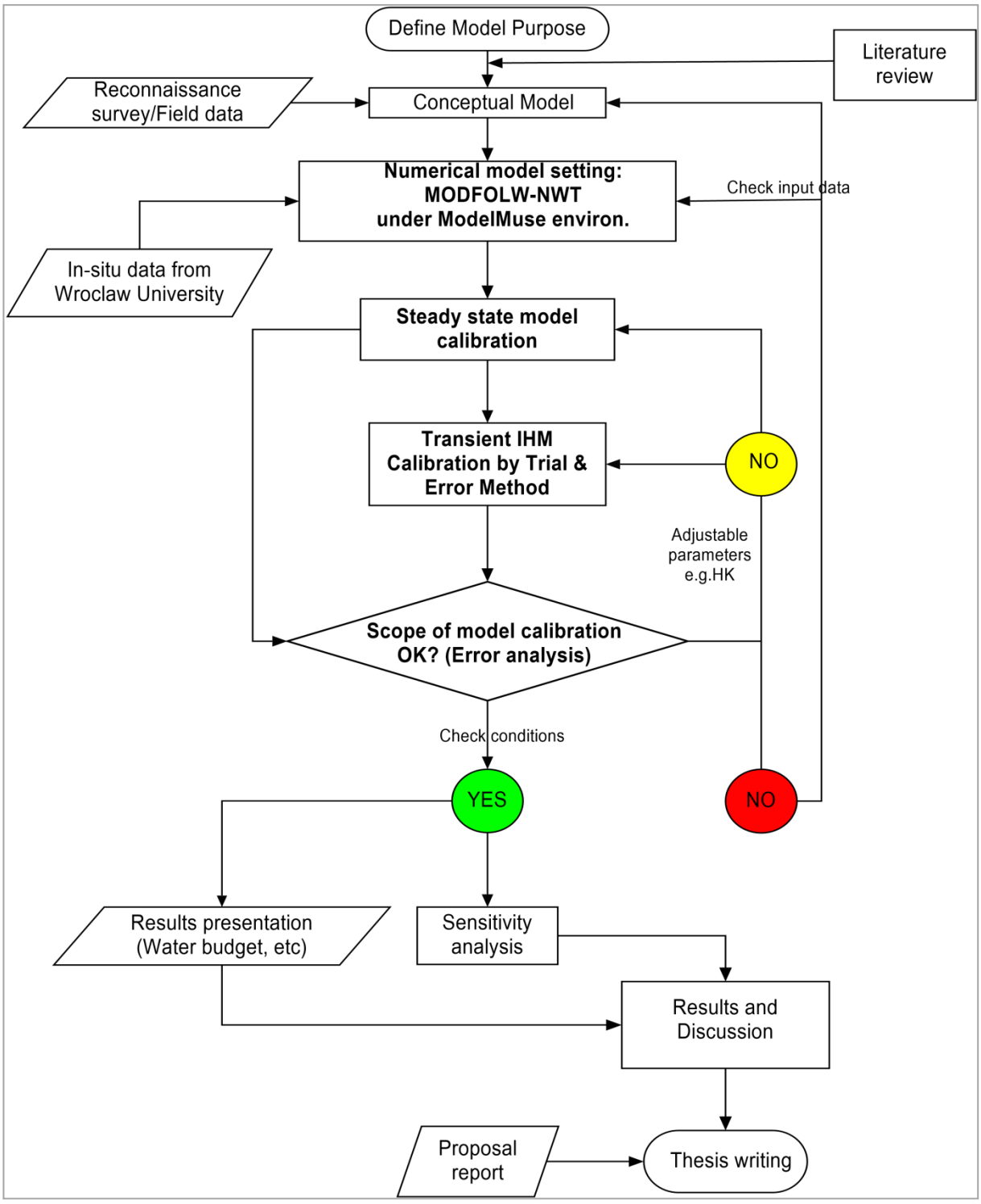

Figure 2-1.Research method

2.2. Reconnaissance survey and data collection

The field work/reconnaissance survey was conducted between 19th and 27th July 2014 that enabled to obtain secondary research data from Wroclaw University in south west part (Poland). The study period was limited from October 01, 2000 to September 30, 2003 and datasets are summarized (Figure 2-2).

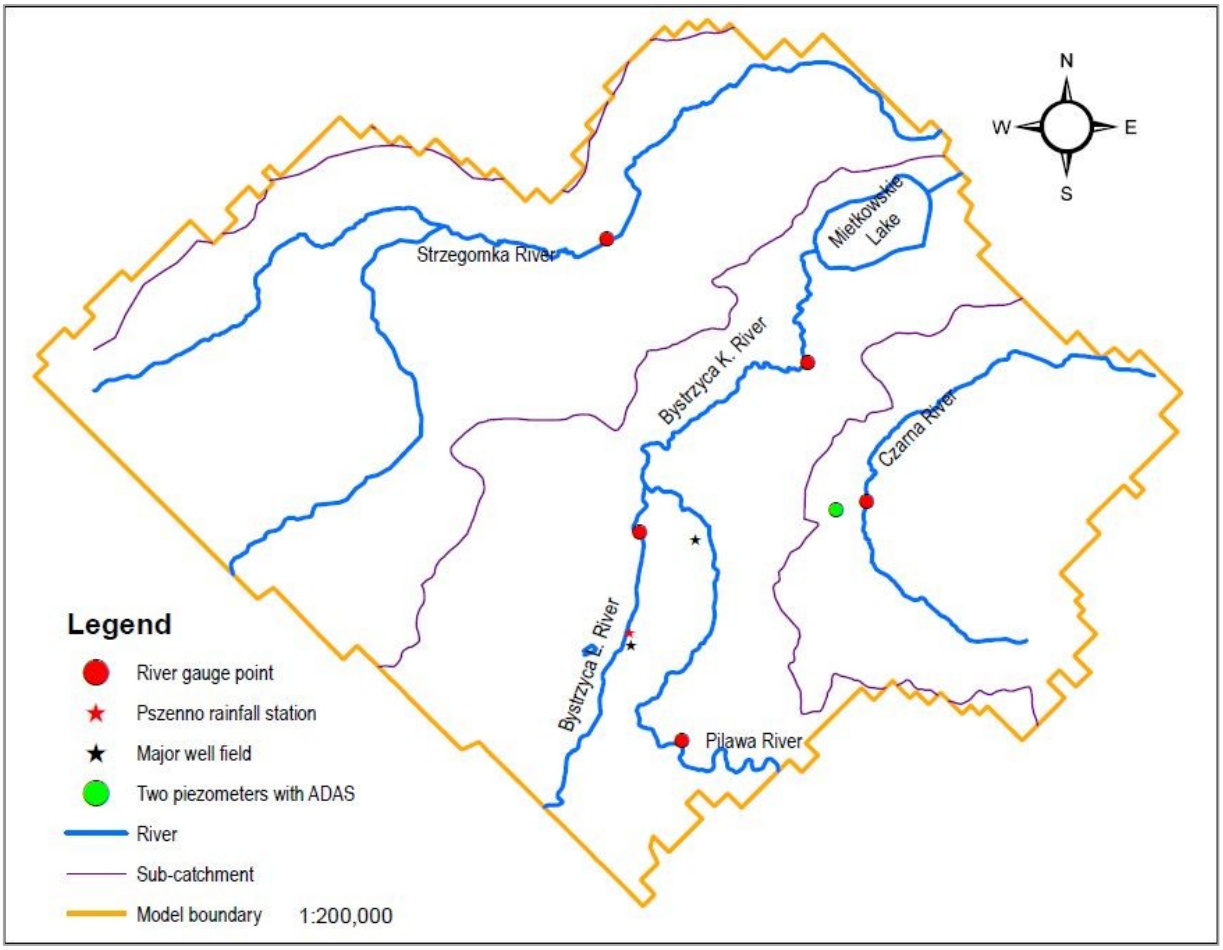

Figure 2-2.Summary of all datasets for the research

2.3. Literature review

Assessment of groundwater resources:

Assessment of groundwater resources by modelling is a data intensive process. It requires availability of data (short or long term) in order to run the steady-state and transient models conditions. Steady-state and transient are the fundamental flow mechanisms used to simulate the groundwater flow. However, each type of the flow has its specific conditions of application depending on the available data. While in the steady-state condition the flow is time independent, thus the change of storage is equal to zero, in the transient condition flow depends entirely on time thus the change of storage is not equal to zero. Therefore, the steady-state flow simulation is more often attributed with non-unique solution, a contrast to the transient simulation. The steady-state simulation produces only one set of average heads and the transient simulation produces a set of heads at each time step (Anderson and Woessner, 1992). The lack of monitoring data in groundwater modelling is limited to the steady-state model calibration (Gurwin and Lubczynski, 2004). Furthermore, the transient modelling requires long term data availability and good monitoring systems.

In the past few decades, there are advancements in science and technology in the field of groundwater modelling. The groundwater modelling expertise plays a big role in the determination of the best

groundwater management solutions. Groundwater modelling software can be addressed in two different types namely: standalone and integrated hydrological models. Likewise, applications of each tool depend on the hydrological nature of the area under investigation. A steady-state standalone model was used in the complex multi aquifer systems and indicated good performance during the assessment of groundwater resources (Gurwin and Lubczynski, 2004). Furthermore, the same model was used by Jaworska-Szulc (2009) to evaluate groundwater resources and it indicated that the groundwater abstractions develop a larger cone of depression extending even outside the study area which cause higher infiltration to the river and lake. Consequently, it led to the decline of groundwater discharges, river discharges and water level in the lake. Lubczynski and Gurwin (2005) and Massuel et al. (2013) used both steady-state and transient standalone models. They concluded that transient model has reliable solutions and it provides a broad knowledge about the hydrological processes. The use of integrated hydrological model (IHM) focusing on the assessment of groundwater resources and surface-groundwater interactions is being practiced. This is because the two water bodies are linked dynamically. The integrated hydrological model is most reliable on the study of the surface-groundwater interactions by Hassan et al. (2014). Moreover, the surface-groundwater interactions with the application of IHM under steady-state model condition was applied by Yimam (2010) and Huntington and Niswonger (2012). They concluded that the model has less reliable solution than the transient model. This is because of the large degree of freedom during steady-state calibration processes which produces higher values of errors in the final results. In addition, Hassan et al. (2014) and Zehairy (2014) conducted the study of surface-groundwater interactions by applying IHM under both steady-state and transient models conditions. They concluded that the model provides good results for the retrieval of water balance.distinct

In Świdnica area only steady-state standalone model had been conducted by Gurwin and Lubczynski (2004) with the aim of groundwater resources evaluation.

2.4. Data processing

2.4.1. Precipitation and potential evapotranspiration (PET)

The Pszenno precipitation station has a complete data for the study period (01/10/2000 to 30/09/2003) and therefore, that station was directly used (Figure 1-2).

The standard climatic data recorded from 03/04/2002 to 22/12/2002 were used to calculate reference evapotranspiration (ET_o) and finally to compute PET by using the FAO main original Penman - Monteith equation (Allen et al., 1998) described (Figure 1-3 and Eqn. 2-1). Because FAO-ET_o/PET has no complete data, it was essential to have the complete data for the study period from 01/10/2000 to 30/09/2003. Therefore, it demanded to use the Hargreaves ET_o equation (Eqn. 2-3) in order to fill the gaps for FAO-ET_o. In order to fill FAO-ET_o gaps, the full study period of temperatures from CLIMVIS website were downloaded which involved two stations (Legnica and Jelenia GORA) to check the best correlation with ADAS station. Legnica station showed the best correlation with the ADAS station for the minimum, maximum and mean temperatures and hence it was selected for further processes (Figure 3-1). The ADAS station temperatures gaps were filled hence used to calculate Hargreaves ET_o (Eqn. 2-3). As a result, the Hargreaves ET_o was used to correlate with the FAO-ET_o and fill the gaps (Figure 3-3).

FAO- ET_o from the main Penman - Monteith equation:

$$ET_o = \frac{0.408\times\Delta\times(R_n-G)+\gamma\times\left(\frac{900}{T+273}\right)\times u_2\times(e_s-e_a)}{\Delta+\gamma\times(1+0.34\times u_2)} \quad \text{Eqn. 2-1}$$

where; ET_o-reference evapotranspiration (mm day^{-1}), R_n -net radiation at the crop surface (MJ m^{-2} day^{-1}), G - soil heat flux density (MJ m^{-2} day^{-1}), T - mean daily air temperature at 2 m height (^{o}C), u_2 - wind speed

at 2 m height (m s^{-1}), e_s -saturation vapours pressure (kPa), e_a- actual vapour pressure (kPa), $e_s - e_a$ - Saturation vapour pressure deficit (kPa), Δ - slope vapour pressure curve (kPa $^oC^{-1}$) and γ - psychrometric constant (kPa $^oC^{-1}$).

PET was calculated using equation:

$$PET = ET_o \times K_c \quad \text{Eqn. 2-2}$$

where; K_c equal to 1

Note: Other equations and constants are described in the appendices.

ET_o from Hargreaves equation:

$$ET_o = 0.0023 \times (T_{mean} + 17.8) \times (T_{max} - T_{min})^{0.5} \times R_a \quad \text{Eqn. 2-3}$$

$$R_a = \left(\frac{24\times60}{\pi}\right) \times (G_{sc} \times d_r) \times [(\omega_s \times \sin(\varphi) \times \sin(\delta)) + (\cos(\varphi) \times \cos(\delta) \times \sin(\omega_s))] \quad \text{Eqn. 2-4}$$

where; G_{sc} - the solar constant equal to 0.0820 (MJ m^{-2} min^{-1}), d_r - the inverse relative distance Earth-Sun, ω_s- the sunset hour angle, φ - the latitude in radians and δ - the solar declination.

The inverse relative distance Earth-Sun (d_r);

$$d_r = 1 + 0.033 \times \cos\left(\frac{2\times\pi}{365} \times J\right) \quad \text{Eqn. 2-5}$$

Where; J - the Julian days.

The sunset hour angle (ω_s);

$$\omega_s = arc\cos[-\tan(\varphi) \times \tan(\delta)] \quad \text{Eqn. 2-6}$$

The solar declination (δ);

$$\delta = 0.409 \times \sin\left(\frac{2\pi\times J}{365} - 1.39\right) \quad \text{Eqn. 2-7}$$

2.4.2. Water level fluctuations for the two piezometers

The heights of groundwater table (heads) above mean sea level were calculated by using the formulas below.

Head above mean seal level:

For piezometer Studnia I/710-2 located in aquifer

$$H_{wt} = 196.95 + 1.3 - D_{wt} \quad \text{Eqn. 2-8}$$

For piezometer Studnia I/710-3 located in aquifer 2:

$$H_{wt} = 197.16 + 1.5 - D_{wt} \quad \text{Eqn. 2-9}$$

where; H_{wt} - is the height of groundwater table (m), 196.95 and 197.16 m - the elevations (m. a. m.s. l), 1.3 and 1.5 - casing heights (m) and D_{wt}- is depth to water table which varies with time (m). The average piezometric heads for Studnia I/710-2 and Studnia I/710-3 were presented in Table 3-2.

2.4.3. Fault groundwater inflow at the SW model boundary

Gurwin and Lubczynski (2004) determined the inflows into aquifer systems along the fault zone in SW, through that study case the total inflows obtained from groundwater budget for aquifer 1 and aquifer 2 were equal to 50277 m^3 d^{-1} and 16846 m^3 d^{-1}, respectively.

2.4.4. Lake Mietkowskie water level fluctuations and river gauge discharges

The average value of lake water level fluctuations (Figure 1-11) was indicated (Table 3-3). Also, there were daily five river gauge discharges data presented (Figure 1-6 to Figure 1-10) with calculated average values (Table 3-4).

2.5. Conceptual model

The conceptual model was adhered to the previous study conducted by Gurwin and Lubczynski (2004) and reconnaissance survey made.

2.5.1. Hydrostratigraphical units

From the data obtained at Wroclaw University and reconnaissance survey made, the study area has 3 hydrostratigraphic units which consist of 2 aquifers and 1 aquitard (Figure 2-3). The upper layer is an unconfined aquifer and one confined aquifer at the lower part which is separated by an aquitard material (clayey).

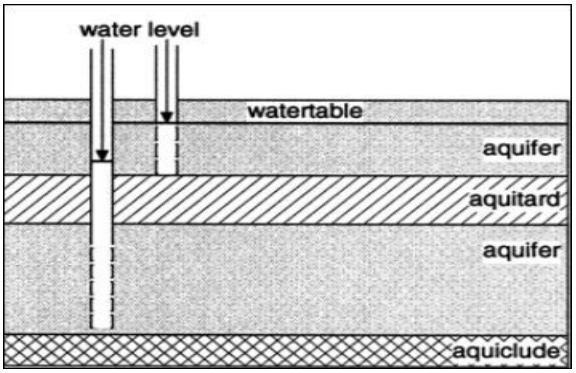

Figure 2-3. Aquifer systems (source: Kovalevsky, Kruseman, and Rushton (2004))

2.5.2. Flow pattern, distribution and flow rate

The groundwater flow pattern and direction can be addressed by the availability of head distributions (Figure 1-15). In addition, it is entirely described by the fault zone, which originates from the Sudety Mountains in SW towards the outflow in NE (Gurwin and Lubczynski, 2004). A flow rate is a function of hydraulic gradient and transmissivity.

2.5.3. Preliminary groundwater balance

It addresses the groundwater budget equation;
The change in groundwater storage by time ($\Delta S/\Delta t$) is equal to the groundwater recharge (inflow, I) minus groundwater discharge (outflow, O).

$$\frac{\Delta S}{\Delta t} = I - O \qquad \text{Eqn. 2-10}$$

Inflow includes; precipitation and percolation from other surface water bodies, e.g. rivers/stream and lakes.

Outflow includes; discharges (pumping wells or spring flow, etc) and groundwater evapotranspiration (ET_{gw}). To close the water balance in steady-state model, the change in storage should be equal to zero (Inflow = Outflow) because it is time independent. In transient state, change in storage should not be equal to zero because it is time dependent (stress periods).

2.5.4. Model boundaries

Considering reconnaissance survey made and data obtained at Wroclaw University, it indicates that the inflows into the aquifer systems are from Sudety Mountains moving along the fault zone and outflows in Mietkowskie Lake side. The external boundaries are considered to be at Bystrzyca, Pilawa and Strzegomka rivers because they act as the inflow and outflow in the study area. Also, the internal boundaries were; Mietkowskie Lake and all three rivers; Bystrzyca, Strzegomka and Czarna (Figure 2-2).

2.6. Numerical model

2.6.1. General concept

Numerical model is the way to illustrate hydrological system for the given environment in nature. The numerical model in groundwater modelling, play a big role, because it enables obtaining the sequential step(s) response of water table. Elevation of the groundwater heads in the aquifers can be contributed by recharges from precipitation. Moreover, Anderson and Woessner (1992) described a numerical method for groundwater modelling and they said that MODFLOW 3D Finite Difference Method is the best in groundwater flow simulation.

2.6.2. Software selection

High advancements in computer hardware and software have been witnessed in the past few decades. Thus, processing software in the field of groundwater modelling has followed the same pace. The modelling software can be addressed in different types of applications depending on the hydrological regime under consideration. MODFLOW is a three dimensional (3D) finite difference groundwater model for flow simulation (McDonald and Harbaugh, 1988). It describes and predicts the performance of groundwater systems. Many new capabilities had been added to the original model. Currently, the integrated hydrological model (IHM) MODFLOW-2005 (Harbaugh, 2005) or MODFLOW-NWT (Niswonger, R.G., Panday, Sorab, and Ibaraki, 2011) are the most important due to the added packages (for example UZF1 and SFR2). The MODFLOW-NWT is a new formulation of MODFLOW-2005. However, its earlier version (MODFLOW-2000) is still in common use (Harbaugh et al., 2000). Generally, MODFLOW simulates both steady state and non-steady model (transient) flow in an irregularly shaped flow system in which aquifer layers can be confined, unconfined, or combination.

The equation is describing groundwater movement in the hydrostratigraphical units and applicable for MODFLOW transient model solution.

$$\frac{\partial}{\partial x}\left(K_x \frac{\partial h}{\partial x}\right)+\frac{\partial}{\partial y}\left(K_y \frac{\partial h}{\partial y}\right)+\frac{\partial}{\partial z}\left(K_z \frac{\partial h}{\partial z}\right)+W=S_s \frac{\partial h}{\partial t} \qquad \text{Eqn. 2-11}$$

where; K_x, K_y, and K_z are the hydraulic conductivities (LT^{-1}); x, y and z are the coordinates axes; h is the potentiometric heads (L); considering the source and sink in the system, W is volumetric flux per unit volume and it can be $W > 0.0$ for outflow or $W < 0.0$ for inflow into the system (T^{-1}); t is the residence time (T) and S_s is the specific storage for confined aquifer (L^{-1}).

Moreover, in this research, MODFLOW-NWT under ModelMuse environment was applied as an integrated hydrological model (Figure 2-4). ModelMuse is a Graphical User Interface (GUI) for the MODFLOW-2005/NWT, ZONEBUDGET, etc and thus, ModelMuse 3.4, 64-bit was chosen following recommendations given by Winston (2005). The IHM MODFLOW-NWT works with different packages to simulates different processes such as; recharge crosses to the water table, leakage from stream/river and lake into aquifers, stream flow, etc.

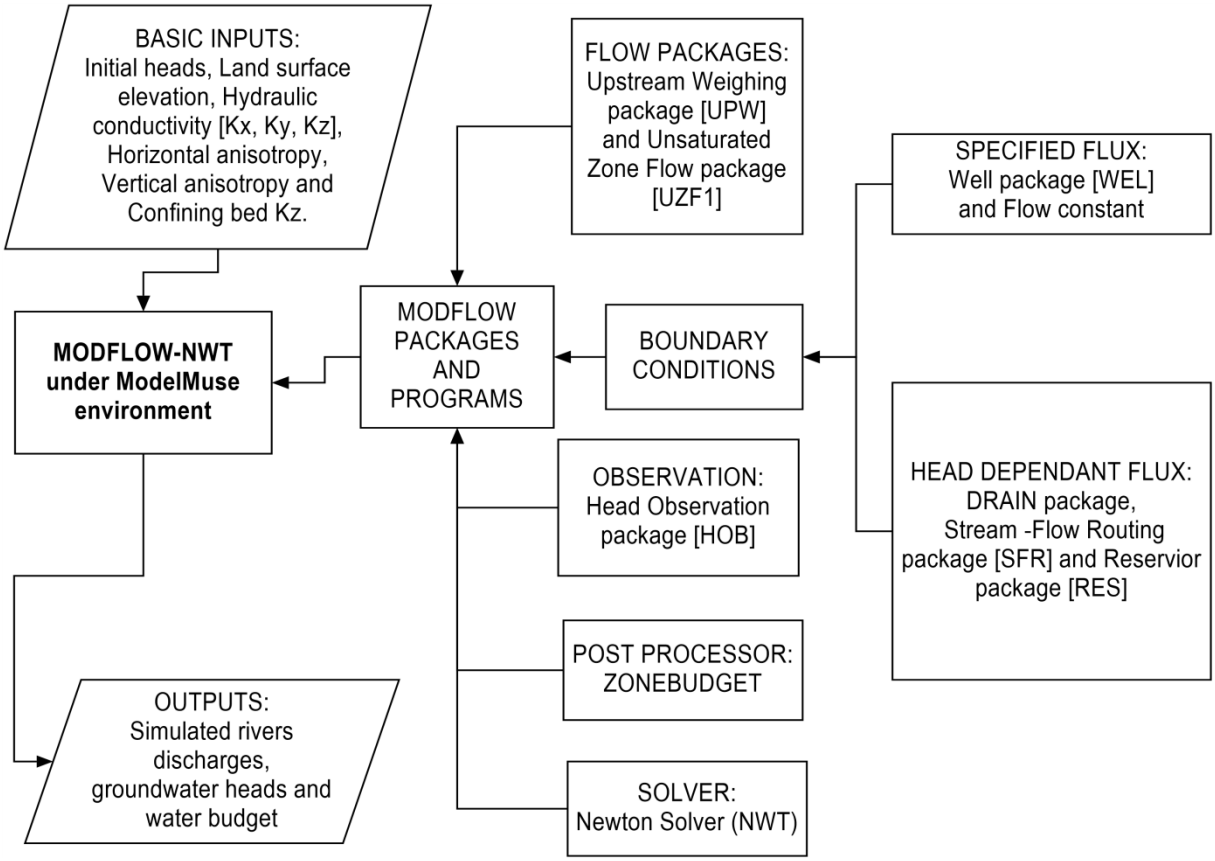

Figure 2-4. MODFLOW-NWT model structure

2.6.3. Grid design

MODFLOW-NWT uses block centred for calculations, thus grid design adhered to the coverage of the study area and complexity of the aquifer systems. The modelled area consists of 71 rows and 76 columns with average grid size of 350 x 450 m as presented in Figure 2-6 and Figure 2-7. The same grid sizes as applied by Gurwin and Lubczynski (2004).

2.6.4. Schematic model setting

The model top was directly imported from Groundwater Modelling System (GMS) model conducted by Gurwin and Lubczynski (2004). ILWIS software was used to interpolate the three (3) layer bottoms adhering to the aquifers and aquitard thickness obtained in Borehole Bank Hydro Data which were gathered from Wroclaw University (Poland). As a result, the interpolated layer bottoms were imported in MODFLOW-NWT model. Therefore, a Quasi-3D model under ModelMuse environment was developed where; layer 1 was unconfined (Quaternary) aquifer, layer 2 was aquitard (confining) and layer 3 was confined (Tertiary) aquifer. In other words, there were two simulated layers and one non simulated layer as described in the conceptual model (Figure 2-3) and being implemented following the schematic model setup (Figure 2-5). All details of the schematic model and the symbols were described in water balance retrieval section (2.6.10.4).

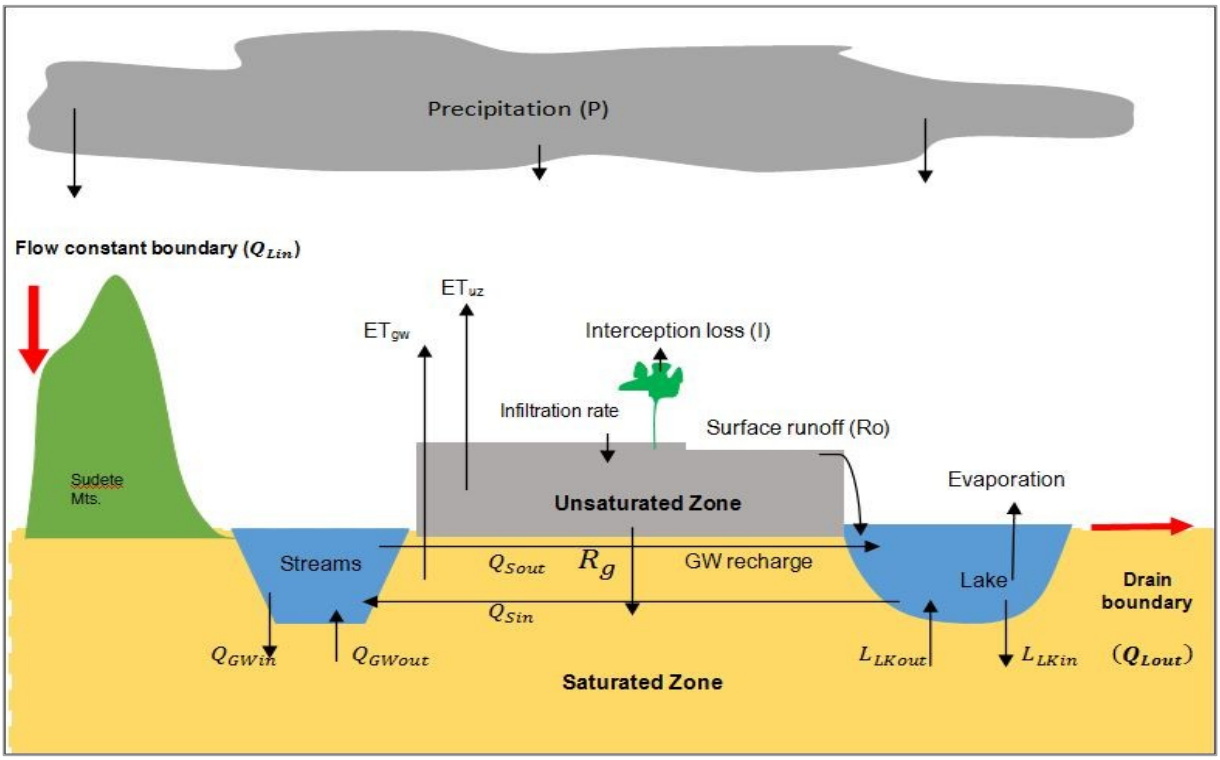

Figure 2-5. Schematic diagram of the model setup in Świdnica study area after Zehairy (2014)

2.6.5. Driving forces

In this study, the assessment of groundwater resources was carried out in the period of 01/10/2000 to 30/09/2003.The driving forces include: precipitation, potential evapotranspiration (PET) and infiltration rate. All the datasets were made complete for the whole simulation period. They were required as inputs for the model. The precipitation was important in MODFLOW-NWT model because it can be converted into recharge under application of UZF1 package. The precipitation dataset was presented in Figure 1-2, where the minimum value was 0 mm d^{-1} and maximum value was 80.5 mm d^{-1}. Also, PET was prepared as an input to the UZF package, where the minimum value was 0 mm d^{-1} and maximum value was 5 mm d^{-1}as presented in Figure 3-3.

The two terms; interception loss and infiltration rate are not separable in a given environment. Interception loss (Ic) is a process at which most of precipitation reaches the ground, but not all of it, because some are stopped by vegetation cover. Normally, precipitation is temporally stored, but immediately evaporation starts from it. In addition, the interception is a function of; 1) the storm character, 2) the characteristics of the prevailing vegetation cover and 3) the season of the year. Wang et al. (2007) determined interception rate at the location of 52^0 20' N, 0^0 42' W in United Kingdom for the different vegetation types, one of them was *Pinus silvestris*. They found that the interception ratio for this vegetation type is 27.3 % of precipitation. Since the vegetation cover were categorized as agriculture farmland and forest, the interception ratio of 27.3 % of precipitation was used for the forest in Świdnica study area (Eqn. 2-8). Also, there was a study conducted by Leuning et al.(1994) to measure soil evaporation and estimating wheat canopy interception. They concluded that interception losses for wheat canopy crops is 33 % of precipitation. As a result, it was used for agriculture farmland which includes wheat crops and grasslands (Eqn. 2-8).

Infiltration rate is the intensity of the process of water which penetrates beneath the earth's surface through faults/joints and plant root zones. It is expressed as flow per unit area of the land surface (Niswonger et al., 2005). Therefore, infiltration rate (P_r) is equal to precipitation (P) minus interception

loss (Ic) (Eqn. 2-12). This can be acceptable when the soil's infiltration capacity is not reached (i.e. the soil layer becomes saturated). In addition, referring to the land use map (Figure 1-5), land use classes with calculated fraction vegetation cover areas (Table 3-1) were used to compute for the infiltration rate in the study area as presented in Figure 3-5.

$$P_r = P - P \times \lfloor (\%F_{area} \times 0.273) + (\%Agr_{area} \times 0.33) \rfloor \quad \text{Eqn. 2-12}$$

where; P- precipitation (mm d^{-1}), P_r - infiltration rate (mm d^{-1}), $\%F_{area}$ -percentage fraction of the forest, 0.273 - constant percentage interception of forest, $\%Agr_{area}$ - percentage fraction of agriculture farmland (wheat and grasslands) and 0.33 - constant percentage interception of agriculture farmland. Therefore, the minimum and maximum interception was 0 and 24 mm d^{-1}, respectively. Also the minimum and maximum infiltration rate was 0 and 56.5 mm d^{-1}, respectively

2.6.6. System parameterization

The Quasi-3D model which was developed requires calibration parameters in order to simulate steady-state or transient model. The core calibration parameters were: horizontal and vertical hydraulic conductivities (HK & VK) for both aquifers and vertical leakance (VKCB) for confining layer. Those parameters were used during the steady-state and transient IHM calibrations. The range of HK for both calibrations in the Quaternary aquifer was from 0.5 m d^{-1} to 180 m d^{-1}, while the VK for both calibrations was ranging from 1 x 10^{-6} to 0.01 x 10^{-3} m d^{-1}. The range of HK for both calibrations in the Tertiary aquifer was from 0.5 m d^{-1} to 100 m d^{-1}, while the VK for both calibrations was ranging from 0.01 x 10^{-3} to 0.5 x 10^{-3} m d^{-1}. The steady-state calibration parameters with their respective zones were transferred to the transient calibration. The transient model requires the addition of other parameters such as specific yield for the unconfined aquifer and specific storage for the confined aquifer (storage parameters). Moreover, it was necessary to add those parameters because during transient calibration, water can be drained to or taken from storage due to variation of hydraulic heads with time in the aquifer systems (Anderson and Woessner, 1992).

2.6.7. Boundary conditions

The boundary conditions in the MODFLOW-NWT were classified into two parts, namely: external and internal boundaries. The external and internal boundaries are the physical boundary features, with well defined hydrological and geological characteristics, that naturally influence the pattern of groundwater flow at a given environment..

2.6.7.1. External boundary conditions

Gurwin and Lubczynski (2004) applied General Head Boundary (GHB) to the natural model in the SW of the model area to estimate lateral groundwater inflows along the Sudety Fault at the SE boundary of the model. Afterward they replaced it with Flow Constant Boundary (FCB) for inflow condition independent on applied stresses on the model. The lateral outflows were observed in the NE of the study area. Hence, the Constant Head Boundary (CHB) was assigned by Gurwin and Lubczynski (2004) while in this study, head dependent boundary.

Flow constant boundary in the SW of the Quaternary and Tertiary aquifers was simulated by using injection wells which were implemented by the use of Well package. The inflows data for the aquifers were considered from groundwater budget retrieved by Gurwin and Lubczynski (2004). Through that study case, the total inflows for the two Quaternary aquifers (Figure 1-15 (a) and (b)) and one Tertiary aquifer (Figure 1-15 (c)) were equal to 50277 m^3 d^{-1} and 16846 m^3 d^{-1}, respectively. Because the two Quaternary aquifers were merged into one, then the total discharge value of 50277 m^3 d^{-1} was divided for 61 cells (Figure 2-6). In Tertiary aquifer, the total discharge value of 16846 m^3 d^{-1} was divided for 42 cells while ignoring clay area which consists of 19 cells (Figure 2-7). The lateral outflows in the NE of both

aquifers, the Drain Boundaries (DB) were assigned using the Drain package in Figure 2-6 and Figure 2-7. No-flow boundaries were used in the North and South of the model for the three layers including the aquitard.

2.6.7.2. Internal boundary conditions

The Well package was used for the wellfield abstractions in the Tertiary aquifer (Figure 2-7). The pumping wells were defined by using objects in ModelMuse. The input parameters were assumed to be constant during a given stress period (s) in steady-state and transient simulation.

The SFR package, for the stream segments was used, where the streams were located in the Quaternary aquifer. The package allowed to assign the flows in the upper streams end and other parameters before simulation. Following the Darcy's equation as presented in equation 2-13 (Prudic et al., 2004), the reservoir package works for the flow between the streams and aquifer.

$$Q_L = \frac{KWL}{m}(h_s - h_a) \quad \text{Eqn. 2-13}$$

where; Q_L - the volumetric flow between a given section of stream and volume of aquifer (m^3d^{-1}), K - the hydraulic conductivity of streambed sediments (md^{-1}), W - representative width of stream (m), L - the length of stream corresponding to a volume of aquifer (m), m - the thickness of the streambed deposits extending from the top to the bottom of the streambed (m), h_s - the head in the stream determined by adding stream depth to the elevation of the streambed (m) and h_a - the head in the aquifer beneath the streambed (m).

Unsaturated Zone Flow package (UZF1) was used with one zone specifically for the first layer (Quaternary aquifer) while excluding the lake cells where the recharge occurs. The main task was to simulate unsaturated zone flow between land surface and groundwater table. The recharge simulated on UZF1 package was depending on water table elevation. The groundwater evapotranspiration and recharges were computed internally in the model, as the precipitation were converted into recharge. (Niswonger et al., 2005).

The Reservoir Boundary package (RES) simulated leakage between a reservoir and an underlying groundwater system. The techniques used to work with this package were described using three equations (Eqn. 2-14, 2-15 and 2-16). The simulation of leakage using Reservoir package was mainly in the demarcated lake area in Figure 2-6, where the model simulated leakage for each cell using Eqn. 2-14 described by Fenske et al.(1996).

$$CRES = \frac{KLW}{M} \quad \text{Eqn. 2-14}$$

Where; $CRES$ - the reservoir-bed conductance (md^{-1}), K - the vertical hydraulic conductivity of the reservoir bed (md^{-1}), L - cell length (m), W - cell width (m) and M - reservoir-bed thickness (m).
Moreover, the land-surface elevation (BRES) was used in the model, because the lake overlay aquifer system. The Reservoir-bed thickness as an input described above was subtracted from the reservoir-bed elevation (land-surface) so as to get reservoir-bed bottom elevation. However, that variable was not used in computing leakage because of two scenarios (Fenske et al., 1996); (1) when the head in the aquifer was above the reservoir-bed bottom.

$$Q_{res} = CRES * (h_{res} - h_{gw}) \quad \text{Eqn. 2-15}$$

(2) when the head in the aquifer was below the reservoir-bed bottom.

$$Q_{res} = CRES * (h_{res} - h_{resbot}) \quad \text{Eqn. 2-16}$$

where; Q_{res} - the leakage from reservoir, h_{res} - the reservoir stage or head (m), h_{gw} - the aquifer head (m) and h_{resbot} - the elevation of the reservoir-bed bottom (m).

In addition, the computation of h_{resbot} was done by subtracting reservoir-bed sediment thickness (M) from the land-surface elevation (BRES) as described by Fenske et al.(1996). Moreover, calibration of steady-state lake stage was updated depending on groundwater heads until the best matching between the observed and simulated stage.

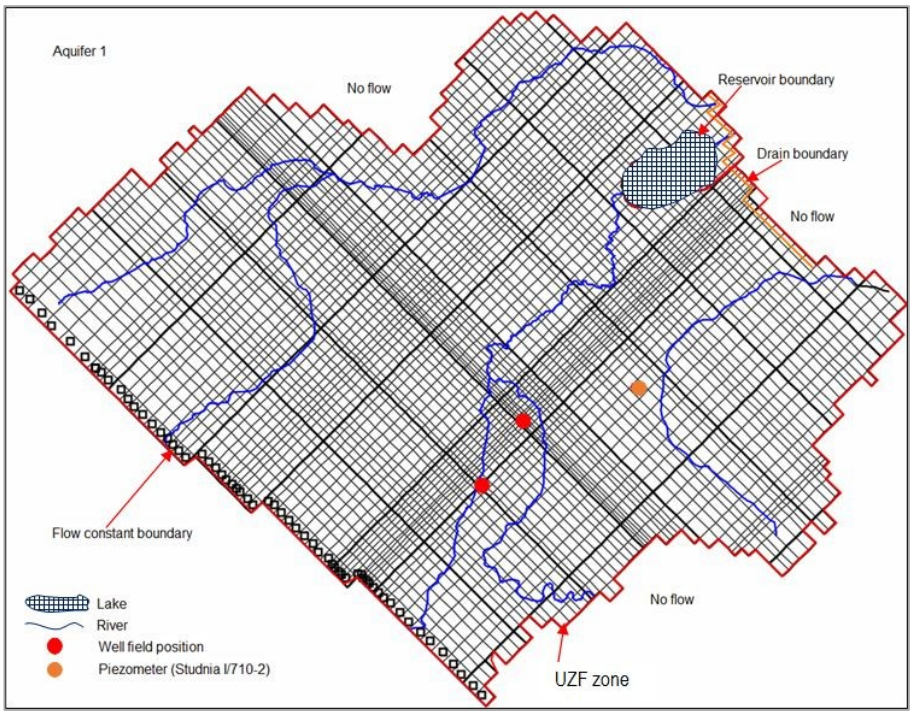

Figure 2-6. Boundary conditions unconfined Quaternary aquifer

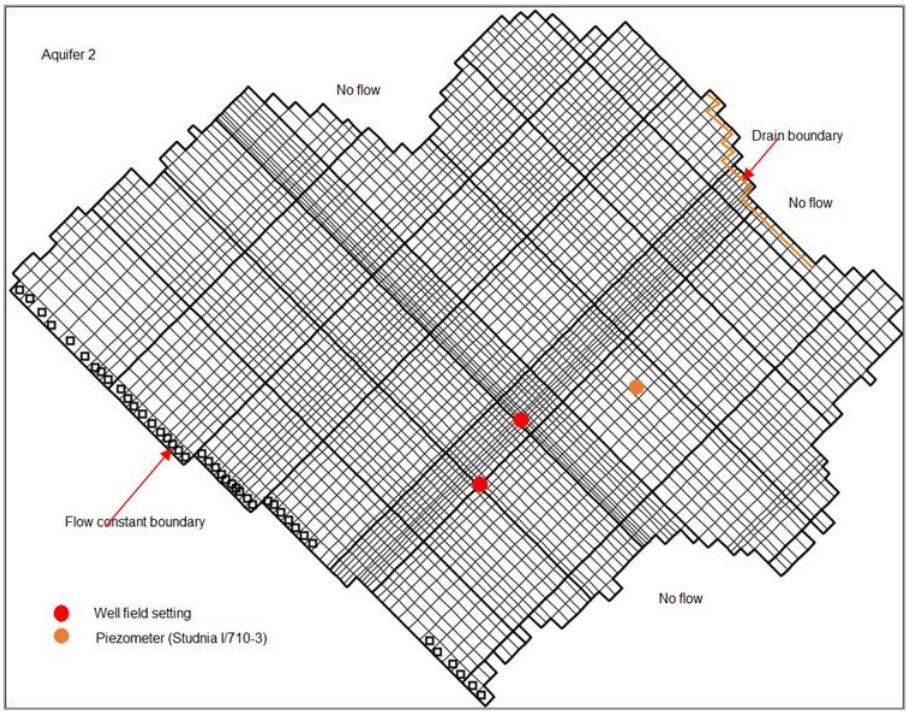

Figure 2-7. Boundary condition for Confined Tertiary aquifer

2.6.8. State variables for model calibration

2.6.8.1. Hydraulic heads

The initial values of hydraulic heads were available and imported from GMS model conducted by Gurwin and Lubczynski (2004). Those heads were used as a good data set of starting heads in steady-state model for the expectation of very fast solution achievement. However, the best heads obtained in steady-state model simulation were the initial condition for transient model calibration simulation. Since groundwater assessment requires groundwater monitoring stations, University of Wroclaw (Poland) enabled to obtain groundwater monitoring datasets from the automatic data acquisition system (ADAS) for the two piezometric points namely: Studnia I/710-2 which is used for monitoring unconfined (Quaternary) aquifer and Studina I/710-3 which is used for monitoring confined (Tertiary) aquifer in the study area (Figure 1-13 and Figure 1-14).

2.6.8.2. River discharges

Gurwin and Lubczynski (2004) on their study case used the baseflow estimated at low river flow discharges in 1999 to 2002. In this research, the total flows obtained from the five river gauges were used to calibrate models. The datasets are presented in Figure 1-6 to Figure 1-10.

2.6.9. Time descretisaton and initial condition

Both steady-state and transient IHM considered data of the three years from 1st October 2000 to 30th September 2003 which was equal to 1096 days as stress periods. Additionally, all internal models calculations were set into meter and day as time step. The initial conditions was determined for the transient model calibration simulation and that was established using the solution of steady-state model calibration.

2.6.10. Numerical model calibration

2.6.10.1. General concept of model calibration

Model calibration is a process which deals with parameter estimation (Anderson and Woessner, 1992). The numerical model calibration was set in two steps: first step was steady-state model calibration to obtain the initial conditions for the transient model. The second step was conducted by trial and error method in transient model calibration while comparing the observed and simulated piezometric heads, lake stages and the monitored Five river gauge discharges in Świdnica area. In this case, MODFLOW-NWT code selected requires the use of Upstream Weighting package (UPW) which uses the NWT-Newton solver (Niswonger, R.G., Panday, Sorab, and Ibaraki, 2011). The solver consists of basic options where the user is required to specify the values or parameters depending on the nature of the model itself. For that matter, head tolerance was set to 0.001 m, flux tolerance was set to 500 $m^3 d^{-1}$, maximum number of outer iterations was set to 1000, model complexity was set to complex and other options remain as by default.

2.6.10.2. Steady-state model calibration

After all boundary conditions were implemented in the model, the calibration of the steady-state model was started. The steady-state model calibration was simulated using average values of hydrological conditions from 1st October 2000 to 30th September 2003. The calibration process was by trial and error method which involved three simultaneous calibrations; two piezomettric heads located in one place (one in Quaternary and other in Tertiary aquifers), lake stage and Five river gauge discharges.

The head observation package (HOB) was applied during peizometric heads calibration, where the input were average head values. The average value of water level fluctuations of the Lake Mietkowskie was used as an input to the Reservoir package (RES), where the other input parameters were; reservoir bed

thickness (M) was set to 0.5 m, reservoir elevation was set to Model Top - 4, reservoir bed vertical hydraulic conductivity (K) was set to 0.003 md^{-1} and specification of the reservoir layer (1). Those parameters were entered into the model as single parameter for the entire lake area. During implementing the package, it was required to assign values to both starting and ending stages of stress period. However, on December 09, 2014 USGS released the new version of ModelMuse 3.4 to make it more efficient when exporting the Reservoir package input file. Therefore, interpolation of reservoir stage was done with respect to starting and ending stage of the time step. In fact, during model calibration the computation of reservoir stage was carried out with respect to Eqn. 2-15 and Eqn. 2-16 in section 2.6.7.2.

Streamflow-Routing package (SFR2) was applied, where the input parameters were; upper and down streams horizontal hydraulic conductivities, flow into the upper stream end, stream elevation, etc. Other different parameters which were assigned in that package, some of them were; stream thickness was set to 0.5 m which was constant to all stream segments, stream width varies from 3 to 4 m and channel roughness was set to 0.035 which was constant to all stream segments. In addition, model simulation using SFR package does not involve directly average values of the input parameters; instead the average values of observed river discharges were used to compare with the simulated values during calibration. The calibration of river gauge discharges involved assigning arbitrary discharge values to the upper streams end. However, SFR package does not possess an observation package like in groundwater heads, instead the calibrated results were retrieved from "SFRg file" which was created in the working folder, it includes all gauge stations but in a separate notepad sheet. The Unsaturated Zone Flow package (UZF1) was used with one zone specifically for the first layer, excluding the lake cells where the recharge occurs. The input parameters were; average values of infiltration rate and potential evapotranspiration (PET), extinction depth was set to 0.5 m as the rooting depth of the dominant vegetation cover in the study area and extinction water content was set to 0.05 m^3. The average values of well field abstraction data were used in Well package.

The steady-state calibration parameters were; horizontal and vertical hydraulic conductivities (HK and VK) for unconfined and confined aquifers and vertical leakance (VKCB) for confining layer. There were 12 and 10 zones, respectively, for HK and VK in the Quaternary (aquifer 1) and 10 VKCB zones in aquitard. Also, there were 16 and 12 zones, respectively, for HK and VK in the Tertiary (aquifer 2). Since there were inactive areas in Tertiary aquifer as shown by Gurwin and Lubczynski (2004) (Figure 1-15(c)), those portions were termed as clay material areas. Therefore, in this research, the entire aquifer 2 was set activate. The calibration process was on by trial and error method until the observed and simulated values (groundwater heads, lake stage and river discharges) were nearly the same.

Error analysis is the way of evaluating the results of the calibration process. The criterion for the steady-state and the transient model calibration was; Root mean square error (RMSE) should be less than 10 % of the change in groundwater heads (maximum minus minimum) within the modelled area (Kelly, B.P., Pickett, L.L., Hansen, C.V., and Ziegler, 2013). Depending on the calibration criterion, the best fit was achieved by matching the observed and simulated values. The results of calibration were reported by listing of measured and simulated heads together with their differences and some type of average of the differences. Three equations used to evaluate the errors between observed (h_o) and simulated heads (h_s) (Anderson and Woessner, 1992) are listed below.

The mean error (ME) is the mean difference between observed (h_o) and simulated head (h_s).

$$ME = \frac{1}{n}\sum_{i=1}^{n}(h_o - h_s)_i \qquad \text{Eqn. 2-17}$$

The mean absolute error (MAE) is the mean of the absolute value of the differences in the observed and simulated head.

$$MAE = \frac{1}{n}\sum_{i=1}^{n}|(h_o - h_s)_i| \qquad \text{Eqn. 2-18}$$

The root mean squared (RMS) error or the standard deviation is the average of the squared differences in the observed and simulated head.

$$RMSE = \left[\frac{1}{n}\sum_{i=1}^{n}(h_o - h_s)_i^{\,2}\right]^{0.5} \quad \text{Eqn. 2-19}$$

2.6.10.3. Transient model calibration

Transient model is a time dependent model, which means that the hydrological conditions vary with time. The initial condition of the transient model was obtained from steady-state model calibration. During steady-state model calibration, the initial condition which includes head distributions was generated from the averaged hydrological conditions. The calibration of transient model was conducted by considering the data for three years from October 01, 2000 to September 30, 2003 which was equal to 1096 days as stress periods. The transient model calibration process by trial and error method involved three simultaneous calibrations following the same parts described in steady-state model simulation above.

The Head observation package (HOB) was applied during peizometric heads calibration, where the input were head values within the stress periods. The Lake Mietkowskie calibration was done in the same way as in the steady-state model without changes of the basic input parameters. During implementing the package in transient model, it was noted that; 'Starting and ending reservoir stage are required input data for each model stress period' (Fenske et al., 1996). Moreover, RES package, simulated leakage between a reservoir and an underneath aquifer system, depending on time variation of lake stage by respecting those three equations described in section 2.6.7.2. The interpolation of reservoir stage was done with respect to starting and ending stage for each time step. In addition, the lake stages were updated at every time step due to the inflows exceeding outflows and vice versa (Fenske et al., 1996).

Streamflow-Routing package (SFR2) was applied in the same way as in steady-state model. However, all stream segments were assigned parameter values in each stress period (1096 days). The Unsaturated Zone Flow package (UZF1) was used in the same way as described in steady-state model. However, the input parameter values were for the full stress periods (1096 days). The two well field abstractions data for the entire stress periods were used in the Well package.

The same calibration parameter zones from steady-state model were transferred to the transient model. In addition, specific yields (Sy) for the unconfined aquifer was comprised of three zones regarding sub-catchments in Figure 2-2 of the study area. Also, specific storage (Ss) for the confined aquifer consists of one zone for the entire area. The calibration process goes on by trial and error method until the observed and simulated values (groundwater heads, lake stages and river gauge discharges) were nearly the same. The error analysis for the transient model calibration process was evaluated using the same criterion as in the steady-state model. The results of calibration were reported by giving an overall ME, MAE and RMSE of the difference between measured and simulated heads. Sensitivity analysis is the way of reporting results as the effects of parameter changes in the model. The final calibrated parameters used to check the sensitivity of the model were; HK, VK, VKCB, Sy and Ss. The parameters were decreased and increased by 10 %. In each parameter change made, the model was run and calculated root mean square errors (RMSE) then compared the sensitivity of the parameters.

2.6.10.4. Water balance using ZONEBUDGET and MODFLOW

The ZONEBUDGET is one of the Post processors available in MODFLOW-NWT under ModelMuse environment. During both steady-state and transient models calibration, it was possible to use ZONEBUDGET and separate the water balance into specific zones. In that case, the specified zones created were; Zone 1 for the Quaternary aquifer, Zone 2 for the Tertiary aquifer and overall water balance (composite zone) as an expected output results. The water balance results obtained in MODFLOW-NWT were the combination of different package applications, namely: UZF package, Well package, Streamflow

package, Reservoir package and Drain package. Since the main task was to justify surface, unsaturated and saturated zone water fluxes in a mm yr^{-1}(Table 3-15), the water balance were calculated using equations described below;

$$P + Q_{Lin} + Q_{Sin} = ET_g + ET_{uz} + I + Exf_{gw} + Q_{Sout} + Q_{Lout} + Q_w + \Delta S \quad \text{Eqn. 2-20}$$

where; P - precipitation Q_{Lin}- lateral inflows from SW of the modelled area Q_{Sin} - stream inflows at the inlet of the modelled area, Q_{Sout} - stream outflows at the outlet of the modelled area, ET - total evapotranspiration, Q_{Lout}- lateral outflows in the SE of the modelled area, Q_w - wellfeild abstraction, and ΔS - total change of storage.

Note: addition equation are found in the appendices.

Water balance on land surface and unsaturated zone were implemented through the application of equations 2-21. The results retrieved from MODFLOW water balance were, unsaturated zone evapotranspiration (ET_{uz}), actual infiltration (P_e), change of storage for unsaturated zone (ΔS) and UZF evapotranspiration.

$$P + Exf_{gw} = R_g + ET_{uz} + I + R_o \pm \Delta S_{uz} \quad \text{Eqn. 2-21}$$

The equation above can be subdivided into two equations below.

$$P + Exf_{gw} = P_e + I + R_o \quad \text{Eqn. 2-22}$$

$$P_e = R_g + ET_{uz} \pm \Delta S_{uz} \quad \text{Eqn. 2-23}$$

where; R_g - gross recharge and ET_{uz} - unsaturated zone evapotranspiration, P_e - actual infiltration and R_o - total surface runoff.

Water balance of the saturated zone was implemented through the application of equations 2-21 to 2-23. The results retrieved from ZONEBUDGET were for the zones and entire model. As a result, it facilitated to obtain groundwater evapotranspiration (GW-ET), UZF recharge (total recharge or gross recharge), surface leakage (S_L), etc. Moreover, those water balance results were used to calculate net recharge in a saturated zone (Eqn. 2-25). In addition, the technique was applied by Hassan et al. (2014), although they called surface leakage as groundwater exfiltration.

$$R_g + Q_{Lin} + Q_{GWin} + L_{LKin} + S_{in} =$$

$$= ET_{gw} + Q_{Lout} + Exf_{gw} + Q_{GWout} + Q_W + L_{LKout} + S_{out} \quad \text{Eqn. 2-24}$$

$$R_n = R_g - Exf_{gw} - ET_{gw} \quad \text{Eqn. 2-25}$$

where; Q_{GWin} - streams leakage to groundwater, Q_{GWout}- groundwater flow to streams, R_n- net recharge, storage change of saturated zone, L_{LKin} - leakage of lake to groundwater, L_{LKout} - leakage of groundwater to lake, R_g- total recharge (gross recharge), Exf_{gw} - groundwater exfiltration or Surface leakage , R_e - effective recharge, Q_W- well abstraction and ET_{gw}- groundwater evapotranspiration.

Furthermore, the net leakage (L_{Net}) was obtained by adding the groundwater inflows to the lake (Lgw_{OUT}) and lake leakage to groundwater(Lgw_{IN}).

$$L_{Net} = Lgw_{IN} + (-Lgw_{OUT}) \quad \text{Eqn. 2-26}$$

3. RESULTS AND DISCUSSION

This chapter describes results and discussion of three parts, namely: (1) data processing, (2) steady-state model calibration and (3) transient model calibration.

3.1. Data processing calculation results

The hydrological calculations were made for the model inputs which includes: precipitation, potential evapotranspiration and infiltration rate. The coefficient of determination (R^2) and correlation coefficient (R) were used during gaps filling in those datasets. R^2 was used to tell how the regression line fits to the data sets which were obtained from the two different sources. The R was used to address the correlation relationship of the data from two different sources and the value of R equal or above 0.5 was considered as the best correlation result.

3.1.1. Potential evapotranspiration (PET)

The coefficient of determination (R^2) for minimum, maximum and mean temperatures from Legnica and ADAS stations were somehow low (Figure 3-1). But the correlation coefficients (R) for the minimum, maximum and mean temperatures were 0.54, 0.55 and 0.57 respectively. From those values it was decided to use the Legnica station data to fill the ADAS station temperature gaps and then calculate ET_o using Hargreaves equation. Also, the coefficient of determination (R^2) for ET_o obtained from FAO and Hargreaves equations were somehow low (Figure 3-2). But correlation coefficient (R) for ET_o was 0.63 and that value was good enough to continue with filling ADAS station ET_o gaps (Figure 3-2).

The average PET for the study period was equal to 1.73 mm d^{-1}. The PET results indicate that the temperature was proportional to PET, which means temperature increases with increase of PET and vice versa (Figure 3-3). Therefore, PET was reasonable to be applied in the model as a driving force.

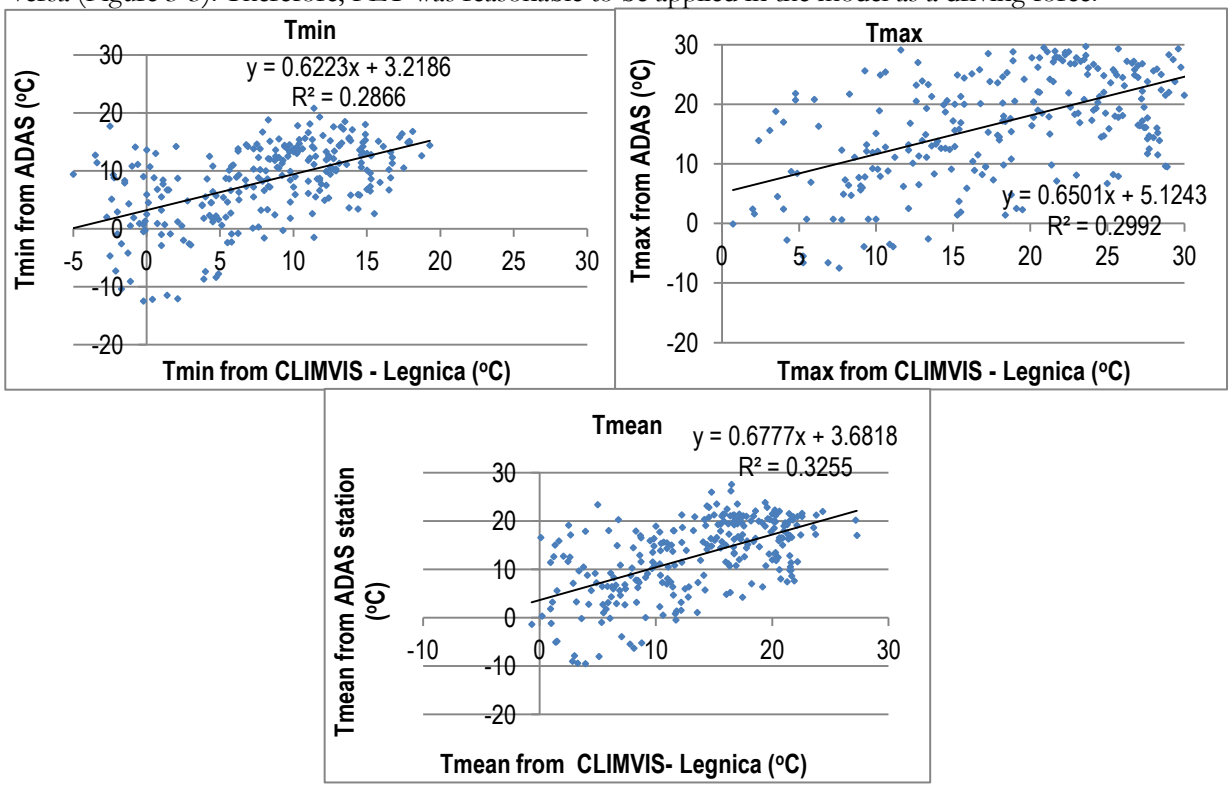

Figure 3-1. Correlation between ADAS and CLIMVIS- Legnica stations (min, max and mean) temps.

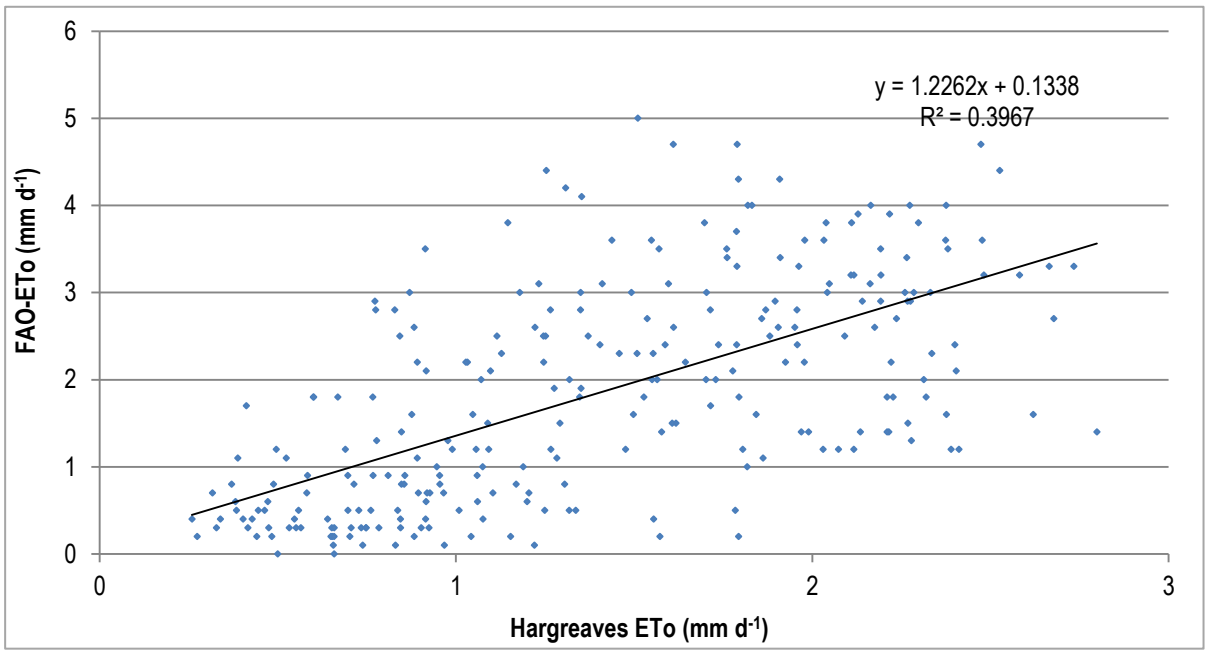

Figure 3-2. Correlation between reference evapotranspiration (ET_o) from FAO and Hargreaves equations

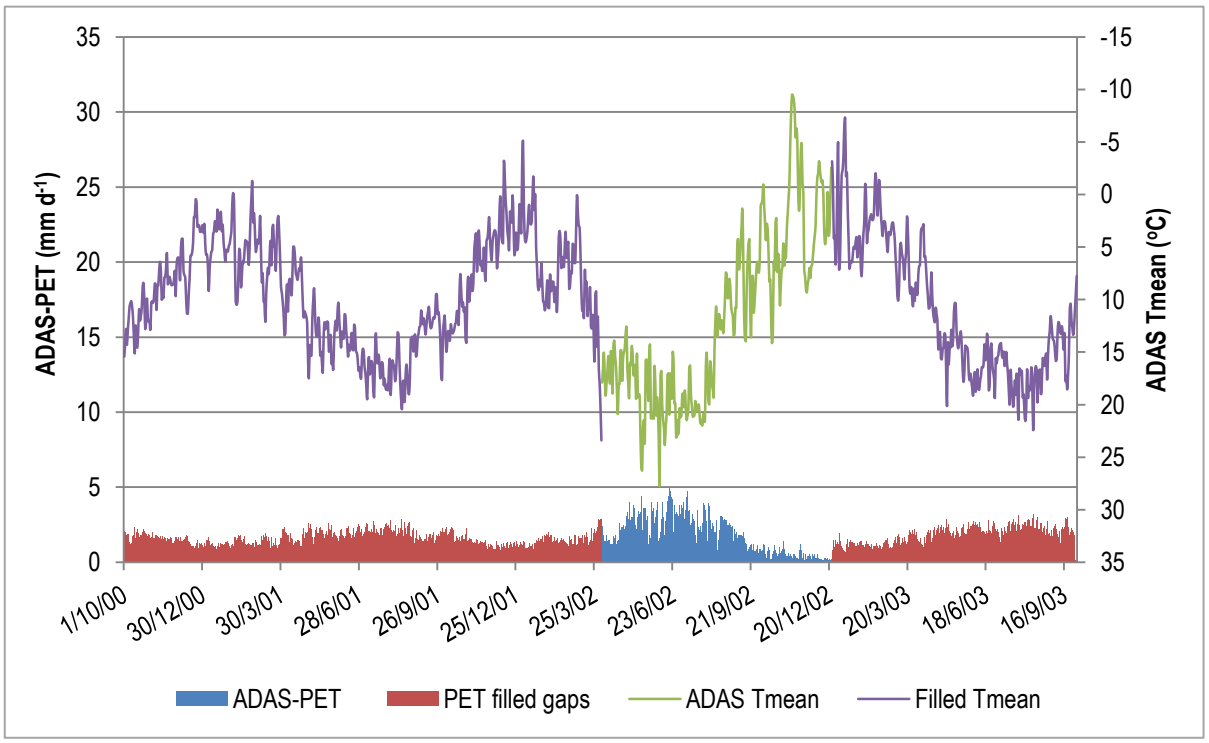

Figure 3-3. Final PET calculated after ET_o gaps filled

3.1.2. Precipitation and infiltration rate

The average precipitation at Pszenno station was about 1.8 mm d^{-1} within the study period. The land use classes were used to calculate fractions of vegetation areas and finally calculate for the infiltration rate (Pr) using Eqn. 2-8, where the summary were presented (Table 3-1) and (Figure 3-4). The average infiltration rate for the vegetation cover categorized (forest and agriculture farmland) was about 1.3 mm d^{-1}. Henceforth, infiltration rates were proportional to precipitation, which means infiltration rate increases

with increases of precipitation and vice versa (Figure 3-5). Therefore, infiltration rate was reasonable to be applied in the model as a driving force.

Table 3-1. Statistical results of fraction of land use classes and vegetation areas in percentages

S/N.	Land use classes	Total area (km²)	Fraction of land use classes in the percentage area (%)	Vegetation cover	Fraction of vegetation cover in the percentage area (%)
1	Town	44.19	7.2	Not applicable	0
2	Forest	41.01	6.7	Applicable	6.7
3	Lake	7.71	1.3	Not applicable	0
4	Agriculture farmland (wheat and grasslands)	521.15	84.9	Applicable	84.9
	Total study area	614.05			

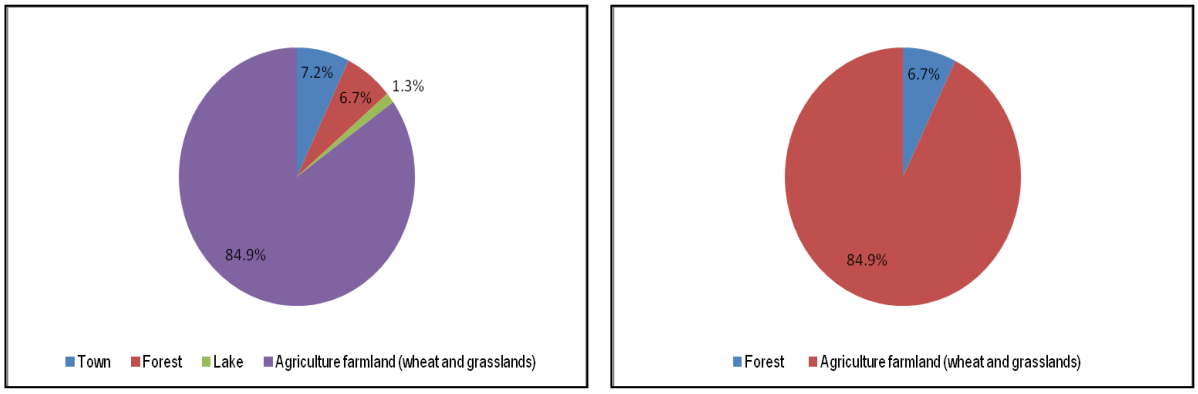

(a) (b)

Figure 3-4. Statistical results of (a) fraction of land use class area in percentage and (b) vegetation area in percentage

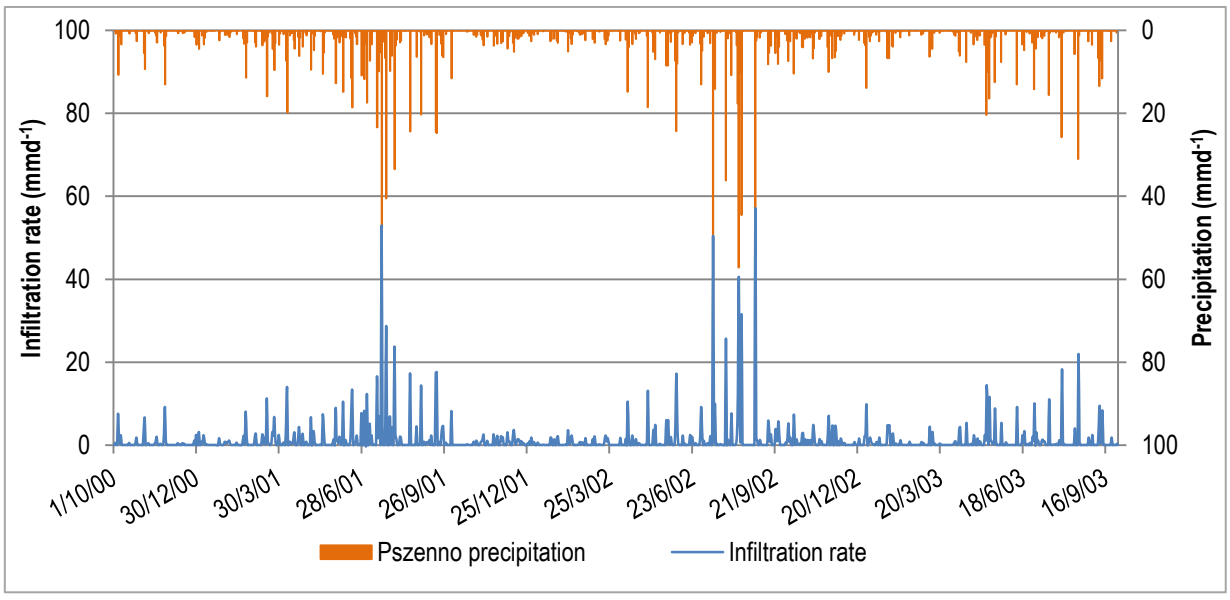

Figure 3-5. The relationships between infiltration rate and prevailing precipitation in Swidnica area

3.2. Steady state model results

This was addressed into seven main parts, namely: 1) calibrated parameters results, 2) head distributions, 3) calibrated piezometric heads, 4) calibrated lake stages, 5) calibrated river discharges), 6) water balance for the aquifers and 7) comparison of this research and the previous study case.

3.2.1. Calibrated parameters results

The final results of calibrated parameters in steady-state model simulation were; HK with a minimum value equal to 0.5 md^{-1} and maximum value equal to 180 m d^{-1} (Figure 3-6 (a)) while the VK were ranging from 5 x 10^{-6} to 0.5 x 10^{-3} m d^{-1} for the Quaternary aquifer. The values of VKCB for confining layer were ranging from 0.1 x 10^{-6} to 0.05 x 10^{-3} m d^{-1} (Figure 3-6 (c)). In the Tertiary aquifer, HK were ranging from minimum value of 0.5 m d^{-1} and maximum value was equal to 100 m d^{-1} (Figure 3-6 (b)) while the VK were ranging from 0.01 x 10^{-3} to 5 x 10^{-3} m d^{-1}.

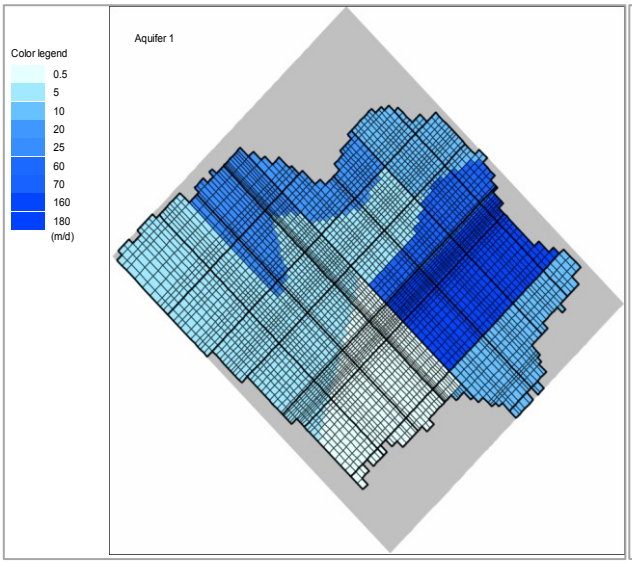

(a) HK for Quaternary aquifer

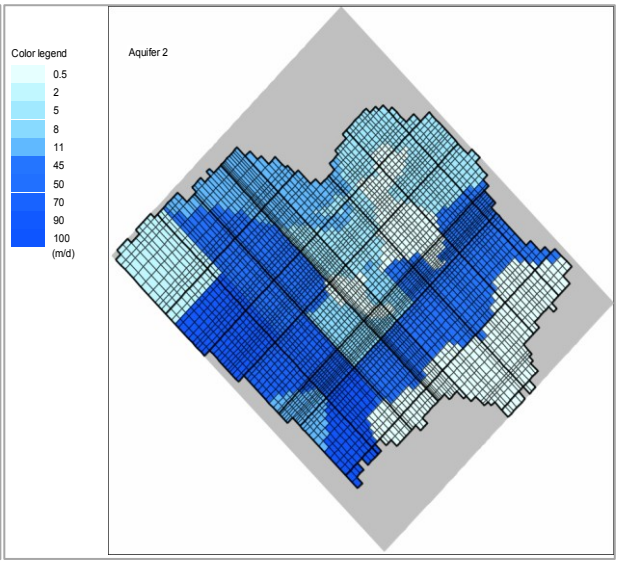

(b) HK for Tertiary aquifer

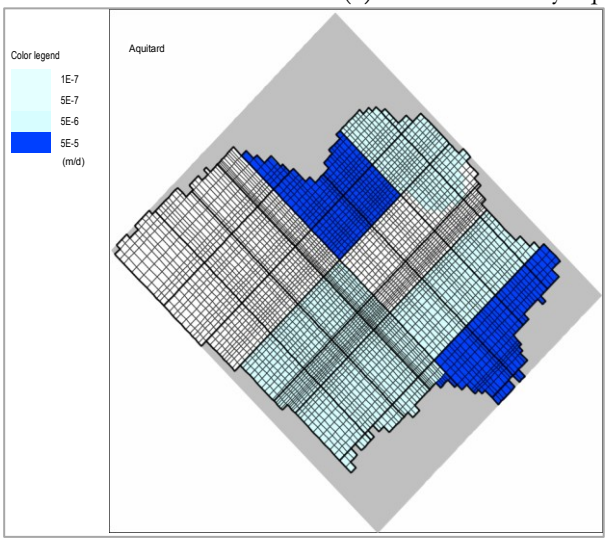

(c) VKCB for aquitard

Figure 3-6. Calibrated parameters results for the steady-state model calibration

3.2.2. Head distributions

The head distributions results were considered for the last simulation day on 30th September 2003 consist of two aquifers namely: Quaternary and Tertiary aquifers (Figure 3-7). The values obtained were more or less the same as compared to steady-state model conducted by Gurwin and Lubczynski (2004) (Figure 1-15). According to the groundwater head results (m. a. m. s. l) indicate that the highest heads values start from southern west (SW) and the lowest heads values in northern east (NE) of the study area (Figure 3-7). As a result, the flow direction is from the SW (inlet side) to NE (outlet side) of the modelled area.

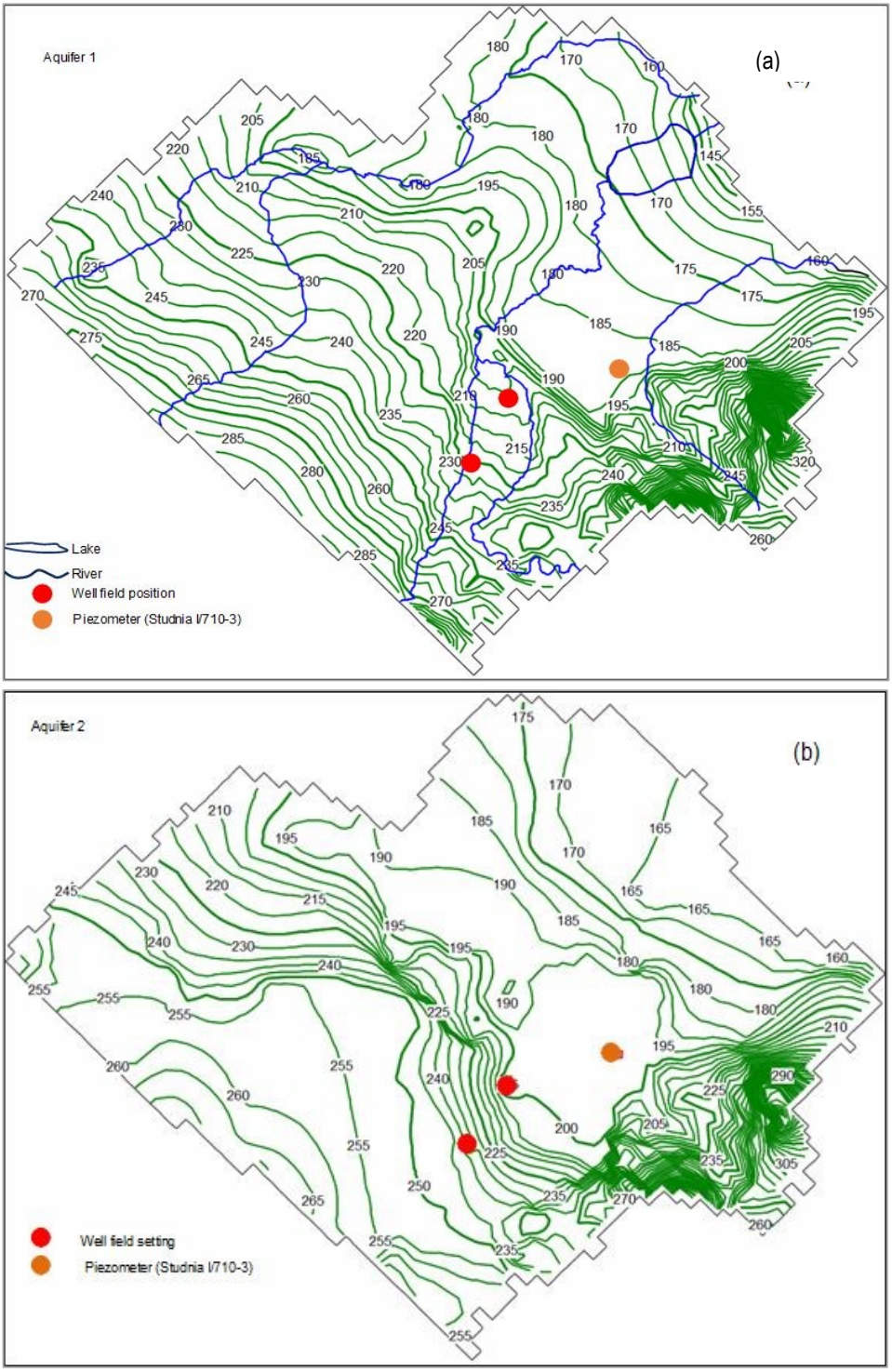

Figure 3-7. Head distributions in meter above mean sea level for (a) Quaternary and (b) Tertiary aquifers

3.2.3. Calibrated piezometric heads

The head observation package which was used during calibration of piezometric heads, retrieved the results of simulated heads from the input averages values of observed heads. The comparison of observed and simulated heads was illustrated using ME, MAE and RMSE (Table 3-2). According to the criterion described in chapter 2 section 2.6.10.2, the results were good.

Table 3-2.Comparison of observed and simulated heads

Piezometer name	Piezometric heads (m)		Errors		
	Observed	Simulated	ME	MAE	RMSE
Studnia I/710_2	186.57	187.40	-0.83	0.83	0.11
Studnia I/710_3	197.29	197.37	-0.08	0.08	0.03
			-0.46	0.46	0.59

3.2.4. Calibrated Lake Mietkowskie water level fluctuations

Reservoir package was used during calibration of Mietkowskie Lake stage, it retrieved simulated value as the result of average water level fluctuations. Therefore, with regards to criterion described in section 2.6.10.2, the result was good (Table 3-3).

Table 3-3. Comparison of observed and simulated lake stage

Lke stage (m)		Errors		
Observed	Simulated	ME	MAE	RMSE
167.93	167.91	-0.02	0.02	0.00
		-0.02	0.02	0.02

3.2.5. Calibrated river discharges

Five river gauge discharges were calibrated in steady-state model using the average values. The results of ME, MAE and RMSE for the comparison of observed and simulated discharges were good despite the consequences of no observation package used during calibration (Table 3-4).

Table 3-4. Comparison of observed and simulated river discharge

Gauge no.	River gauge name	River gauge discharge ($m^3\ d^{-1}$)		Errors		
		Observed	Simulated	ME	MAE	RMSE
1	Pelcznica	87666	87391	276	276	76093
2	Pilawa	166283	165844	439	439	193014
3	Bystrzyca L.	145803	146711	-908	908	824675
4	Bystrzyca K.	473690	474907	-1217	1217	1480558
5	Strzegomka	242369	242806	-436	436	190352
				-369	655	744

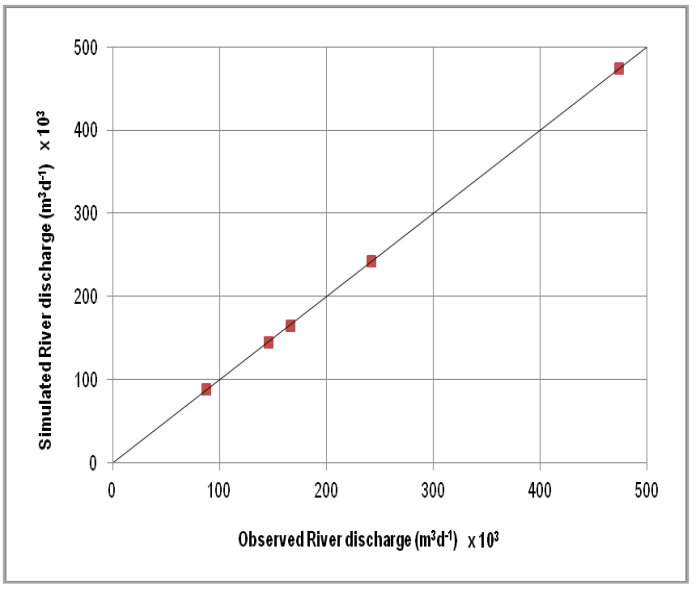

Figure 3-8. Comparison of observed and simulated river discharges

3.2.6. Water balance for the steady-state model calibration

ZONEBUDGET a post processor was used to retrieve water balance for the aquifer systems in the study area. The water balance was subdivided into three parts, namely: Zone 1 for the Quaternary aquifer and Zone 2 for the Tertiary aquifer and the composite zone (entire aquifer systems). The average precipitation (1110337 $m^3\ d^{-1}$) was used as the reference for the water balance components (input and output) in Table 3-5 and Table 3-6 because it cannot be affected in the model like the other input parameters.

The total groundwater input for the Quaternary aquifer was equal to 965580 $m^3\ d^{-1}$, which consists of different components such as: gross groundwater recharge which was 62.7 % of precipitation followed by 17.5 % stream leakage, 4.5 % lateral inflows, 1.8 % reservoir leakage and 0.43 % the exchange between aquifers. The total groundwater output was the same as input, which consists of different components such: GW-ET 32 % of precipitation followed by 20 % lateral outflows, 19.7 % stream leakage, 14.6 % surface leakage, 0.3 % the exchange between aquifers and 0.1 % reservoir leakage as presented in Table 3-5. Moreover, no percentage discrepancy, but the acceptable limit is within ±1% (Harbaugh, 2005).

The total groundwater input for the Tertiary aquifer was equal to 20137 $m^3\ d^{-1}$, which consists of two different water budget components, namely: lateral inflows 1.5 % of precipitation and 0.3 % exchange between aquifers in Table 3-5. In addition, the total output was equal to the total input, thus there were three outflow components: wellfield abstractions 1.3 % of precipitation followed by 0.43 % the exchange between aquifers and last 0.1 % lateral outflows. No percentage discrepancy in the Tertiary aquifer in Table 3-5

In the entire aquifer systems, there were different contribution of water budget components in the input such as: gross groundwater recharge 62 % of precipitation followed by 32 % GW-ET, 17.8 % stream leakage, 6 % lateral inflows and 1.8 % reservoir leakage. The total input was equal to the total output, therefore, the outflow components were; dominated by 19.7 % stream leakage followed by 14.6 % surface leakage, 2 % lateral outflows, 1.3 % well abstractions and 0.1 % reservoir leakage . No discrepancy between the flows into and out of the aquifer systems in Table 3-6.

Table 3-5. Steady-state groundwater budget in the Quaternary and Tertiary aquifers

Groundwater budget component	Quaternary aquifer ($m^3 d^{-1}$)		Tertiary aquifer ($m^3 d^{-1}$)	
	IN	OUT	IN	OUT
Lateral inflows from SW (a and b) to the aquifers and well field abstractions	50277 (a)	0	16846 (b)	14500
Lateral outflows in the NE of the aquifers	0	223530	0	907
Reservoir leakage	19611	1134	0	0
Stream leakage	194890	218510	0	0
Groundwater - ET	0	356860	0	0
UZF recharge	696070	0	0	0
Surface leakage	0	162260	0	0
Exchange between aquifers	4730	3290	3290	4730
Total	965580	965580	20137	20137
IN - OUT		0		0
Percent discrepancy		0		0

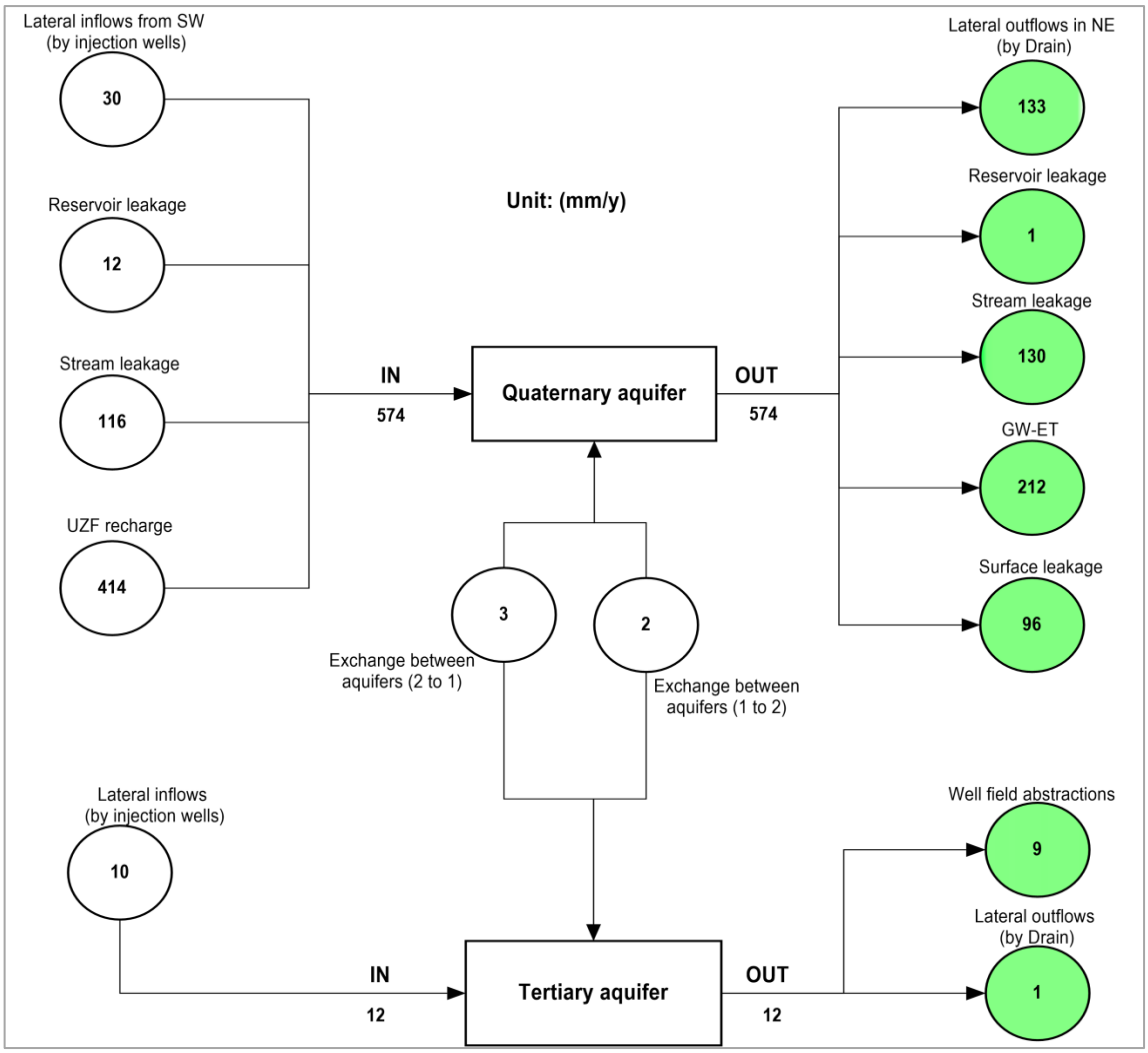

Figure 3-9. Steady-state groundwater budget for the Quaternary and Tertiary aquifers

Table 3-6. Steady-state groundwater budget for the entire aquifer systems

	Aquifer systems	
Groundwater budget component	IN ($m^3 d^{-1}$)	OUT ($m^3 d^{-1}$)
Lateral inflows from SW to the aquifers and well field abstractions	67123	14500
Lateral outflows in the NE of the aquifers	0	22440
Reservoir Leakage	19611	1134
Stream leakage	194890	218510
Groundwater - ET	0	356860
UZF recharge	696070	0
Surface leakage	0	162260
Total	977700	977700
IN - OUT		0
Percent discrepancy		0

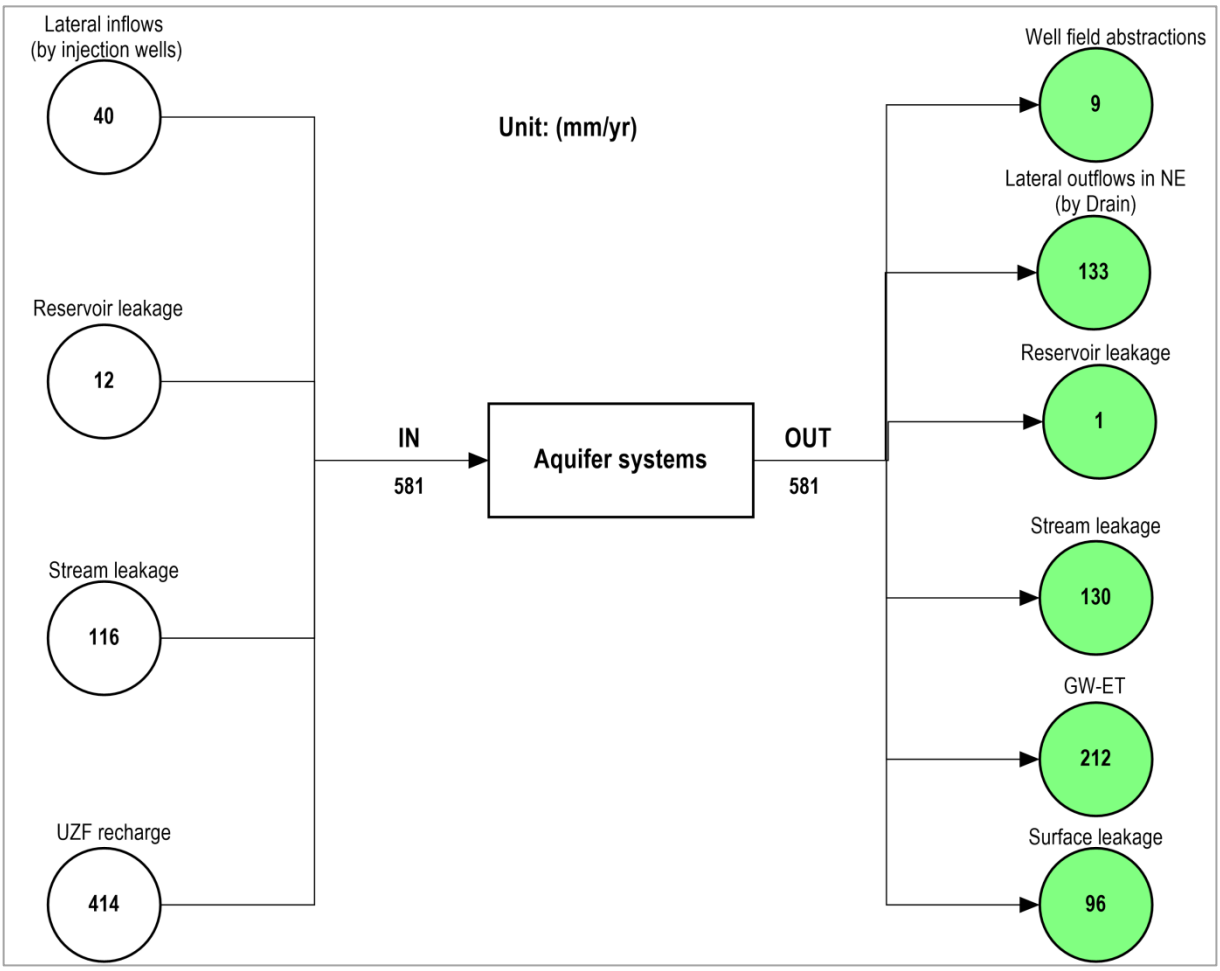

Figure 3-10. Schematic diagram of the steady-state groundwater budget for the entire aquifer systems

3.2.7. Comparison of this research and the previous study model results

The calibration of steady-state model was successfully done using MODFLOW-NWT under ModelMuse environment. The steady-state model results in this research were better and of course very comparable to the study case conducted by Gurwin and Lubczynski (2004). This research and the previous work were compared using the head distributions in Figure 3-7 and Figure 1-15, respectively. The head contour lines in both studies were more or less the same.

Furthermore, the comparison between the two studies provided the following conclusions:
First, the calibrated parameter results: This research have high values of HK in both aquifers, the range was between 0.5 to 180 m d^{-1} in the Quaternary aquifer and 0.5 to 100 m d^{-1} in the Tertiary aquifer. In the previous study HK in both aquifers was ranging between 0.5 to 100 m d^{-1} in the Quaternary aquifer and 5 to 50 m d^{-1} in the Tertiary aquifer. However, the two studies have more or less the same range of VKCB (0.1×10^{-6} to 0.05×10^{-3} m d^{-1}) as presented in Table 3-7.

Second, the calibrated piezometric head errors were good in this research where; in the Quaternary aquifer ME (-0.25), MAE (0.25) and RMSE (0.25) and in the Tertiary aquifer the ME (-0.08), MAE (0.08) and RMSE (0.08). But in the previous study the ME range between (0.18 to 0.42), MAE (1.32 to 1.54) and RMSE (1.6 to 1.79) for the Quaternary aquifer, while in the Tertiary aquifer the ME (-0.09), MAE (1.65) and RMSE (2.09).

Third, the groundwater balance components indicated small difference for the relationships of lake from or to groundwater in both models. In this study the stream leakage to groundwater was less by 10.7 % of the previous study value. Also, this study indicated two time of the stream gaining water from the aquifer as compared to the previous study value. The precipitation recharge to the aquifer indicated large value in this research as compared to the previous study value (Table 3-7). The exchange between the aquifers from Tertiary to Quaternary in this research was higher by 40 % of the previous study value, while in this research the exchange between the aquifers from Quaternary to Tertiary was less by 89.2 % of the previous study value.

Finally, although there were some differences in other components, this could be due to the different software used and the number of simulated layers, where in this research the two Quaternary aquifers (Figure 1-15 (a) and (b)) from Gurwin and Lubczynski (2004) model were merged into one. Additionally, Gurwin and Lubczynski (2004) did not activate the other parts in the Tertiary aquifer (Figure 1-15 (c)), while in this research those areas were activated. Conclusively, both research models were good to address the real relationships of surface and ground water system in the study area. However, this research model could be more detailed to address the links between the surface and ground water fluxes.

Table 3-7. Comparison of this research and the previous study by Gurwin and Lubczynski (2004)

This research model (Steady-state IHM using MODFLOW-NWT)			**Previous study case model** (Steady-state standalone model using GMS)	
Calibrated parameter results (m d^{-1})				
Quaternary aquifer				
HK	0.5 to 180		1st : 0.5 to 30 and 2nd: 1 to 100	
VK	5 x 10^{-6} to 0.5 x 10^{-3}		Not directly applied (Transmissivity)	
Aquitard (s)				
VKCB	0.1 x 10^{-6} to 0.05 x 10^{-3}		1st : 5 x 10^{-6} to 0.5 x 10^{-3} and 2nd: 0.1 x 10^{-6} to 0.04 x 10^{-3}	
Tertiary aquifer				
HK	0.5 to 100		5 to 50	
VK	0.01 x 10^{-3} to 5 x 10^{-3}		Not directly applied (Transmissivity)	
Errors of calibrated piezometric heads (m. a. m. s. l)				
	Quaternary aquifer	Tertiary aquifer	Quaternary aquifer	Tertiary aquifer
ME	-0.25	-0.08	0.42 and 0.18	0.09
MAE	0.25	0.08	1.54 and 1.32	1.65
RMSE	0.25	0.08	1.79 and 1.60	2.09
Groundwater balance components (m^3 d^{-1})				
Aquifer gaining from lake leakage		19611	21971	
Aquifer discharge to lake		1134	1124	
Aquifer gaining from stream leakage		194890	32481	
Aquifer discharge to streams		218510	109681	
Precipitation recharge		696070	56051	
Q. aquifer gaining from Tr.		4730	3357	
T. aquifer gaining from Q.		3290	30417	
Percent discrepancy		0	0	

3.3. Transient model results

The transient model results were expressed by eleven main components, namely: 1) calibrated parameters results, 2) head distributions, 3) UZF recharge and groundwater-ET, 4) calibrated piezometric heads, 5) calibrated lake stages, 6) calibrated river gauge discharges, 7) water balance for the aquifers, 8) spatial variability of surface and groundwater fluxes, 9) temporal variability of surface and groundwater fluxes, 10) quantification of surface and groundwater fluxes and 11) sensitivity analysis.

3.3.1. Calibrated parameters results

The calibrated parameters together with associated zones of steady-state model were used. The final results of calibrated parameters retrieved from the transient model were; HK where the minimum value was equal to 0.5 m d^{-1} and the maximum value was equal to 180 m d^{-1} (Figure 3-11 (a)) while the VK were ranging from 1 x 10^{-6} to 0.01 x 10^{-3} m d^{-1} for the Quaternary aquifer. The VKCB for confining layer were used with the final values ranging from 0.1 x 10^{-6} to 0.05 x 10^{-3} m d^{-1} (Figure 3-11 (e)).
In the Tertiary aquifer, HK were ranging from the minimum value of 0.5 m d^{-1} and the maximum value was equal to 100 m d^{-1} (Figure 3-11 (b)) while the VK were ranging from 0.01 x 10^{-3} to 5 x 10^{-3} m d^{-1} . Additionally, the transient model used specific yield (Sy) for unconfined (Quaternary) aquifer which consists of three zones regarding sub-catchments in the study area, where zone 1 (0.25) was within the Czarna river area, zone 2 (0.2) was within the Bystrzyca river area and zone 3 (0.05) was within the Strzegomka river area (Figure 3-11 (c)). Also, specific storage (Ss) was applied for confined (Tertiary) aquifer which consists of one zone (0.01 x 10^{-3}) for the entire area (Figure 3-11 (d)).

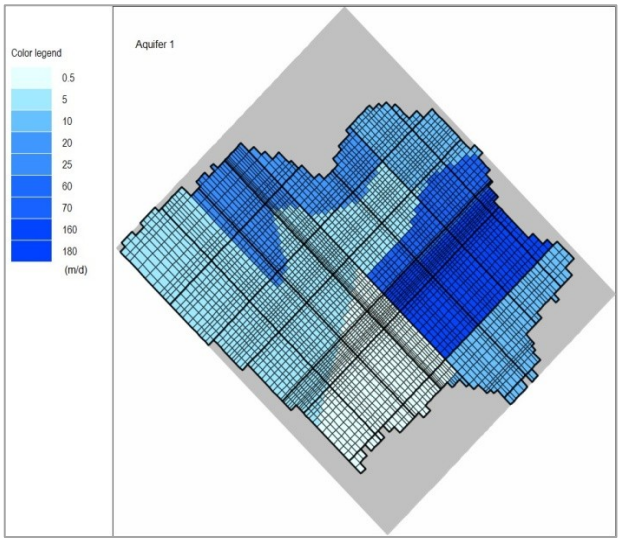

(a) HK for Quaternary aquifer

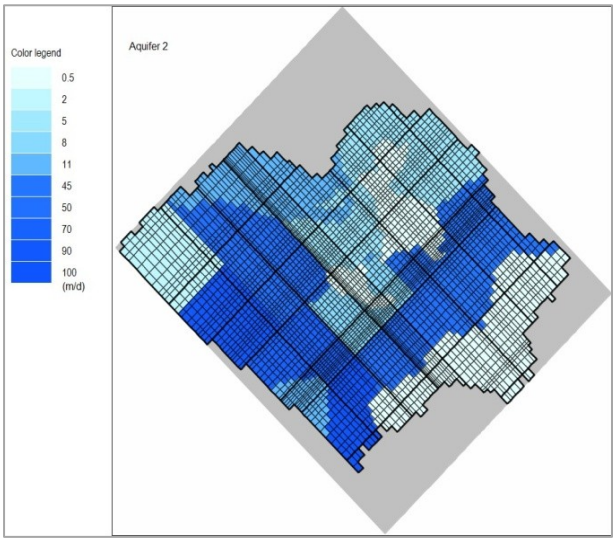

(b) HK for Tertiary aquifer

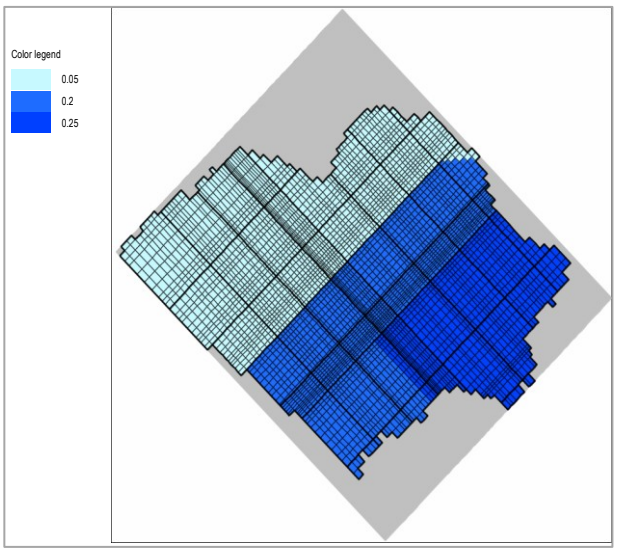

(c) Sy for Quaternary aquifer

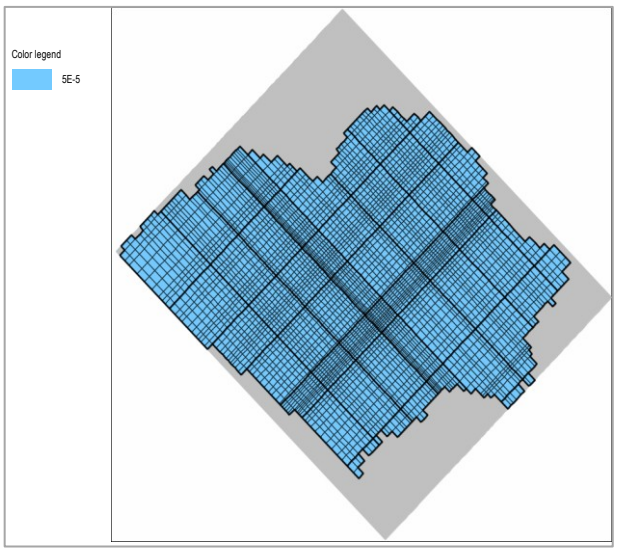

(d) Ss for Tertiary aquifer

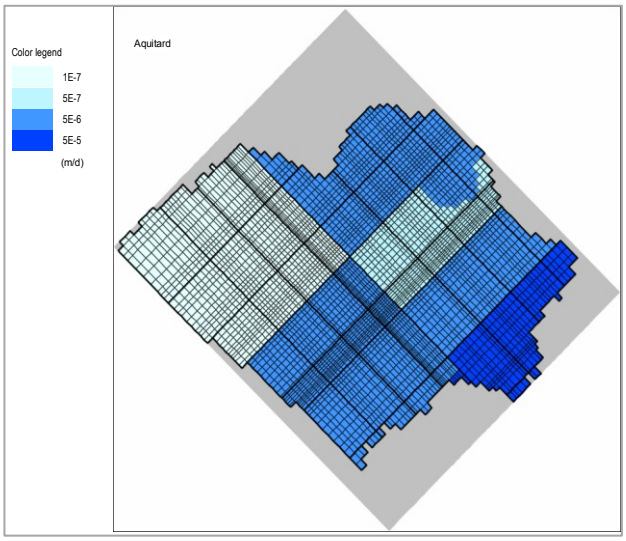

(e) VKCB for aquitard layer

Figure 3-11. Calibrated parameters for the transient model

3.3.2. Head distributions

The head distributions consist of two aquifers, namely: Quaternary and Tertiary (Figure 3-12 (a) and (b)), respectively. The head contour lines displayed for both aquifers were considered for the last simulation period on 30th September 2003,. The values obtained were better as compared to the steady-state model calibration. The reason could be due to the fact that the steady-state model was used as the initial condition for the transient model calibration. The groundwater head results indicated that the highest head values start from the SW and the lowest head values in the NE of the study area (Figure 3-12 (a) and (b)). As a result, the flow directions are from SW to NE of the modelled area and this was also addressed in the study case conducted by Gurwin and Lubczynski (2004) in Figure 1-15.

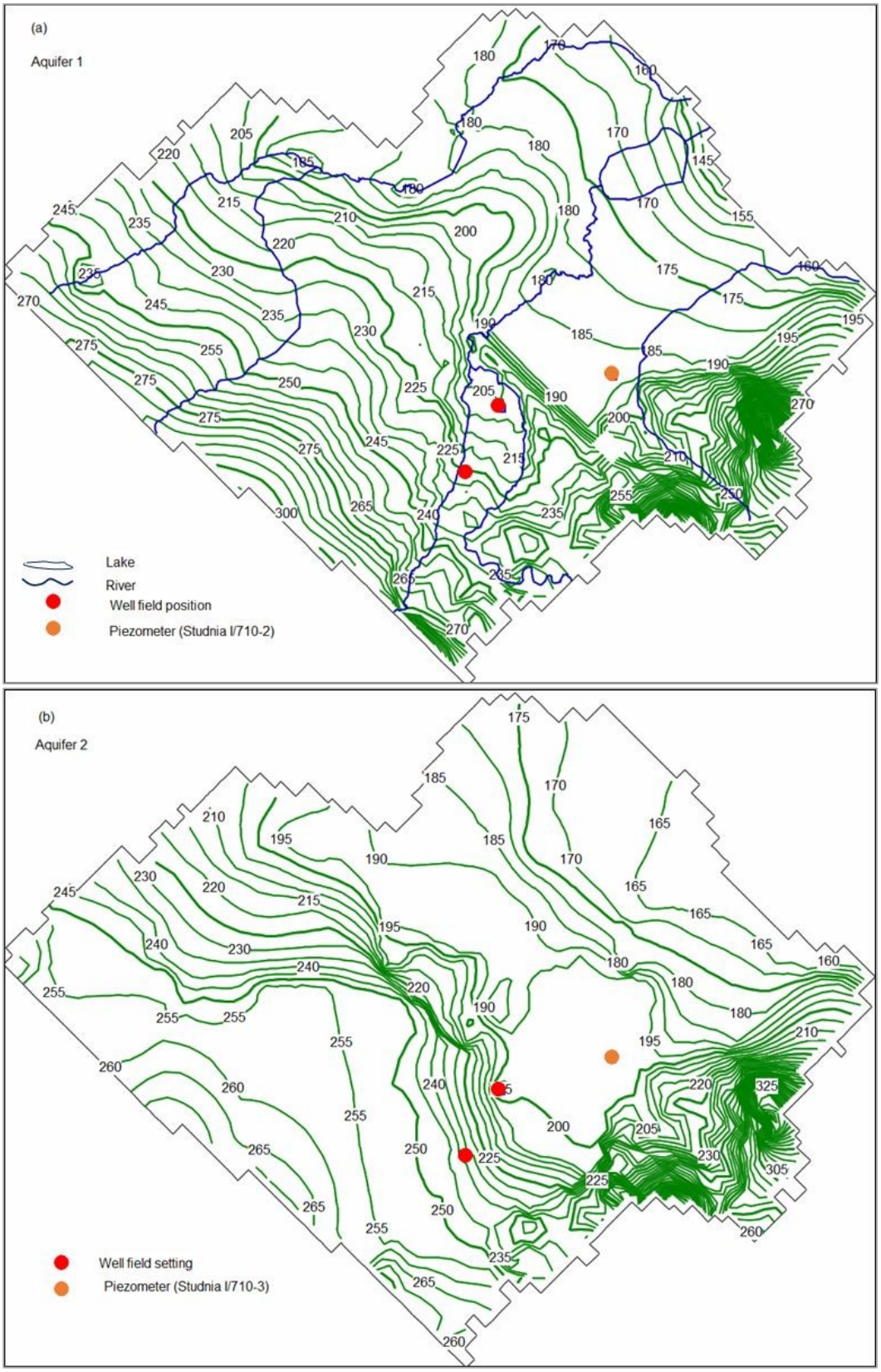

Figure 3-12. Head distributions in meter above mean sea level for the (a) Quaternary and (b) Tertiary aquifers taken at the last simulation period on 30th Sept, 2003

3.3.3. Calibrated piezometric heads

The calibration of piezometric heads was done in the transient mode from 1st October 2000 to 30th September 2003. The result of ME, MAE and RMSE for the comparison of observed and simulated piezometric heads, namely: Studnia I/710-2 and 701-3 (Table 3-8) was good to meet the criterion described in Chapter 2 section 2.6.10.2, where the results were presented in Figure 3-13. The time series for the comparison of observed and simulated heads from the two piezometric heads were illustrated in Figure 3-14 and Figure 3-15. The results were good for both two piezometers, however they are not enough to describe the entire Quaternary and Tertiary aquifers. Additionally, precipitation was playing a role on piezometric heads, although there was a delay because of low velocity of groundwater movement in the aquifers.

Table 3-8. Calibrated piezometric head errors

Piezometer name	Piezometric head errors (m)		
	ME	MAE	RMSE
Studnia I/710-2 and 710-3	-0.08	0.15	0.18

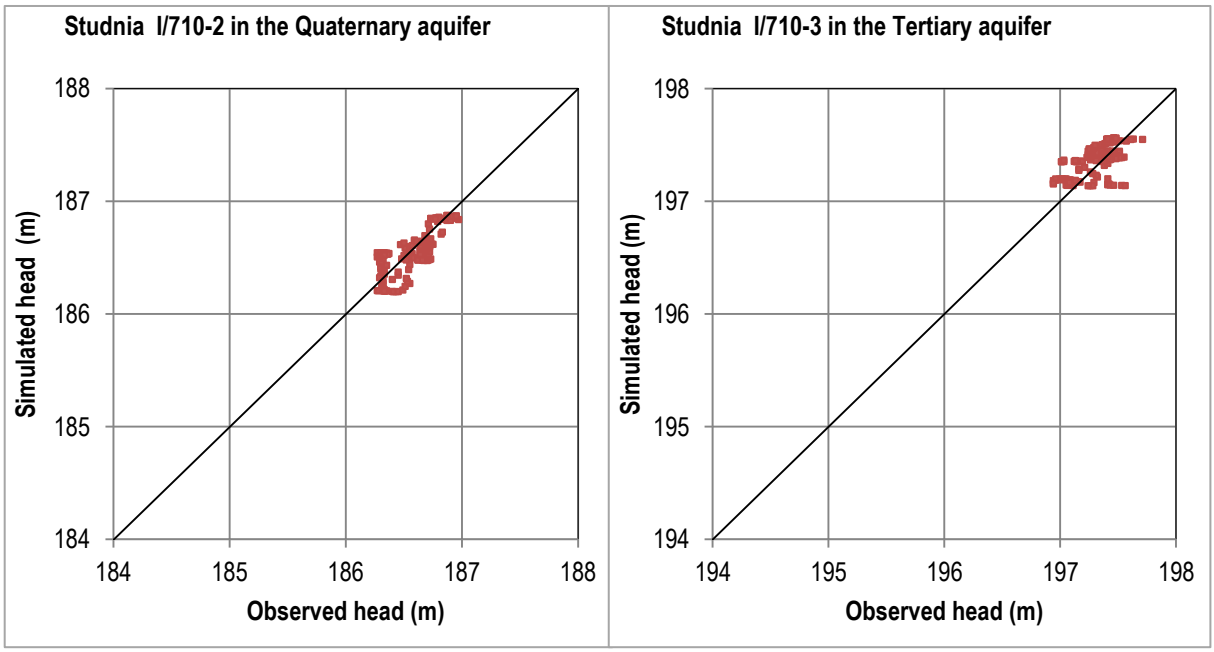

Figure 3-13. Observed against simulated head for the two piezometers

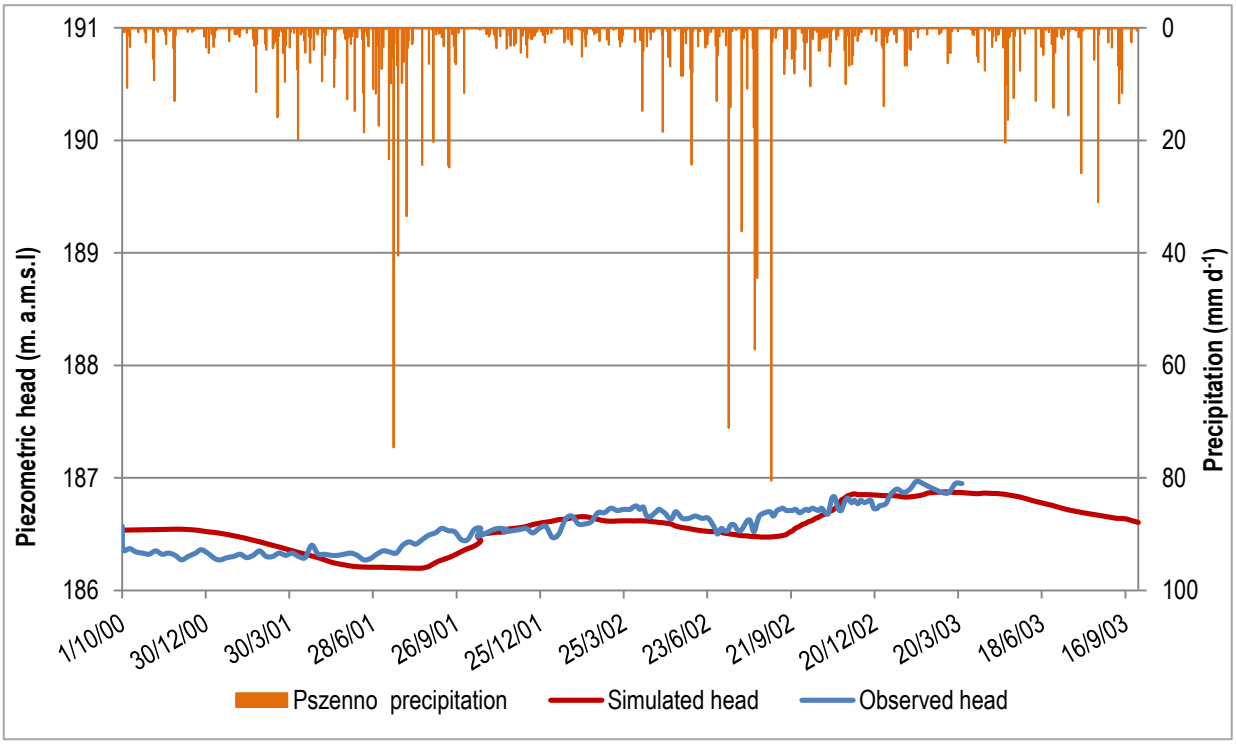

Figure 3-14. Time series for the comparison of observed and simulated heads for Studnia I/710-2 in Quaternary aquifer

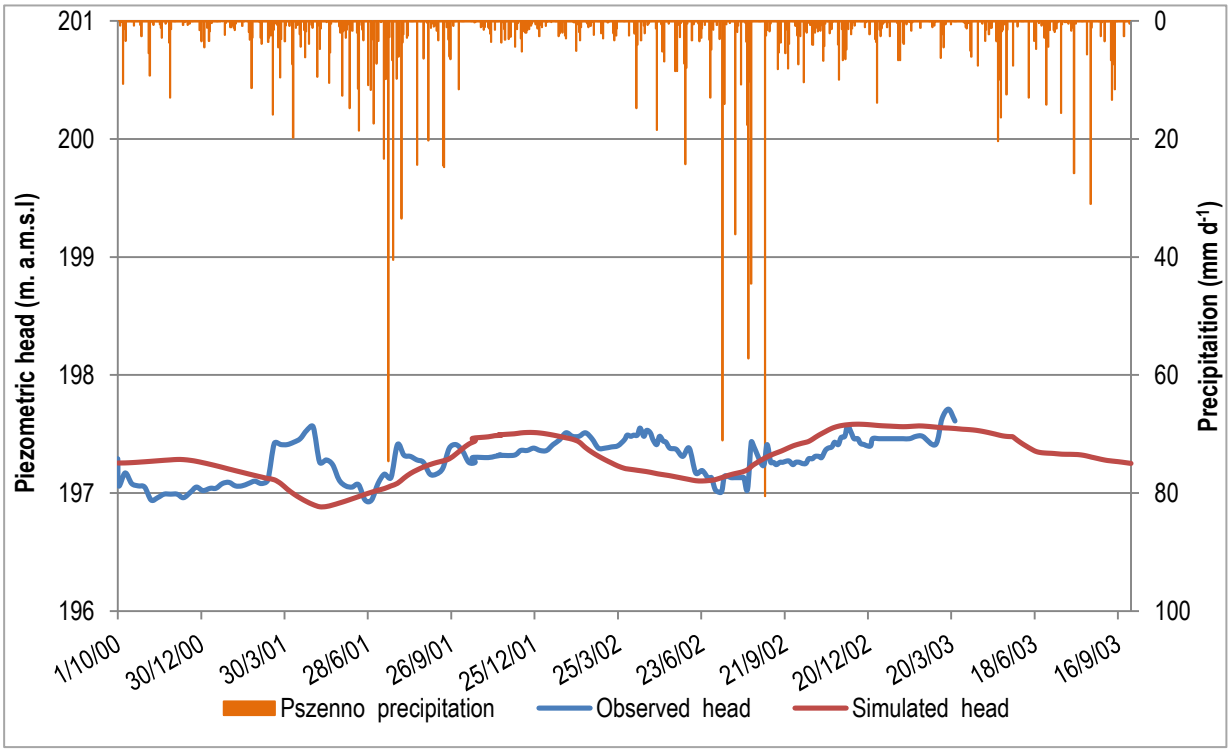

Figure 3-15. Time series for the comparison of observed and simulated heads for Studnia I/710-3 in the Tertiary aquifer

3.3.4. Calibrated lake stages

The lake was simulated by using Reservoir package and calibrated successively with the retrieval of simulated lake stages which were compared with observed (Table 3-9) and (Figure 3-16). The results were good hence the time series for the comparison of observed and simulated lake stages illustrated in Figure 3-17. Additionally, there were good matching between the observed and simulated lake stages, although in the most stress periods the simulated stages were lower than the observed stages. Moreover, precipitation was playing a role on lake stages because of the high velocity of the surface runoff to the Lake Mietkowskie.

Table 3-9. Calibrated lake stage errors

Lake stage errors		
ME	MAE	RMSE
0.13	0.23	0.31

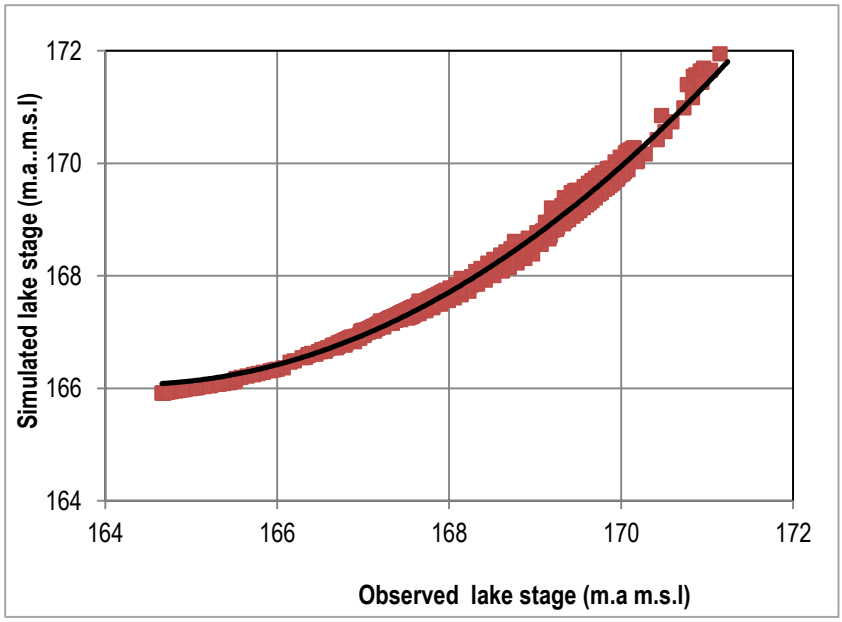

Figure 3-16. The comparison of observed and simulated lake stages

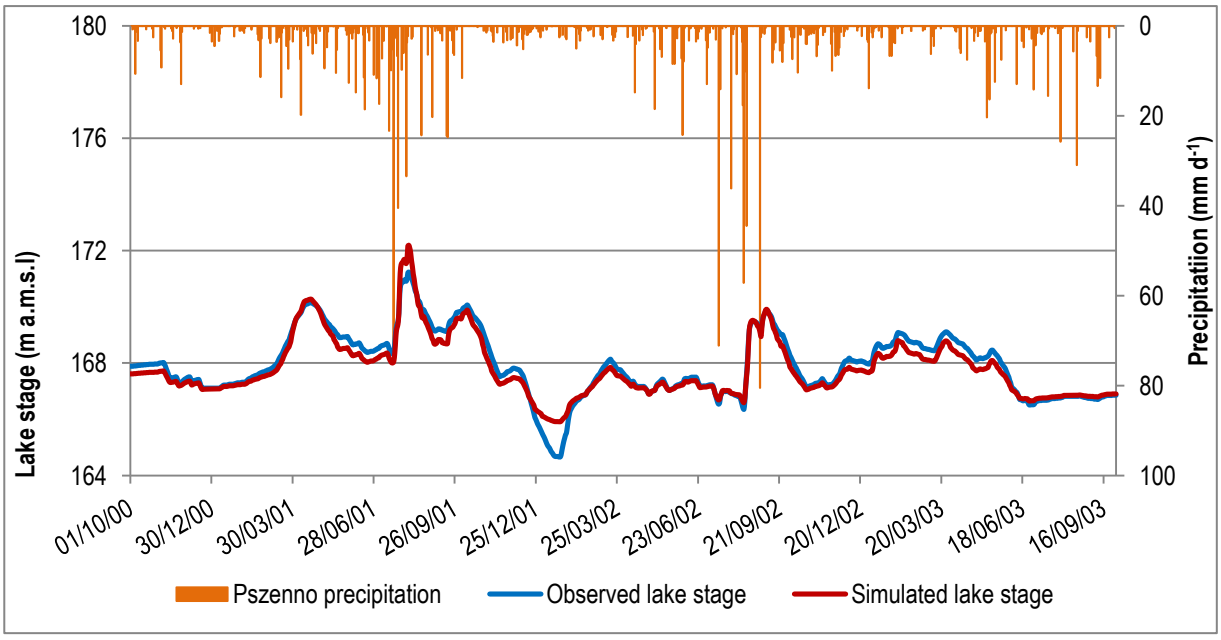

Figure 3-17. Time series for the comparison of observed and simulated lake stages

Moreover, the transient model calibration simulation retrieved groundwater inflows to the lake and lake water flow to groundwater table. The relationship of lake leakages to and from groundwater table was described using a Reservoir component from water balance results. The net leakage was obtained by adding the groundwater inflows to the lake and lake leakage to groundwater in equation 2-26. The trend of net recharge and lake leakage to groundwater were the same (Figure 3-18). In addition, when groundwater inflows to the lake was higher the lake leakage to groundwater and the net leakage was higher and vice versa (Figure 3-18).

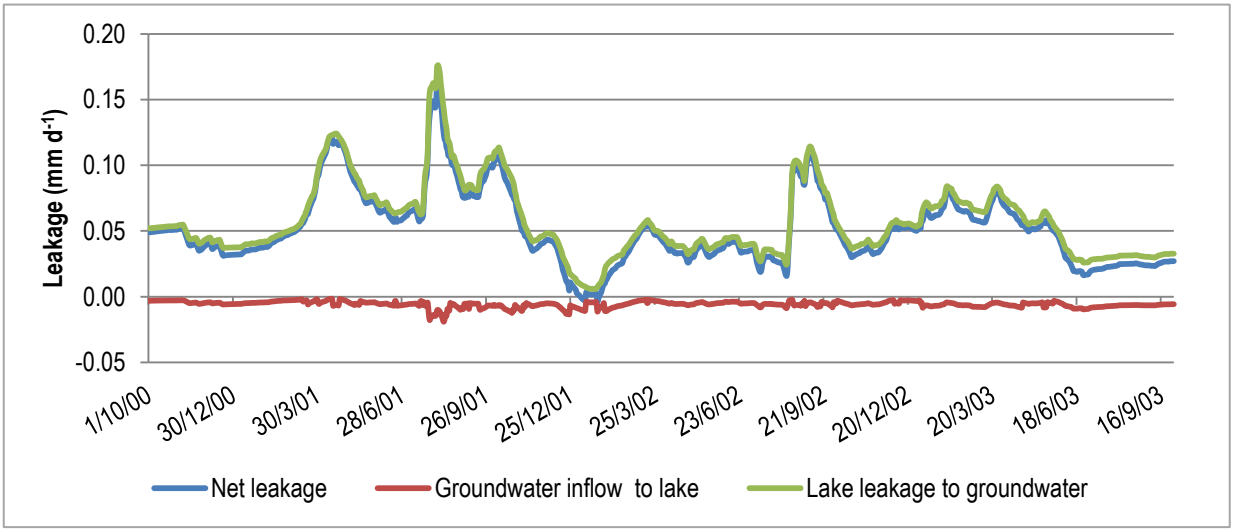

Figure 3-18. Comparison of the reservoir leakages and net leakage from groundwater balance results

3.3.5. Calibrated river gauge discharges

The Five river gauge discharges were calibrated in transient model by considering the variations of discharges with time. The results of ME, MAE and RMSE for the comparison of observed and simulated discharges were good despite the consequences of no observation package used during calibration (Table 3-10). In addition, the discrepancy in each river gauge discharge for the comparison of observed and simulated discharges were presented in Figure 3-19, Figure 3-21, Figure 3-23, Figure 3-25 and Figure 3-27. Additionally, the results were good hence the trend of time series for the comparison of observed and simulated in each river gauge discharges were presented in Figure 3-20, Figure 3-22, Figure 3-24, Figure 3-26 and Figure 3-28. In general, precipitation was playing a role of all river flows discharges because of high velocity for the surface runoff to the rivers.

Table 3-10. Comparison of observed and simulated river gauge discharges

S/No	River gauge	River gauge discharges errors (m^3 d^{-1})		
		ME	MAE	RMSE
1	Pelcznica	-413	3754	5612
2	Pilawa	9622	9632	14500
3	Bystrzyca L.	-4992	5866	9198
4	Bystrzyca K.	762	6304	10042
5	Strzegomka	9119	30268	49246
		2820	11165	17719

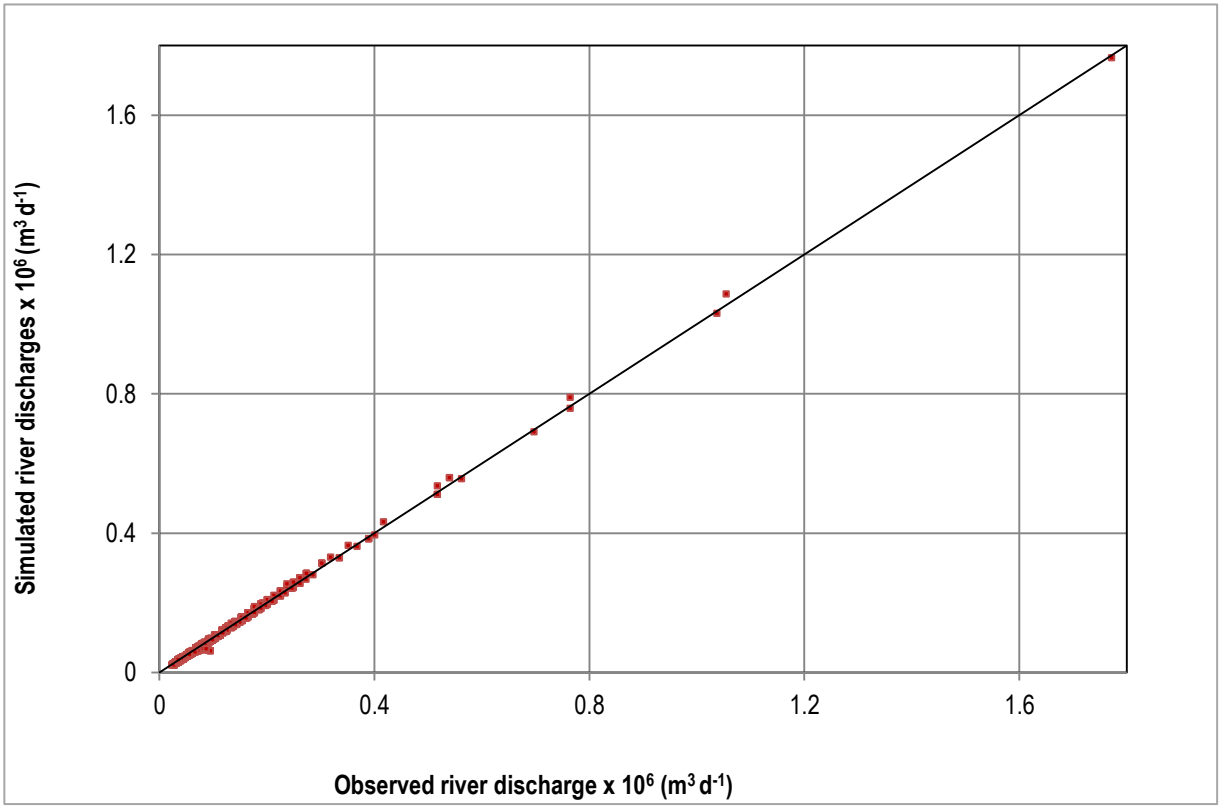

Figure 3-19. The discrepancy for the comparison of observed and simulated river gauge discharges - Pelczarna

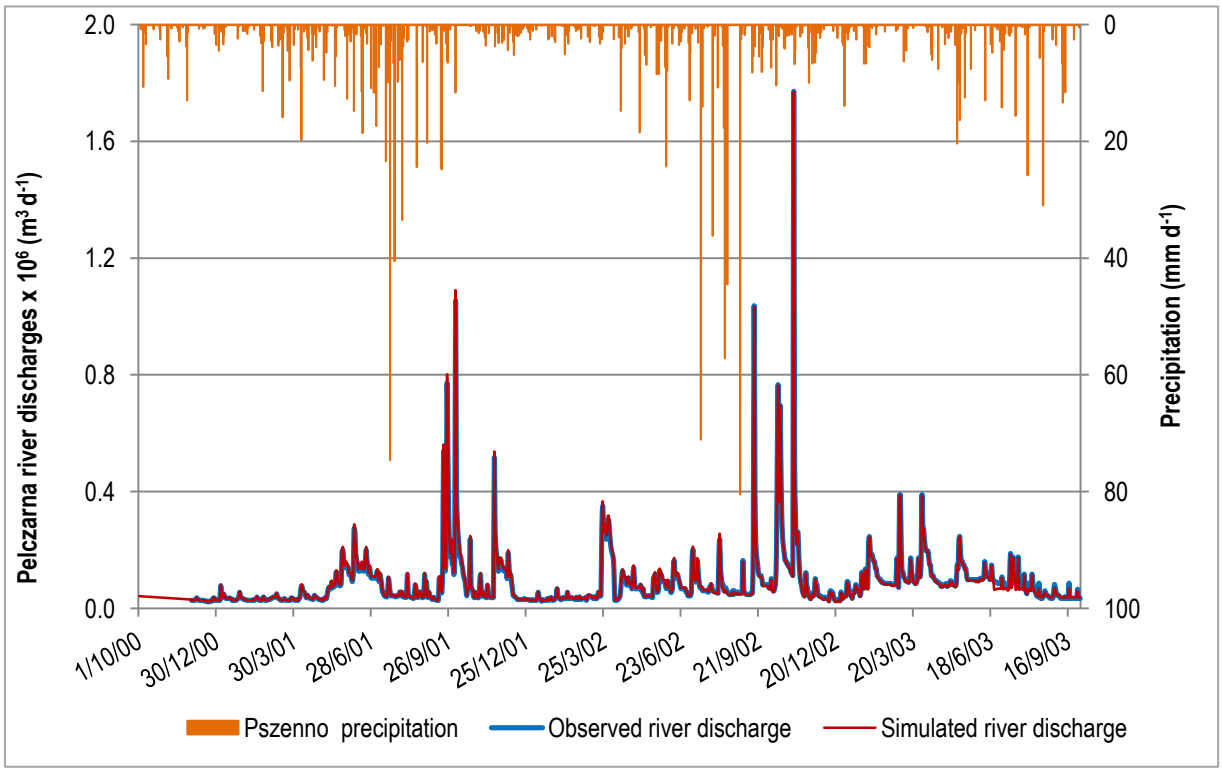

Figure 3-20. Time series for the comparison of observed and simulated river gauge discharges - Pelczarna

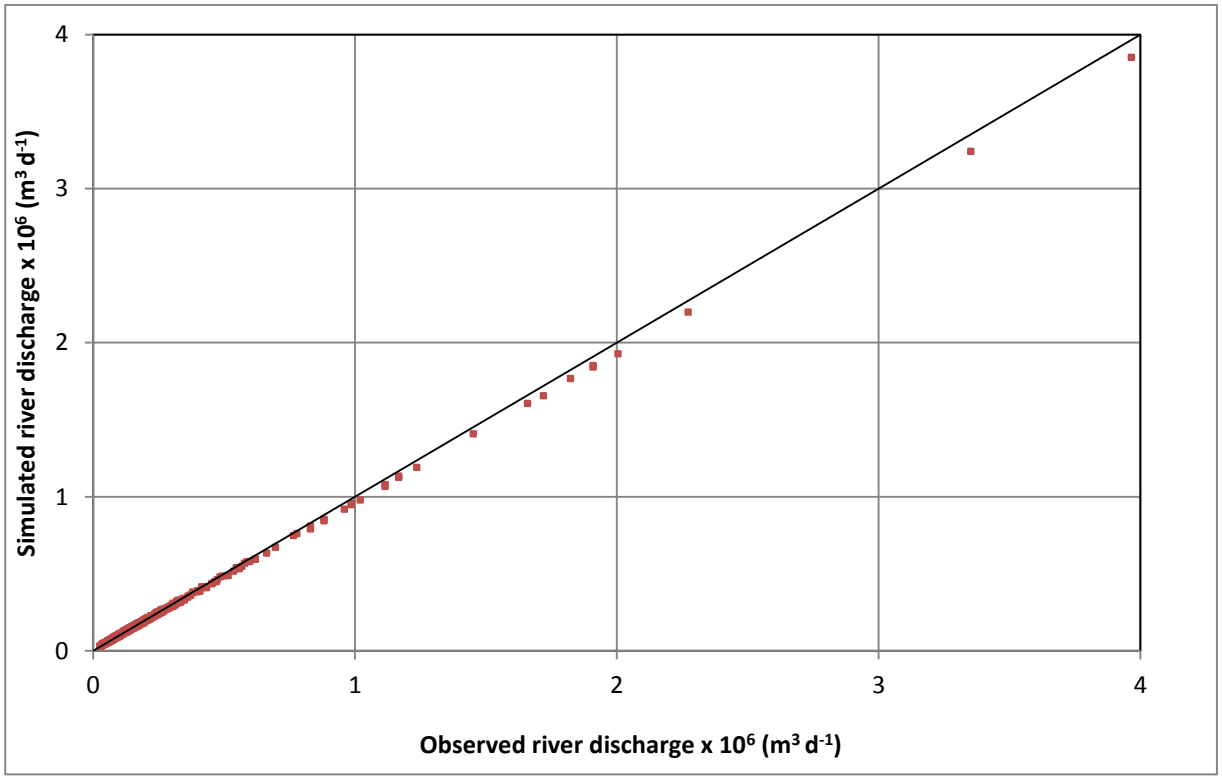

Figure 3-21. The discrepancy for the comparison of observed and simulated river gauge discharges - Pilawa

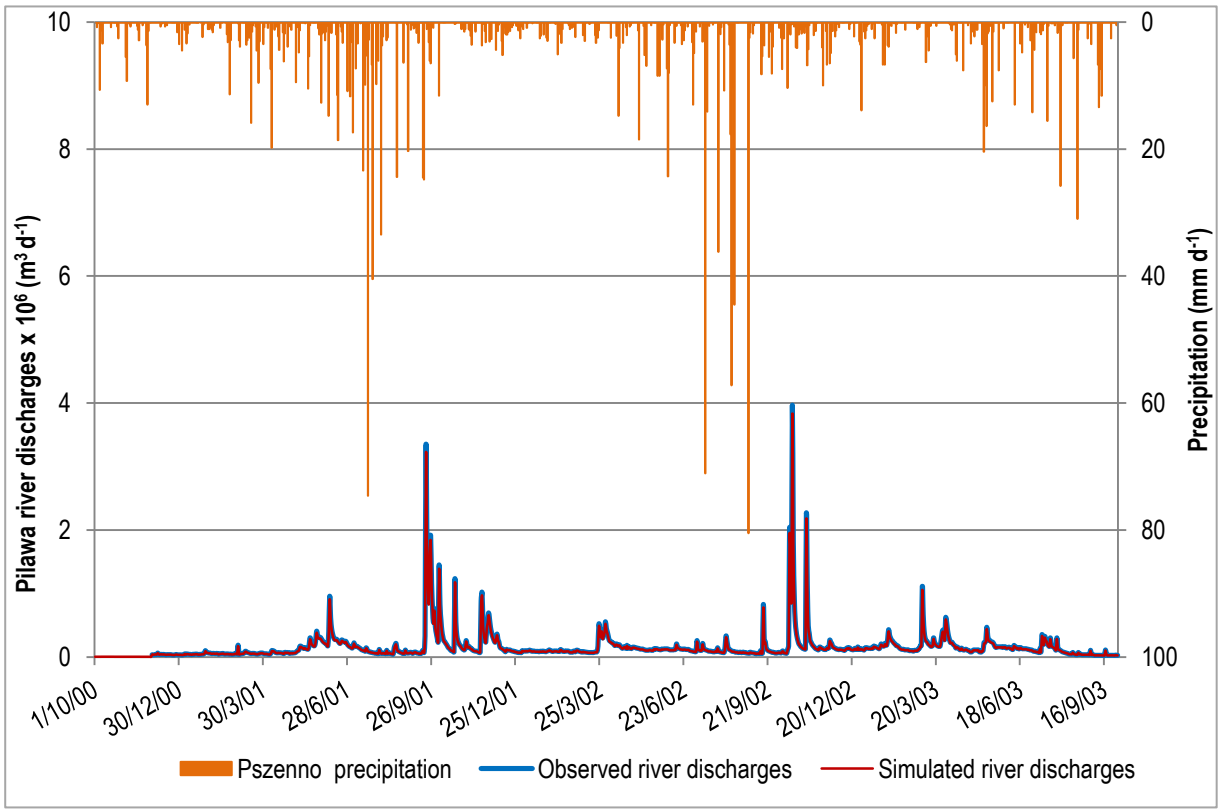

Figure 3-22. Time series for the comparison of observed and simulated river gauge discharges - Pilawa

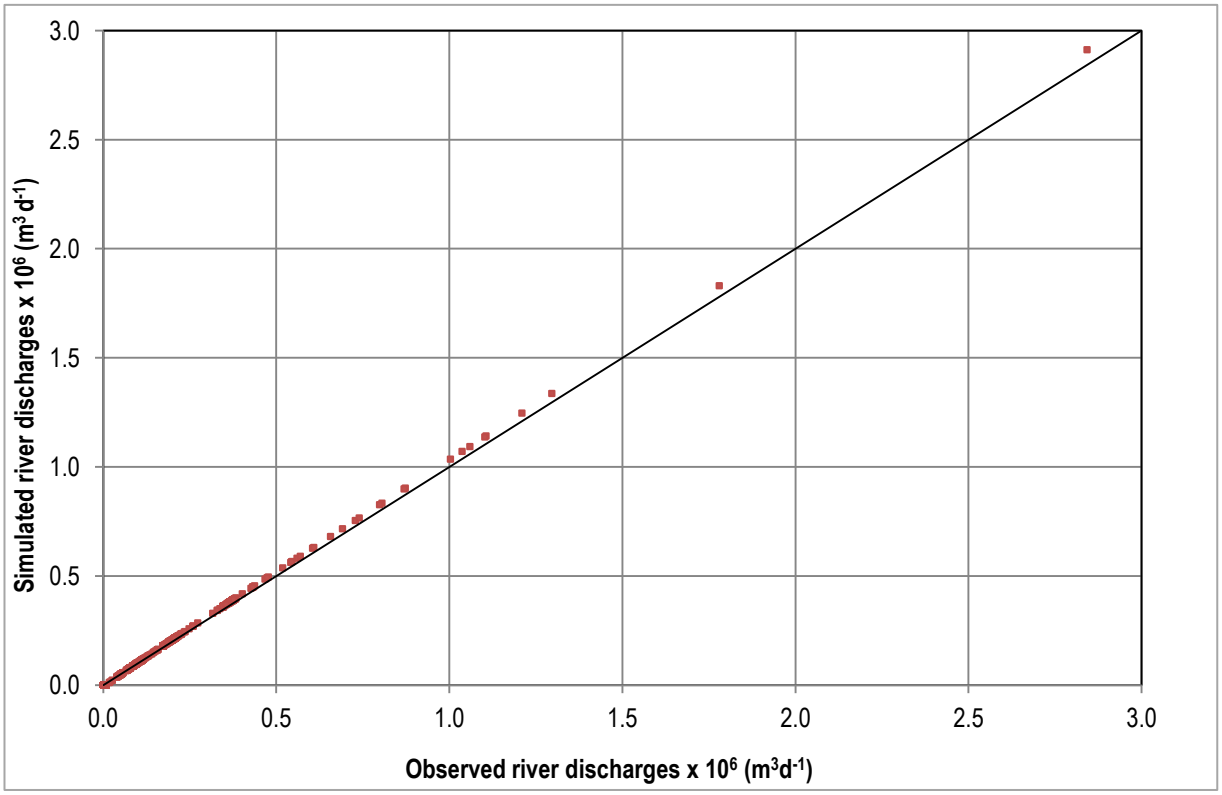

Figure 3-23. The discrepancy for the comparison of observed and simulated river gauge discharges - Bystrzyca L.

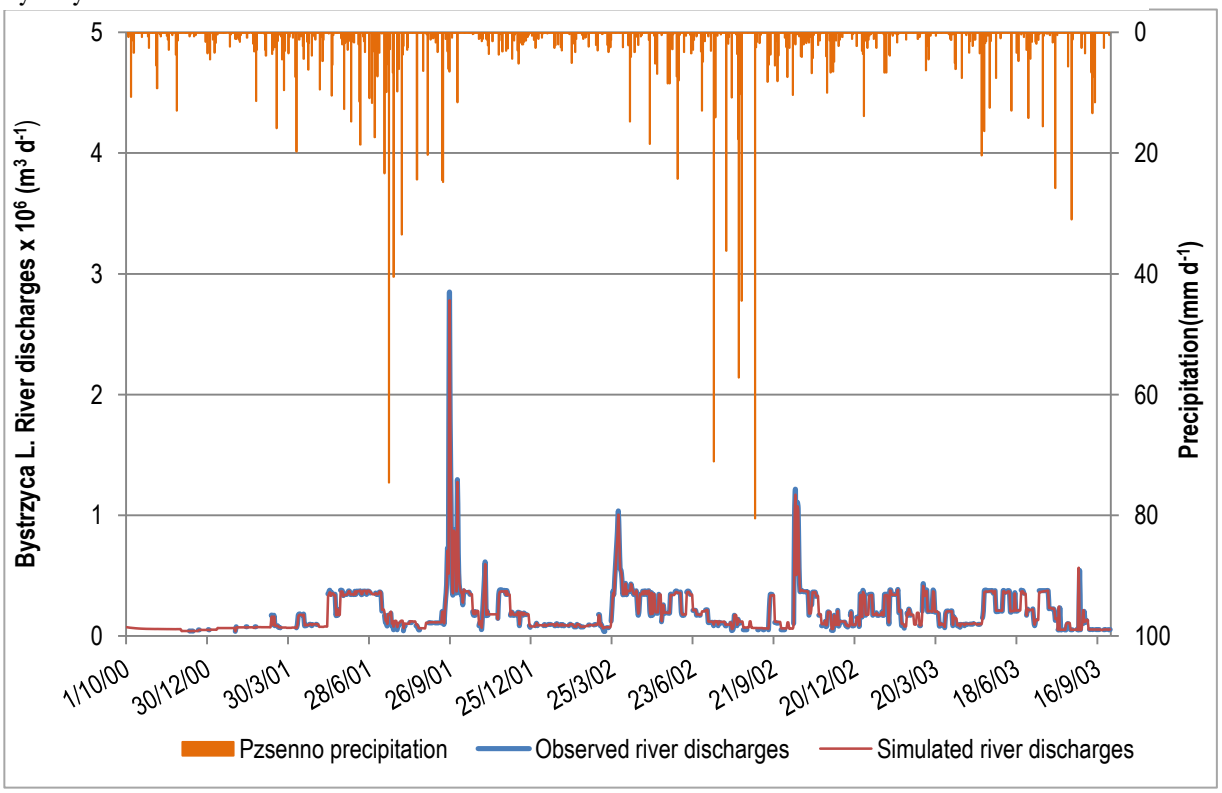

Figure 3-24. Time series for the comparison of observed and simulated river gauge discharges - Bystrzyca L.

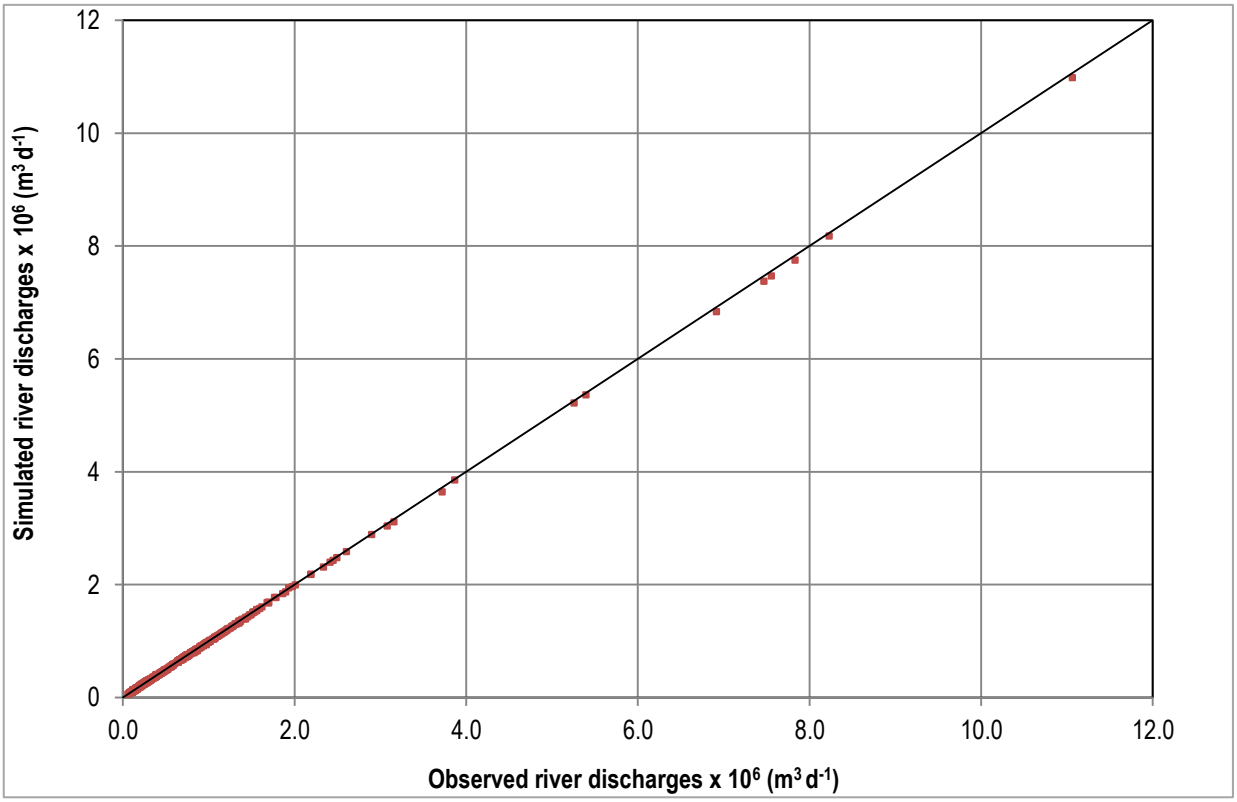

Figure 3-25. The discrepancy for the comparison of observed and simulated river gauge discharges - Bystrzyca K.

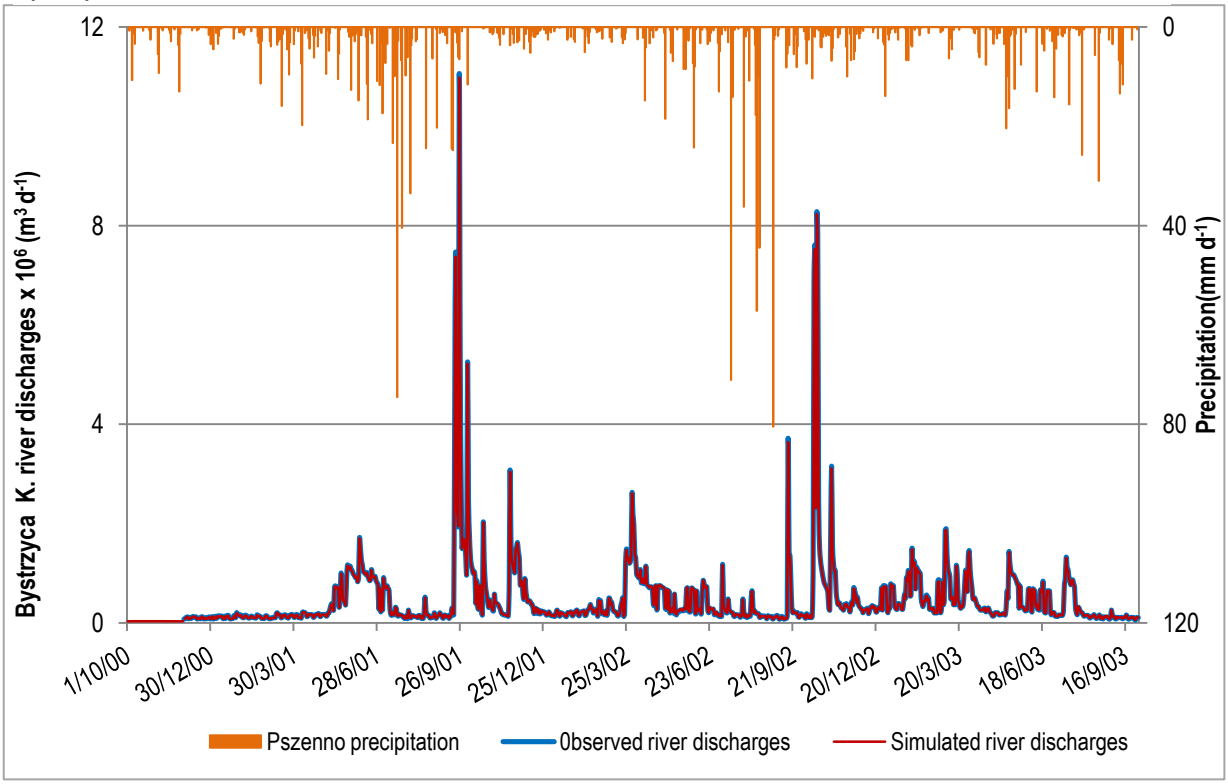

Figure 3-26. Time series for the comparison of observed and simulated river gauge discharges - Bystrzyca K.

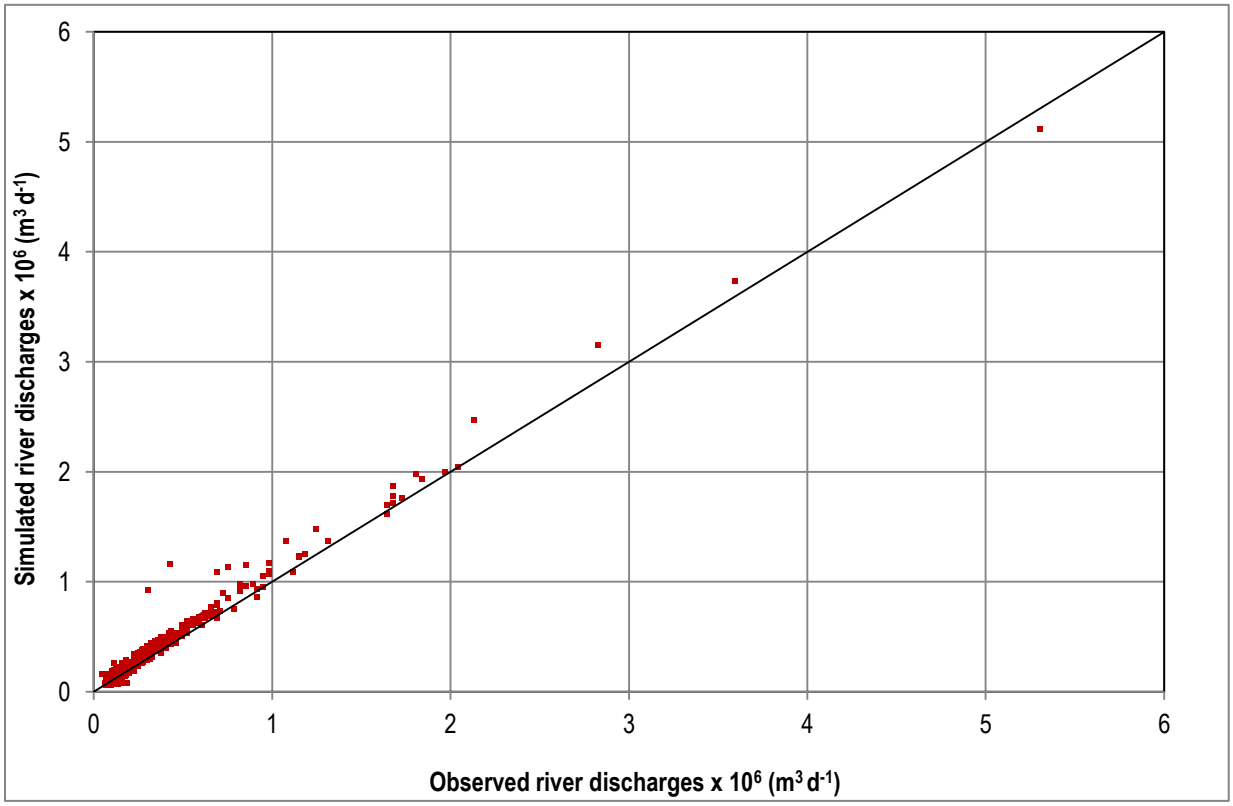

Figure 3-27. The discrepancy for the comparison of observed and simulated river gauge discharges-Strzegomka

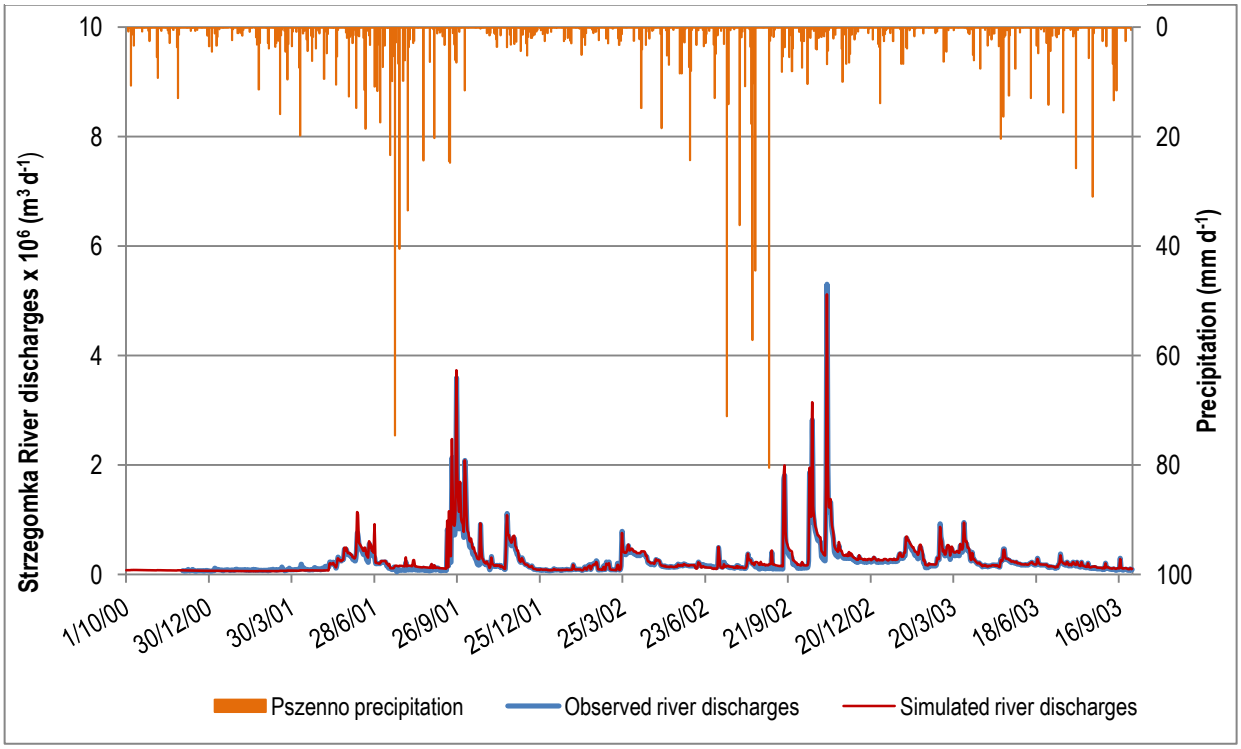

Figure 3-28. Time series for the comparison of observed and simulated river gauge discharges-Strzegomka

3.3.6. Water balance for the transient model calibration

The integrated hydrological model MODFLOW-NWT using ZONEBUDGET retrieved water balance for the aquifer systems with the same zones as it was conducted in steady-state model. However, the average of the three years (1st October, 2000 to 30th September, 2003) for the water balance results were calculated as described in Table 3-11, Table 3-12, Figure 3-29 and Figure 3-30. The average precipitation (1110337 $m^3 d^{-1}$) was used as the reference for the water balance components (input and output) in Table 3-11 and Table 3-12.

The total groundwater input for the Quaternary aquifer was equal to 1064369 $m^3 d^{-1}$, which consists of different components such as: gross groundwater recharge 49.9 % of precipitation which was the dominant followed by 17.2 % stream leakage, 4.5 % lateral inflows, 3.2 % reservoir leakage and 0.4 % the exchange between aquifers. The total groundwater output was equal to 1064340 $m^3 d^{-1}$, which consists of different components such: 31 % surface leakage followed by 21 % lateral outflows, 20.5 % stream leakage, 1.1 % GW-ET, 0.3 % reservoir leakage, 0.3 % the exchange between aquifers and groundwater storage change was 0.8 % of precipitation in the Quaternary aquifer as presented in Table 3-11. No percentage discrepancy.

The total groundwater input for the Tertiary aquifer was equal to 20442 $m^3 d^{-1}$, which consists of different water budget components, namely: 1.5 % lateral inflows and 0.3 % the exchange between aquifers in Table 3-11. In addition, the total output was equal to the total input, thus there were three outflow components: 1.3 % wellfield abstractions, 0.4 % the exchange between aquifers, 0.1 % lateral outflows and groundwater storage change was ~ 0 % of precipitation. No percentage discrepancy in the Tertiary aquifer.

Table 3-11. Three years average of groundwater budget for the Quaternary and Tertiary aquifers in the transient model

Groundwater budget component	Quaternary aquifer ($m^3 d^{-1}$)		Tertiary aquifer ($m^3 d^{-1}$)	
	IN	OUT	IN	OUT
Lateral inflows from SW (a & b) to the aquifers and well field abstractions	50277 (a)	0	16846 (b)	14500
Lateral outflows in the NE of the aquifers	0	234067	0	1398
Reservoir leakage	35081	3503	0	0
Stream leakage	190495	227801	0	0
Groundwater - ET	0	11770	0	0
UZF recharge	553611	0	0	0
Surface leakage	0	344263	0	0
Exchange between aquifers	4521	3582	3582	4521
Storage	230384	239354	14	23
Total	1064369	1064340	20442	20442
IN - OUT		29		0
Percent discrepancy		0		0

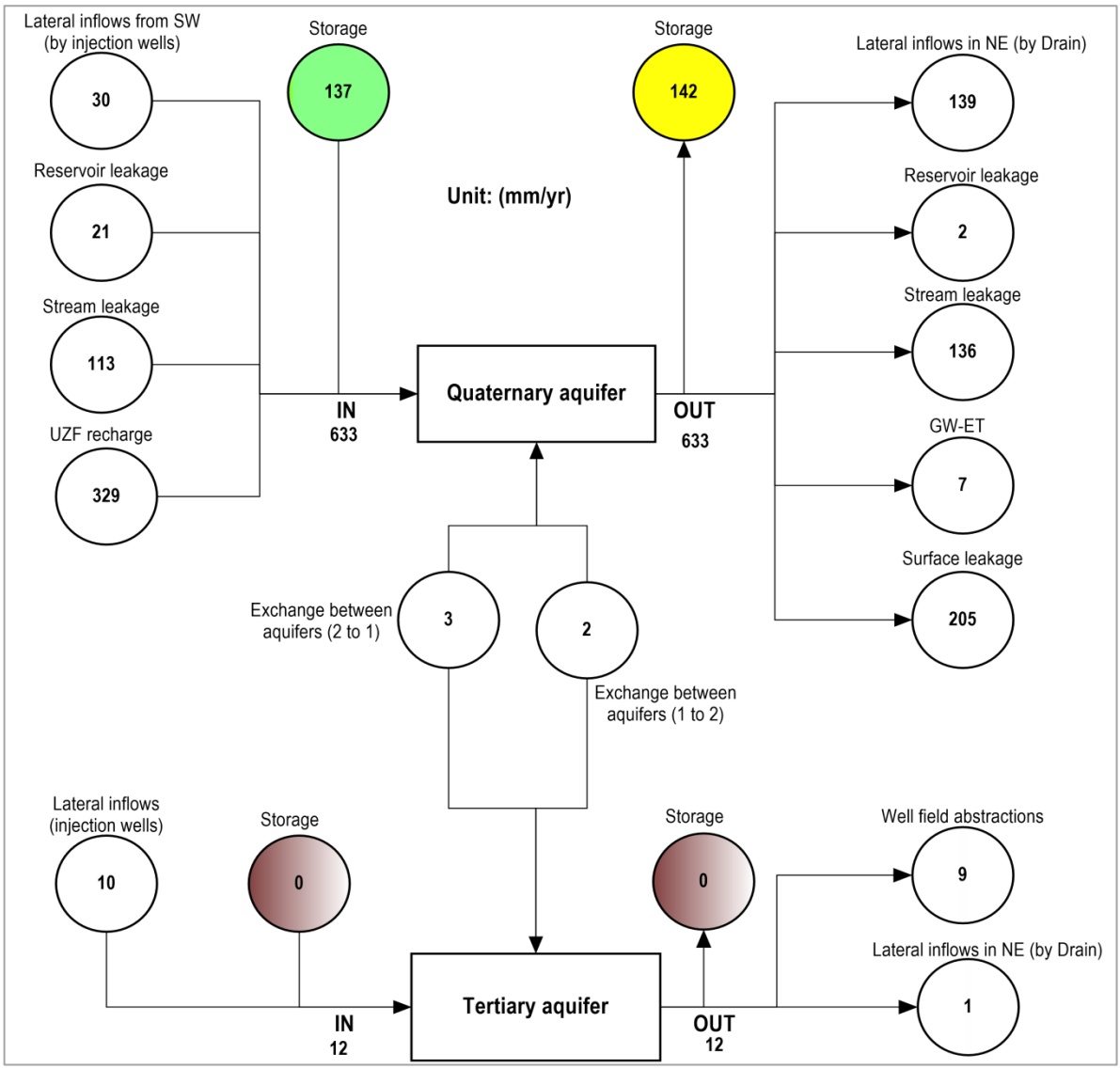

Figure 3-29. Schematic diagram of the three years average of groundwater balance for the Quaternary and Tertiary aquifers in the transient model

In the entire aquifer systems (composite zone) the total input was equal to 1076708 m^3 d^{-1}, there were different contribution of water budget components in the input such as: gross groundwater recharge 49.9 % of precipitation which was the dominant followed by 17.2 % stream leakage, 6 % lateral inflows and 3 % reservoir leakage. The total output was equal to 1076679 m^3 d^{-1}, therefore, the outflow components were; 31 % surface leakage followed by 21.2 % lateral outflows, 20.5 % stream leakage, 1.3 % well abstractions, 1.2 % GW-ET and 0.3 % reservoir leakage. The groundwater storage change was 0.8 % of precipitation. No discrepancy between the flows into and out of the aquifer systems.

Table 3-12. Three years average of groundwater balance of the entire aquifer systems for the transient model

	Aquifer systems	
Groundwater budget component	IN (m^3d^{-1})	OUT(m^3d^{-1})
Lateral inflows from SW to aquifers and well field abstractions	67123	14500
Lateral outflows in the NE of the aquifers	0	235466
Reservoir leakage	35081	3503
Stream leakage	190495	227801
Groundwater - ET	0	11770
UZF recharge	553611	0
Surface leakage	0	344263
Storage	230398	239377
Total	1076708	1076679
IN - OUT		29
Percent discrepancy		0

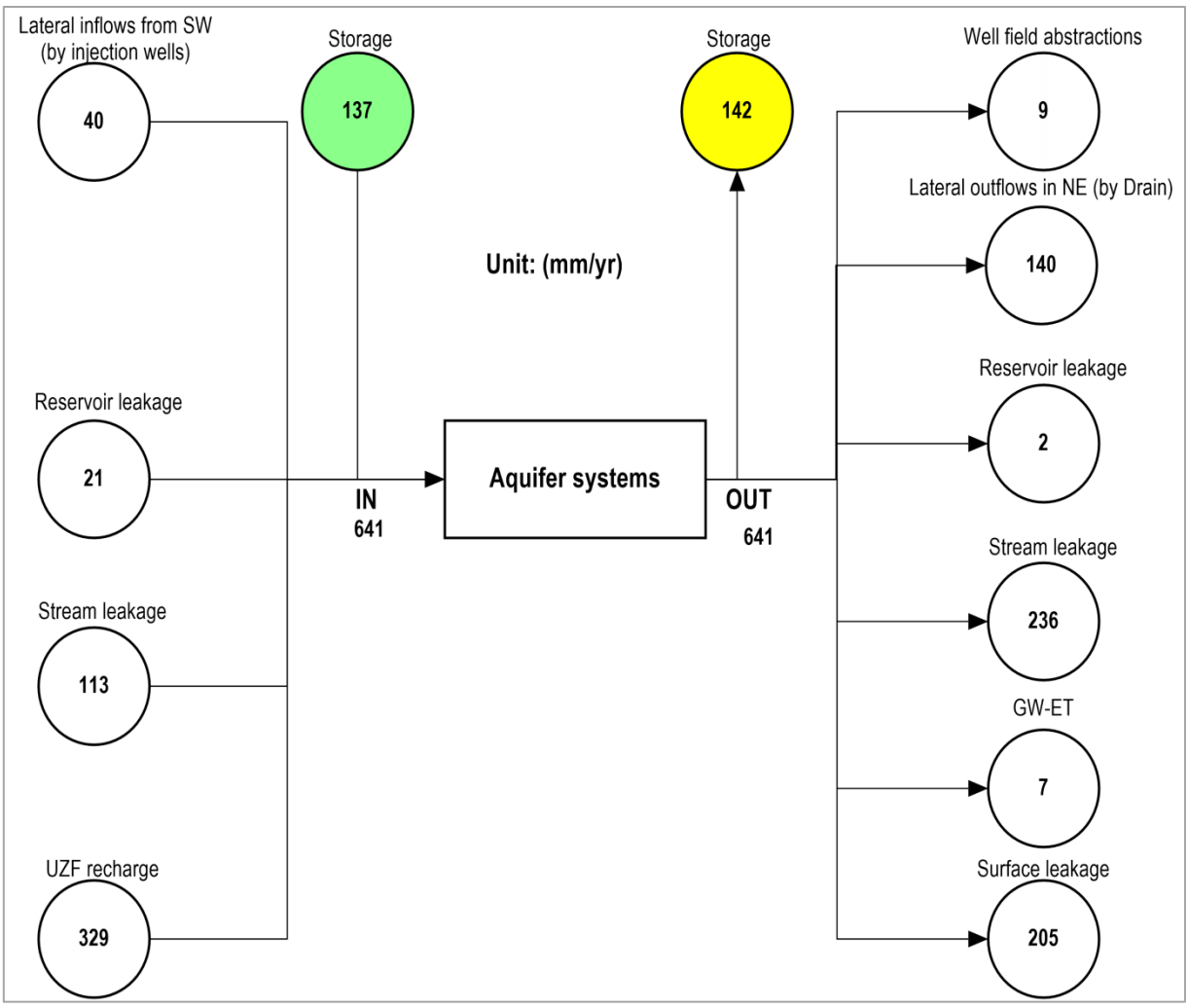

Figure 3-30. Schematic diagram of the three years average of groundwater balance for the entire aquifer systems in the transient model

3.3.7. Spatial variability of surface and ground water fluxes

The datasets of precipitation, infiltration rates and potential evapotranspiration (Figure 3-3 and Figure 3-5) were applied in UZF package. Through the use of these data, MODFLOW-NWT under ModelMuse environment retrieved the spatial variability of surface and groundwater fluxes, namely: UZF recharge (total recharge), Groundwater evapotranspiration (GW-ET) and Surface leakage in a unit of $m^3\ d^{-1}$, which means a depth (m) per unit area (m^2) of the grid cells. Since the software was retrieving the results in each stress period and not the average or cumulative of the whole simulated period, it was decided to select one stress period (for example was taken in the last stress period on 30th September 2003). Therefore, it was required to convert the fluxes into mm d^{-1} after importing the model results. The process involved was to create a new data set and use the function in MODFLOW-NWT, hence write the formula (UZF recharge ,GW-ET or Surface leakage was divided by ModelTopArea times 1000), the results were converted into mm d^{-1}. The UZF recharge (total recharge) results obtained were good (Figure 3-31 (a)). GW ET is removed from the unsaturated zone and if the ET demand is not fulfilled GW ET it is removed from the groundwater system if the water table is above the extinction depth (0.5 m) in Figure 3-32 (b). Additionally, the negative sign of GW-ET and surface leakage indicates that water was taken out of the groundwater table.

The spatial variability of UZF recharge range from 1 to 3 mm d^{-1} in the study area (Figure 3-31). The distribution of recharges were controlled by the availability of precipitation which is mostly originates from Sudety Mountains in the SW of the study area as indicated in Figure 3-31. Moreover, it was noted that the precipitation average was 1.8 mm d^{-1}. The spatial variability of GW-ET range between 0.2 to 1.8 mm d^{-1} in the study area. The rivers indicated in Figure 3-32 demonstrates how the GW-ET depend on extinction depth. Because they are spatially distributed mostly along the river flows, where the water table was within the extinction depth (0.5 m). The extinction depth is the depth below which no GW- ET occurs. In addition, the GW-ET depends mostly on the land cover and soil properties or the subsurface characteristics. The land cover in the area is dominated by the wheat and grasslands in Figure 1-5, therefore the rooting depth are approximately 0.5 m. Through that classification, the extinction depth was set to 0.5 m in the model, thus extinction depth increase with the increase in the rooting depth. Moreover, Soil characteristics play a big role on the GW-ET, because the soil properties like soil texture can influence, thus the fine texture can cause the decline of GW-ET and vice versa. The spatial variability of surface leakage range from 10 to 50 mm d^{-1} in the study area. The highest were spatially distributed mostly in the upper part area, where the three river flows originate as indicated in Figure 3-33. In general, both GW-ET and surface leakage, they are characterized by the high availabilities of groundwater rate along the streams where the water table is possibly close to the land surface in Figure 3-32 and Figure 3-33.

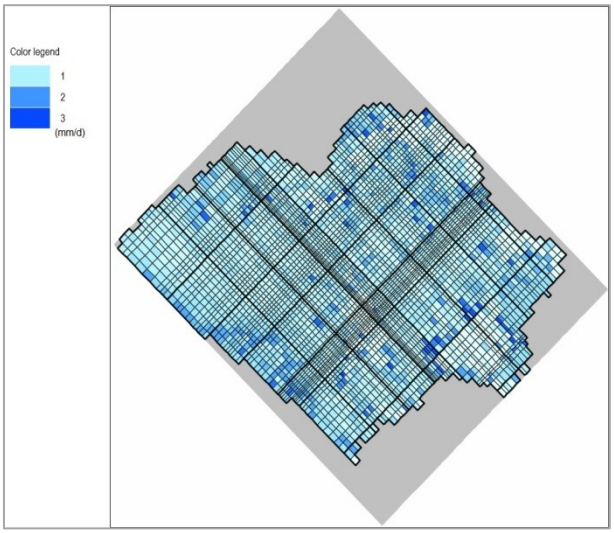

Figure 3-31.UZF recharge (gross GW recharge)

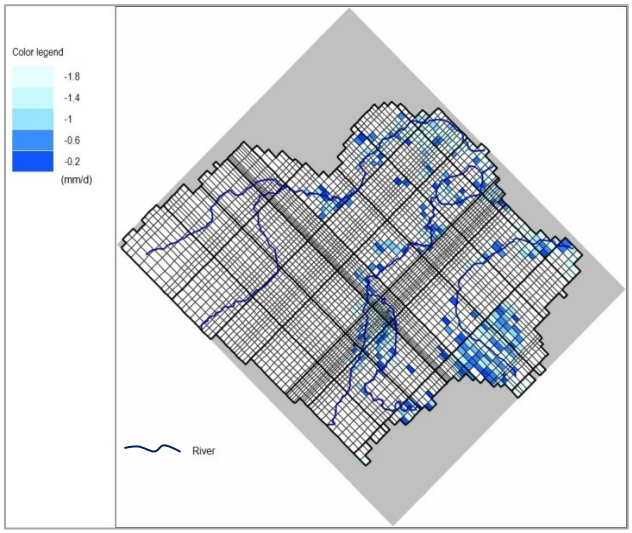

Figure 3-32. Groundwater - ET

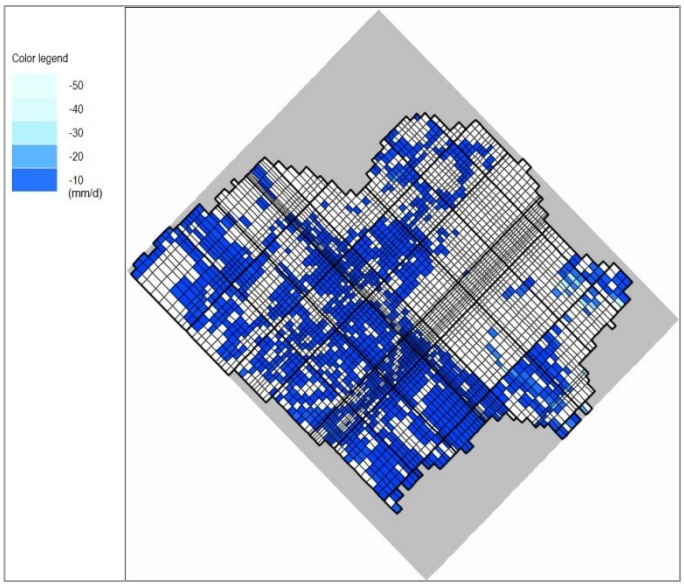

Figure 3-33.Surface leakage (groundwater exfiltration)

3.3.8. Temporal variability of surface and ground water fluxes

The three hydrological years data (1st Oct. 2000 to 30th Sept. 2003) were used to classify the temporal variability of surface and ground water fluxes. Each year was started from 1st October to 30th September (Table 3-15). The temporal variability of groundwater fluxes was detailed illustrated by different water balance components, namely: GW-ET, surface leakage and total recharge. The total recharge (R_g) were directly retrieved by the model (UZF package). Additionally, the net recharge (R_n) were calculated, where GW-ET were taken with negative sign before subtraction in Eqn.2-25. The temporal variability of surface and groundwater fluxes were considered for the last stress period (30th Sept. 2003), where all components were converted into mm yr^{-1} as presented in Figure 3-34.

The temporal variability of driving forces (precipitation, potential evapotranspiration and infiltration rate) as an input to the model were moderate. Because the study area is dominated by hilly topography towards the Sudety and Sleza Mountains and mostly flat land toward the Lake Mietkowskie (Figure 1-4). In

addition, the climate situation of the study area is termed as a temperate orographic influence due to the presence of Sudety Mountains at the SW boundary of the modelled area (Gurwin and Lubczynski, 2004). In that case, the minimum, maximum and average precipitation for the three years were 506, 765 and 660 mm yr^{-1}, respectively (Table 3-15). In general, precipitation was the key of everything because each item depends direct or indirect on it. Similarly, calculations in mm yr^{-1} were applied to the other driving forces and to the model results of groundwater balance as presented in Table 3-15. As a result, the aquifer systems in the study area were gaining the high UZF recharge as compared to the other groundwater balance components in Table 3-15. In addition, streams were much gaining more water from the aquifer than lake (Table 3-15), due to the spatial distributions of the streams in the study area.

The daily variability of GW-ET depend on the availability of water contents in the soil. It indicated that there were high variation of GW-ET within the period of 28/06/2001 to 26/09/2001 and 23/06/2002 to 21/09/2002 in Figure 3-34, this demonstrate that the precipitation was higher as presented in Figure 3-5. To emphasize, both GW-ET and surface leakage results indicated the same trends on the negative side (Figure 3-34). The total recharge indicated to be higher, because it is the summation of net recharge, GW-ET and Surface leakage while considering the negative sign of the two components as in Eqn.2-25. The rounded part in Figure 3-34, showed that there were negative values for the net recharge (Figure 3-35).

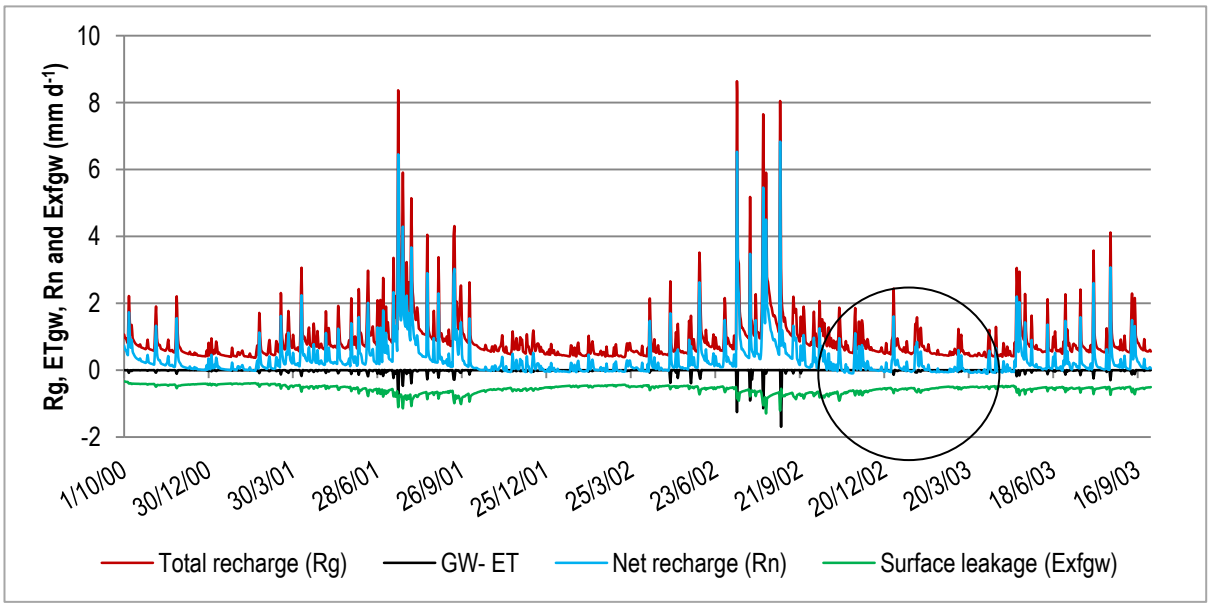

Figure 3-34. Daily variability of different groundwater balance components over the 3 years (1096 days) MODFLOW-NWT simulation period retrieved under the use of UZF package

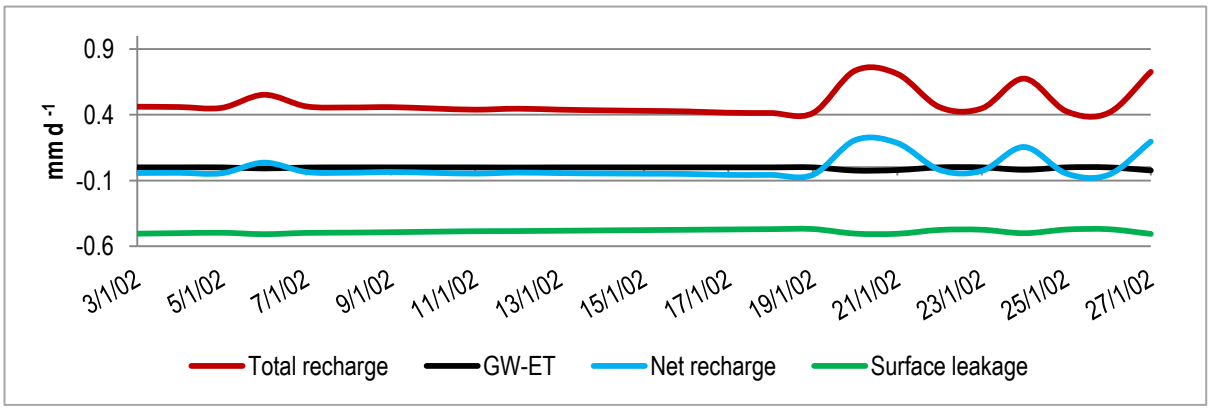

Figure 3-35. More clarification of Figure 3 34

3.3.9. Quantification of surface and ground water fluxes for the steady-state and the transient model calibration

The quantification of surface and groundwater fluxes (mm yr^{-1}) was started by considering the transient model, where the fluxes were subdivided into three hydrological years as presented in Table 3-15. In addition, the comparison of the surface and ground water fluxes for the steady-state and the average value of the transient model were conducted as presented in Table 3-14. The calculations implemented in Table 3-13 and Table 3-14 adhered to the three parts, namely: surface, unsaturated and saturated zone water fluxes. All the three parts were implemented using the three main equations (Eqn. 20, Eqn. 21 and Eqn. 24) described in section 2.6.10.4. In that case, the results of three year transient model simulation in Table 3-15 were used to quantify the surface and ground water fluxes. Referring in Eqn. 20, the quantification of surface and ground water fluxes was conducted for the entire modelled area. The results presented in Table 3-13 and Table 3-14 were almost better in the first hydrological year as shown in Table 3-13. However, the percentage discrepancy of the results were not good in the last year (Oct 01, 2002 to Sept 30, 2003) in Table 3-13, which might be due to the low precipitation as presented in Table 3-15 and Figure 3-5. By considering Eqn. 21, it addresses the unsaturated zone water fluxes. The calculated results in Table 3-13, it indicates almost 0 % percentage discrepancy of the water fluxes in the study area. Likewise, Eqn. 24, it addresses the saturated zone water fluxes. The calculated results in Table 3-13, it indicates 0 % percentage discrepancy of the water fluxes. Moreover, the comparison of the steady-state and the transient model was almost good according to the percentage discrepancy. The transient model calibration indicated to be the best because of less percentage discrepancy as presented in Table 3-14. Generally, the quantification of the temporal variability of surface and ground water fluxes was reasonable according to the transient integrated hydrological model.

Table 3-13. Quantification of surface and ground water fluxes for the transient model calibration

Yr	Eqn. 20			% Error	Eqn. 21			% Error	Eqn. 24			% Error
1	1070	≠	1102	-3	960	=	960	-0.1	652	=	652	0.0
2	1079	≠	1240	15.7	918	≠	919	-0.1	665	=	665	0.0
3	967	≠	1320	36.5	716	=	716	0.0	603	=	603	0.0

Table 3-14. Comparison of the surface and ground water fluxes for the steady-state and the average of the transient model in Table 3-15

Steady-state model												
Eqn. 20			% Error	Eqn. 21			% Error	Eqn. 24			% Error
1113	≠	1435	-28.9	756	=	756	0.0	582	=	581	0.1
Average value of the transient model											
1151	≠	1360	-18.2	865	=	865	0.0	640	=	640	0.0

Table 3-15. The yearly variability of driving forces and different groundwater balance components over the 3 years (1096 days) MODFLOW-NWT simulation period

Hydrological year	Driving forces (mm yr^{-1})						GW (IN)) (mm yr^{-1})						GW (OUT) (mm yr^{-1})									UZF) (mm yr^{-1})		
	Precipitation(P)	PET	Interception (I_c)	Infiltration rate (P_r)	Net recharge (R_n)	Runoff (R_o)	Lateral inflows (Q_{Lin})	Lake leakage (L_{LKin})	Streams leakage (Q_{GWin})	UZF recharge (R_g)	Stream inflows (Q_{Sin})	Storage (in)	Lateral outflows (Q_{Lout})	GW to lake (L_{LKout})	GW to Streams (Q_{GWout})	GW-ET (ET_{gw})	Surface leakage (SL)	Stream outflows (Q_{Sout})	Storage (out)	GW storage change (ΔS_g)	Well abstraction (Q_W)	Actual infiltration(P_e)	UZF-ET (ET_{uz})	Storage change (ΔS_{uz})
Steady-state model	660	632	197	463	105	145	40	12	116	414	297	0	133	1	130	212	96	664	0	0	9	414	0	0
Transient model																								
Oct 01, 2000 - Sept 30, 2001	765	615	228	537	166	350	40	26	108	369	265	108	140	2	132	8	195	568	167	-59	9	382	10	3
Oct 01, 2001- Sept 30, 2002	709	715	211	497	121	366	40	18	112	339	329	156	140	2	140	9	209	659	156	0	9	341	10	-7
Oct 01, 2002 - Sept 30, 2003	506	565	151	355	65	303	40	18	119	279	421	146	140	2	134	4	210	782	104	42	9	262	5	-23
Statistics																								
MIN.	506	565	151	355	65	303	40	18	108	279	265	108	140	2	132	4	195	568	104	-59	9	262	5	-23
MAX.	765	715	228	537	166	366	40	26	119	369	421	156	140	2	140	9	210	782	167	42	9	382	10	3
AVERAGE	660	632	197	463	117	340	40	21	113	329	338	137	140	2	135	7	205	670	142	-5	9	328	8	-9
STD	136	76	41	96	51	33	0	5	6	46	79	25	0	0	4	3	8	107	34	51	0	61	3	13

3.3.10. `Comparison of steady-state and transient IHM calibration results

The calibration of steady-state and transient models were accomplished by comparing the results of from the steady-state and the transient model calibrations. The results of calibrated parameters in the steady-state model were as follows; HK in aquifer 1 range from 0.5 to 180 m d^{-1} (Figure 3-6 (a)), while the VK range from 5 x 10^{-6} to 0.5 x 10^{-3} m d^{-1}. The VKCB in aquitard range from 0.1x 10^{-6} to 0.05 x 10^{-3} m d^{-1}. Additionally, in aquifer 2; HK range from 0.5 to 100 m d^{-1} (Figure 3-6 (b)), while the VK range from 0.01 x 10^{-3} to 0.5 x 10^{-3} m d^{-1}. However, the results of the calibrated parameters in the transient model were as follows; HK in aquifer 1 range from 0.5 to 180 m d^{-1} (Figure 3-11(a)) while the VK range from 1 x 10^{-6} to 0.01 x 10^{-3} m d^{-1}. The VKCB in aquitard range from 0.1x 10^{-6} to 0.05 x 10^{-3} m d^{-1}. Additionally, in aquifer 2; HK range from 0.5 to 100 m d^{-1} (Figure 3-11 (b)) while the VK range from 0.01 x 10^{-3} to 0.5 x 10^{-3} m d^{-1}. It means both models follow the same range of the calibrated parameter values.

The head distributions in both models were slightly different and it was noted in the contour lines distributions (Figure 3-7 and Figure 3-12). The calibrated results for the piezometric heads in the steady-state model gives the RMSE equal to 0.59 m while in the transient model, it was equal to 0.18 m. The calibrated lake stage in the steady-state model possess the RMSE equal to 0.02 m, while in the transient mode, it was equal to 0.31 m. The water balance in both models, followed the zones as described above. In steady-state model, the total groundwater input and output in the Quaternary aquifer was equal to 965580 $m^3 d^{-1}$, respectively while in the Tertiary aquifer, the total groundwater input and output was equal to 20137 $m^3 d^{-1}$, respectively. However, in the transient model, the total groundwater input and output in the Quaternary aquifer was equal to 1064369 $m^3 d^{-1}$, respectively, while in the Tertiary aquifer, the total groundwater input and output was equal to 20442 $m^3 d^{-1}$, respectively. Therefore, it is almost the same results of the total groundwater balance.

The yearly variability fluxes which include the driving forces and different groundwater balance components over the 3 years MODFLOW-NWT simulation period was demonstrated in Table 3-15. By considering the steady-state model result and the statistic average in the transient model result, it indicates that the groundwater to the lake, stream leakage, stream inflow and outflow and others, were almost the same in both model calibration. However, GW-ET was noted to be higher in the steady-state model than in the transient model. This could possibly be attributed by the high surface leakage in Figure 3-33 and Table 3-15, because during the calibration process, when the GW-ET rise the surface leakage decline and vice versa.

3.3.11. Sensitivity analysis for the transient model

Sensitivity analysis was conducted with the aim of assessment of groundwater in Świdnica area and the results were described into three key points: 1) Effect of changing calibrated parameters on piezometric heads, 2) Effect of changing calibrated parameters on river gauge discharges and 3) Effect of changing river inflows (total flow) on piezometric heads.

3.3.11.1. The effect of changing calibrated parameters on piezometric heads

The effect of changing calibrated parameters such as HK and VK, VKCB, Sy and Ss were conducted separately where the RMSE was higher than MAE in each case (Table 3-16 up to Table 3-20 and Figure 3-36 up to Figure 3-40. The effect was evaluated with respect to the RMSE of each calibrated parameter and the final effect results were combined (Table 3-21 and Figure 3-41). Therefore, HK was more sensitive (larger effect on piezometric heads) than the other calibrated parameters, while the Sy was less sensitive with almost constant effect in Figure 3-41.

Table 3-16. Effect of changing HK parameter

Percentage changes (%) of HK	Piezometric head errors (m)		
	ME	MAE	RMSE
-30	-8.29	8.29	11.05
-20	-5.24	5.24	6.98
-10	-2.08	2.08	2.75
0	-0.08	0.15	0.18
10	2.21	2.21	2.91
20	4.25	4.25	5.59
30	6.12	6.12	8.04

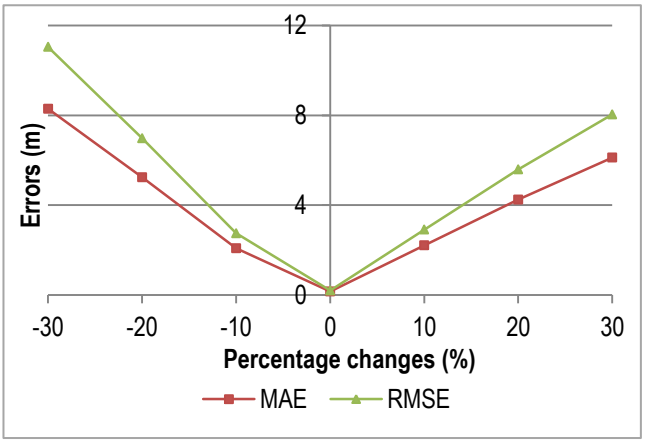

Figure 3-36. Effect of changing HK parameter

Table 3-17. Effect of changing VK parameter

Percentage changes (%) of VK	Piezometric head errors (m)		
	ME	MAE	RMSE
-30	0.25	0.29	0.37
-20	0.14	0.19	0.26
-10	0.05	0.16	0.20
0	-0.08	0.15	0.18
10	-0.08	0.19	0.25
20	-0.14	0.23	0.30
30	-0.18	0.27	0.35

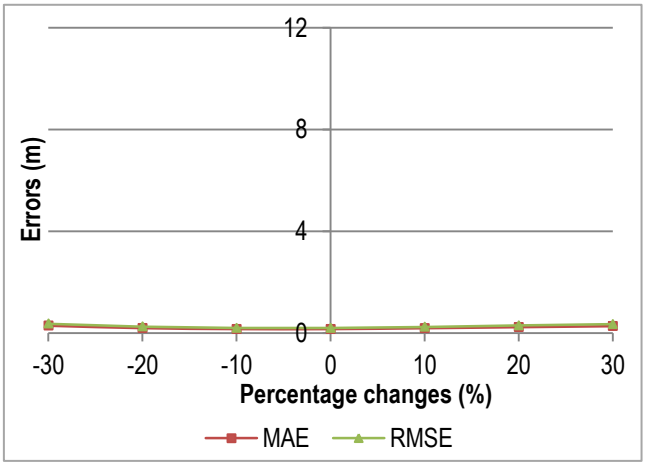

Figure 3-37. Effect of changing VK parameter

Table 3-18. Effect of changing Sy parameter

Percentage changes (%) of Sy	Piezometric head errors (m)		
	ME	MAE	RMSE
-30	-0.06	0.20	0.25
-20	-0.04	0.18	0.23
-10	-0.03	0.17	0.22
0	-0.08	0.15	0.18
10	-0.01	0.15	0.20
20	0.00	0.15	0.19
30	0.01	0.14	0.18

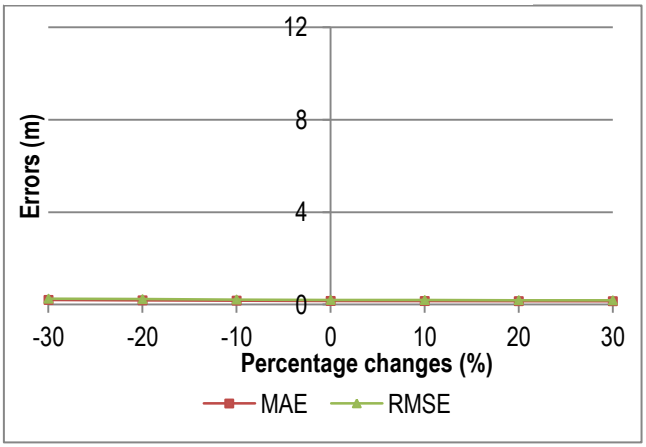

Figure 3-38. Effect of changing Sy parameter

Table 3-19. Effect of changing VKCB parameter

Percentage changes (%) of VKCB	Piezometric head errors (m)		
	ME	MAE	RMSE
-30	0.44	0.48	0.63
-20	0.42	0.47	0.61
-10	0.41	0.46	0.59
0	-0.08	0.15	0.18
10	0.39	0.43	0.56
20	0.38	0.43	0.55
30	0.44	0.48	0.63

Figure 3-39. Effect of changing VKCB parameter

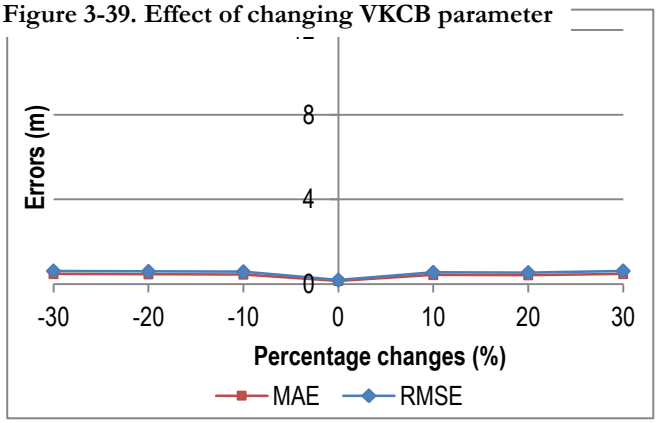

Table 3-20. Effect of changing Ss parameter

Percentage changes(%) of (Ss)	Piezometric head errors (m)		
	ME	MAE	RMSE
-30	0.40	0.45	0.58
-20	0.40	0.45	0.58
-10	0.40	0.45	0.58
0	-0.08	0.15	0.18
10	0.40	0.45	0.58
20	0.40	0.45	0.58
30	0.40	0.45	0.58

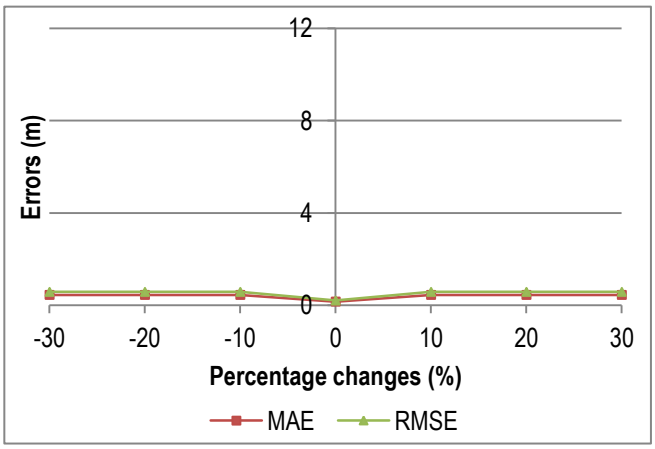

Figure 3-40. Effect of changing Ss parameter

Table 3-21. General effect of calibrated parameters

Percentage changes (%) of all	Piezometric heads -RMSEs (m)				
	HK	VK	Sy	VKCB	Ss
-30	11.05	0.37	0.25	0.63	0.58
-20	6.98	0.26	0.23	0.61	0.58
-10	2.75	0.20	0.22	0.59	0.58
0	0.18	0.18	0.18	0.18	0.18
10	2.91	0.25	0.20	0.56	0.58
20	5.59	0.30	0.19	0.55	0.58
30	8.04	0.35	0.18	0.63	0.58

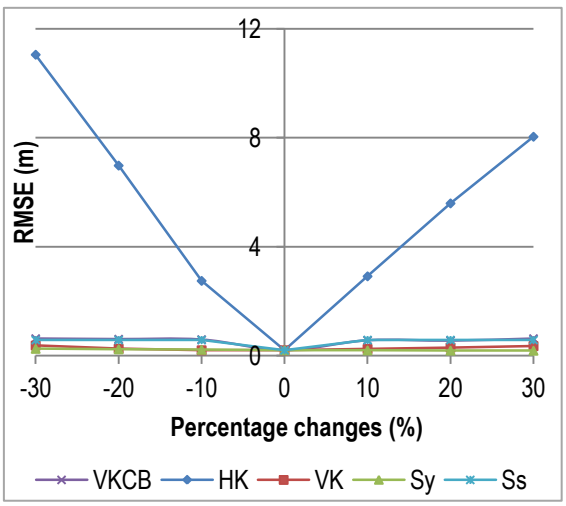

Figure 3-41. General effect of calibrated parameters

3.3.11.2. The effect of changing calibrated parameters on river gauge discharges

The effects were conducted in the same ways as section 3.3.11.1, but vertical leakance (VKCB) and specific storage (Ss) was excluded, because the elevation formulas (Z) for streams were set in layer 1 only. The sensitivity was conducted separately where the RMSE was higher than MAE in each case (Table 3-22 to Table 3-24) and (Figure 3-42 to Figure 3-44) and then were combined (Table 3-25 and Figure 3-45). Therefore, HK was more sensitive (larger effect on river gauge discharges) than the other calibrated parameters, while specific yield (Sy) was less sensitive when the values decrease and vice versa. In addition, VK was less sensitive when the values increase and vice versa (Figure 3-45).

Table 3-22. Effect of changing HK parameter

Percentage changes (%) of HK	River Q errors (m^3d^{-1})		
	ME	MAE	RMSE
-30	-3076	13059	19105
-20	-1473	12594	18807
-10	-19	12045	18376
0	2820	11165	17719
10	2851	11429	17989
20	4261	11709	18338
30	5668	12399	19047

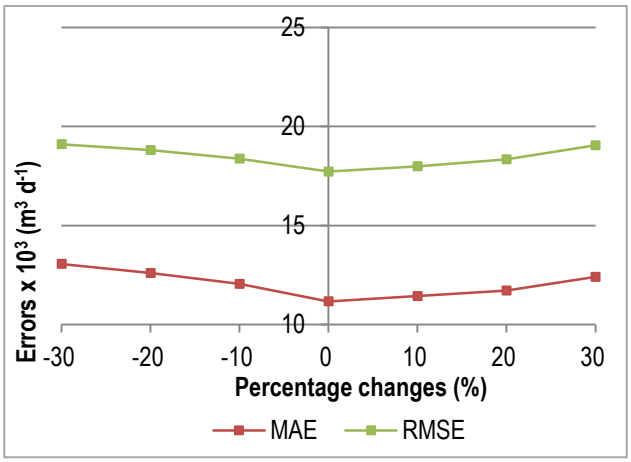

Figure 3-42. Effect of changing HK parameter

Table 3-23. Effect of changing VK parameter

Percentage changes (%) of VK	River Q errors (m^3d^{-1})		
	ME	MAE	RMSE
-30	1417	11588	18040
-20	1421	11587	18040
-10	1424	11587	18040
0	2820	11165	17719
10	1422	11586	18039
20	1432	11585	18040
30	1435	11584	18039

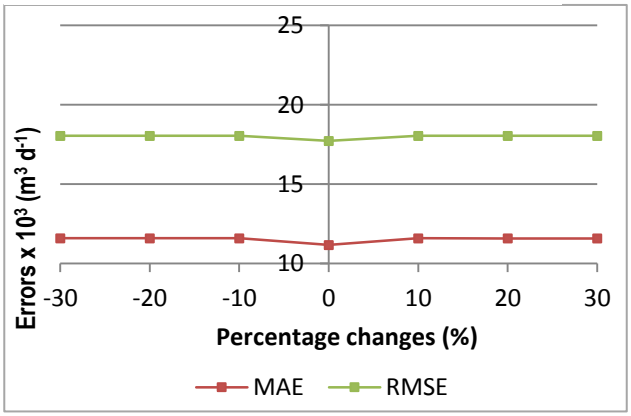

Figure 3-43. Effect of changing VK parameter

Table 3-24. Effect of changing Sy parameter

Percentage changes (%) of Sy	River Q errors (m^3d^{-1})		
	ME	MAE	RMSE
-30	617	11382	17563
-20	910	11439	17734
-10	1180	11505	17892
0	2820	11165	17719
10	1653	11668	18179
20	1861	11747	18309
30	2051	11823	18431

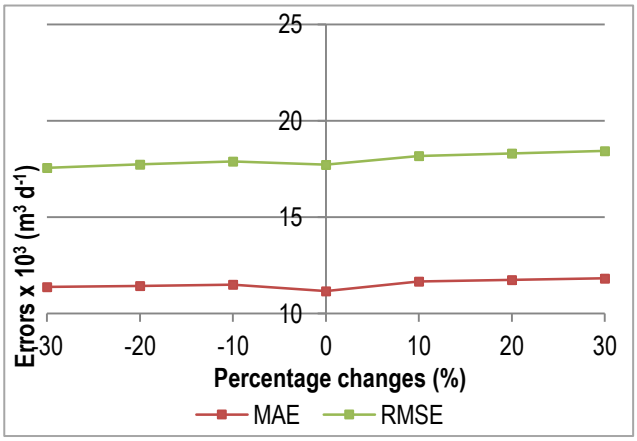

Figure 3-44. Effect of changing Sy parameter

Table 3-25. General effect of changing calibrated parameters on river discharges

Percentage changes (%) of all	River discharges - RMSE (m^3d^{-1})		
	HK	VK	Sy
-30	19105	18040	17563
-20	18807	18040	17734
-10	18376	18040	17892
0	17719	17719	17719
10	17989	18039	18179
20	18338	18040	18309
30	19047	18039	18431

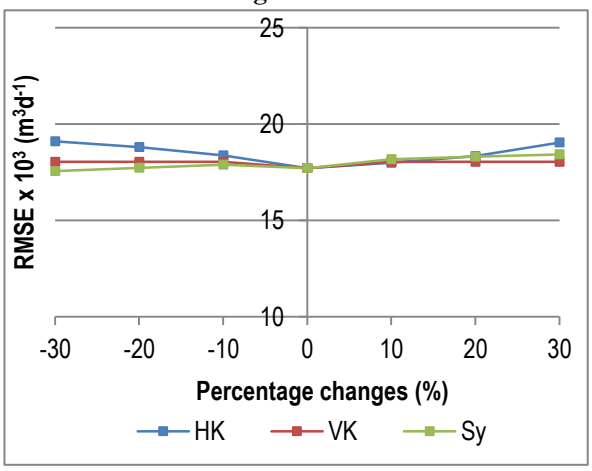

Figure 3-45. General effect of changing calibrated parameters on river discharges

3.3.11.3. The effect of changing river inflow (total flow) on piezometric heads

The effect was conducted by changing total flows that were assigned at the upper end streams as arbitrary values in different stress periods. The sensitivity was conducted with respect to all streams discharges in the whole area. The results indicate that RMSE was higher than MAE (Figure 3-46) but the effect was noted within the percentage change of -10 % to +10 % and also it was constant in other changes.

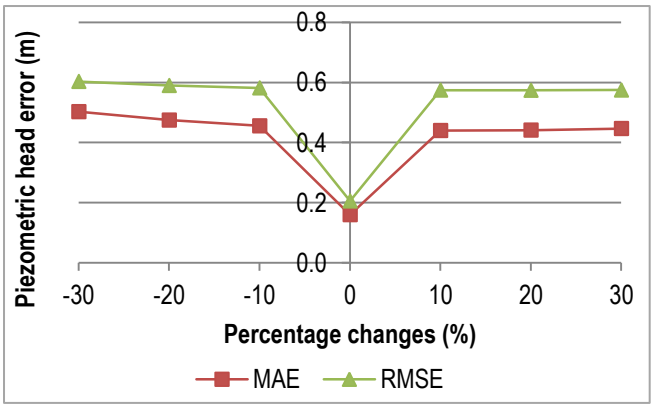

Figure 3-46. Effect of changing river inflow

4. CONCLUSIONS AND RECOMMENDATIONS

4.1. Conclusions

The Quasi-3D model was made for the assessment of groundwater resources in Świdnica area. Numerical model calibration started with steady-state model run which facilitated initial conditions for the transient model simulation, the target of this research. The transient model simulation period was from 1st October 2000 to 30th September 2003 and involved abstractions of two wellfields.

The calibration process started with the steady-state model where the errors in the piezometric head were: ME (-0.46 m), MAE (0.46 m) and RMSE (0.5 m). The piezometric head errors after transient calibration were: ME (-0.08 m), MAE (0.15 m) and RMSE (0.18 m). Additionally, the stream flows for the five river gauges and lake stage were calibrated concurrently with groundwater heads in the model. The sensitivity of hydraulic conductivity indicated larger effect on piezometric heads and river gauge discharges than the other parameters. The changing river inflows indicated that there was small effects on RMSE for the piezometric heads and this was limited due to the less number and spatial distributions of piezometers in the study area.

The groundwater budget showed that the Quaternary aquifer was gaining water from different water balance components such as gross groundwater recharge which was 49.9 % of precipitation followed by 17.2 % of stream leakage. The lateral inflows from the SW contributed 4.5 %, reservoir leakage 3.2 %, the exchange between aquifers 0.4 %. Additionally, the aquifer was losing water through different water balance components where the large contribution was from surface leakage 31 % followed by lateral outflows 21 % and stream leakage 20.5 %. Moreover, GW-ET, reservoir leakage and exchange between aquifers were: 1.1, 0.3 and 0.3 %, respectively. The groundwater storage change was 0.8 % of precipitation. The Tertiary aquifer was gaining water from the two different water balance components: lateral inflows from the SW which contributed (1.5 % of P) and the exchange between aquifers (0.3 % of P). In addition, the aquifer was losing water through three outflow components: wellfield abstractions (1.3 % of P), lateral outflow (0.1 % of P) followed by the exchange between aquifers (0.4 % of P).

The spatial variability of ground water fluxes in the study area indicated even distribution. The gross recharge was almost uniform over the entire modelled area. The surface leakage was highly concentrated at the middle part of the study area towards the SW boundary with a minimum and maximum of 1.29 and 34 mm d^{-1}, respectively. The temporal variability of fluxes indicated the gross groundwater recharge varied between 0.37 and 8.63 mm d^{-1} and net recharge varied between -0.11 and 6.83 mm d^{-1}. GW-ET had a maximum value of 1.69 mm d^{-1}. Moreover, the steady-state fluxes were more or less close to the average fluxes of the transient model.

Finally, the transient integrated hydrological model led to the better solution of the assessment of groundwater resources in the study area. This model was the appropriate method for analysing water balance of the multi-aquifer systems in Świdnica area.

4.2. Recommendations

1) There is a need to have a collaborative initiative in groundwater management for the future plans. This could enable development of a detailed research programme to gather more groundwater data directly from government and other stakeholders in the communities, so as to improve the picture of groundwater use and conditions. The real picture would be a pre-requisite for developing more informed assessments which address the situations of groundwater conditions for domestic water supply, scientific strategy towards managing water resources database.
2) Groundwater monitoring and data collection in the study area are inadequate, because there were only two piezometers from ADAS station, where one piezometer is used to monitor unconfined (Quaternary) aquifer and other confined (Tertiary) aquifer. As the result, it was not sufficient for the clear knowledge about aquifer systems in Świdnica area. Furthermore, additional of groundwater monitoring network (piezometers) should be made so as to solve water problems by reflecting and sticking to uncertainty, change and understanding of aquifer systems and their interactions. Because the availability of data collected would enable solving water resources conflicts for the users.
3) Data dissemination and access should be taken into consideration, because the dissemination of groundwater data to groundwater users would help them in knowing water problems and hence develop the research on it.
4) To ensure groundwater resources are well managed for sustainable development and future generation, the following target studies could be considered: a) the effect of communities located on recharge and discharge areas of aquifer systems, b) socio-economic impacts resulting from over abstractions and pollution in Świdnica area, c) competition intense within water users (public and private) and d) groundwater management failure.

List of references

Allen, R.G., Pereira, L.S., Raes, D., Smith, M., Ab, W., 1998. Crop evapotranspiration - Guidelines for computing crop water requirements - FAO Irrigation and drainage paper 56 By 1–15.

Anderson, M.P., Woessner, W.W., 1992. Applied Groundwater Modeling: Simulation of Flow and Advective Transport (Google eBook). Academic Press.

Fenske, J.P., Leake, S.A., Prudic, D.E., 1996. Documentation of a computer program (RES1) to simulate leakage from reservoirs using the modular finite-difference ground-water flow model (MODFLOW). Open-File Rep.

Gurwin, J., 2010. Renewal Assessment of Water-bearing Structures within the Fore-Sudetic Blocks Integration of Monitoring and GIS/RS Data with Numerical Flow Models.

Gurwin, J., Lubczynski, M., 2004. Modeling of complex multi-aquifer systems for groundwater resources evaluation—Swidnica study case (Poland). Hydrogeol. J. 13, 627–639. doi:10.1007/s10040-004-0382-9

Harbaugh, A.W., 2005. MODFLOW-2005 : The U.S. Geological Survey modular ground-water model--the ground-water flow process. B. 6 Model. Tech. Sect. A. Ground-water.

Harbaugh, A.W., Banta, E.R., Hill, M.C., McDonald, M.G., 2000. MODFLOW-2000, The U.S. Geological Survey Modular Ground-Water Model - User Guide to Modularization Concepts and the Ground-Water Flow Process.

Hassan, S.M.T., Lubczynski, M.W., Niswonger, R.G., Su, Z., 2014. Surface–groundwater interactions in hard rocks in Sardon Catchment of western Spain: An integrated modeling approach. J. Hydrol. 517, 390–410. doi:10.1016/j.jhydrol.2014.05.026

Huntington, J.L., Niswonger, R.G., 2012. Role of surface-water and groundwater interactions on projected summertime streamflow in snow dominated regions: An integrated modeling approach. Water Resour. Res. 48, n/a–n/a. doi:10.1029/2012WR012319

Jaworska-Szulc, B., 2009. Groundwater flow modelling of multi-aquifer systems for regional resources evaluation: the Gdansk hydrogeological system, Poland. Hydrogeol. J. 17, 1521–1542. doi:10.1007/s10040-009-0473-8

Kelly, B.P., Pickett, L.L., Hansen, C.V., and Ziegler, A.C., 2013. USGS Scientific Investigations Report 2013–5042: Simulation of Groundwater Flow, Effects of Artificial Recharge, and Storage Volume Changes in the Equus Beds Aquifer near the City of Wichita, Kansas Well Field, 1935–2008 [WWW Document]. URL http://pubs.usgs.gov/sir/2013/5042/ (accessed 2.2.15).

Kovalevsky, V.S., Kruseman, G.P., Rushton, K.R., 2004. G r o u n d w a t e r s t u d i e s : An international guide for hydrogeological investigations.

Leuning, R., Condon, A.G., Dunin, F.X., Zegelin, S., Denmead, O.T., 1994. Rainfall interception and evaporation from soil below a wheat canopy. Agric. For. Meteorol. 67, 221–238. doi:10.1016/0168-1923(94)90004-3

Łowicki, D., 2008. Land use changes in Poland during transformation. Landsc. Urban Plan. 87, 279–288. doi:10.1016/j.landurbplan.2008.06.010

Lubczynski, M.W., Gurwin, J., 2005. Integration of various data sources for transient groundwater modeling with spatio-temporally variable fluxes—Sardon study case, Spain. J. Hydrol. 306, 71–96. doi:10.1016/j.jhydrol.2004.08.038

Massuel, S., George, B.A., Venot, J.-P., Bharati, L., Acharya, S., 2013. Improving assessment of groundwater-resource sustainability with deterministic modelling: a case study of the semi-arid Musi sub-basin, South India. Hydrogeol. J. 21, 1567–1580. doi:10.1007/s10040-013-1030-z

McDonald, M.G., Harbaugh, A.W., 1988. A modular three-dimensional finite-difference ground-water flow model.

Niswonger, R.G., Prudic, D.E., Regan, R.S., 2005. Documentation of the Unsaturated-Zone Flow (UZF1) Package for Modeling Unsaturated Flow Between the Land Surface and the Water Table with MODFLOW-2005 Techniques and Methods 6-A19 Documentation of the Unsaturated-Zone Flow (UZF1) Package for Modeling.

Niswonger, R.G., Panday, Sorab, and Ibaraki, M., 2011. MODFLOW-NWT , A Newton Formulation for MODFLOW-2005.

Prudic, D.E., Konikow, L.F., Banta, E.R., 2004. A New Streamflow-Routing (SFR1) Package to Simulate Stream-Aquifer Interaction with MODFLOW-2000.

Wang, D., Wang, G., Anagnostou, E.N., 2007. Evaluation of canopy interception schemes in land surface models. J. Hydrol. 347, 308–318. doi:10.1016/j.jhydrol.2007.09.041

Wikipedia, 2014. Groundwater_model.

Winston, R.B., 2005. ModelMuse — A Graphical User Interface for MODFLOW – 2005 and PHAST.

Yimam, Y.T., 2010. Groundwater – Surface Water Interaction Modeling of the Grote Nete Catchment using GSFLOW.

Zehairy, A.M.R.E.L., 2014. Assessment of lake-groundwater interactions.

APPENDICES:

Other equations used to compute ETo and PET above:

Variables	Symbol	Value	Unit
Height	z	2	m
Elevation of ADAS	z_e	198.660	m
Atmospheric Pressure	P	98.974	atm
Psychrometric	ɣ	6.582E-02	
Average temperature max	Tmax,K	290.36	K
Average temperature min	Tmin,K	281.36	K
Stefan Boltzmann	σ	4.90E-09	$MJK^{-4}m^{-2}d^{-1}$
Gsc		0.082	MJm-2d-1
latitude=φ		50.84378=0.88739	Degree/rad
albedo of grass	α	0.23	
Crop factor	Kc	1	
Mean Temp	Tmean	286.14	K
Average temperature max	Tmax,C	17.2	C
Average temperature min	Tmin,C	8.2	C
Mean temperature	Tmean	12.7	C
Average relative humidity max	Rhmax	101.7	%
Average relative humidity min	Rhmin	44.5	%

Summary of variables used to accomplish calculation of FAO- ET_o and PET.

Slope vapour pressure curve;

$$\Delta = \frac{498 * \left[0.6108 * \exp\left(\frac{17.27 * T}{T + 237.3} \right) \right]}{(T + 237.3)^2}$$

Mean daily air temperature in centigrade (°C);

$$T_{mean} = \frac{T_{max-} T_{min}}{2}$$

Net radiation at the crop surface;

$$R_n = R_{ns} - R_{nl}$$

$$R_{ns} = (1 - \alpha) * R_s$$

where;

α - albedo is 0.23 of the grass reference crop

R_s - the incoming solar radiation ($MJm^{-2}day^{-1}$),

R_{ns} - net shortwave radiation ($MJm^{-2}day^{-1}$),

Net longwave radiation (R_{nl});

$$R_{nl} = \sigma * \left[\frac{T_{max,K^4} + T_{min,K^4}}{2} \right] * \left(0.34 - 0.14 * \sqrt{e_a} \right) * \left(1.35 * \frac{R_s}{R_{so}} - 0.35 \right)$$

where;
σ - Stefan-Boltzmann constant 4.903 x 10^{-9} ($MJm^{-2}day^{-1}$),
$T_{max, K}$ - maximum absolute temperature during 24 hours period in kelvin,
$T_{min, K}$ - minimum absolute temperature during 24 hours period in kelvin,
e_a - actual vapour pressure (kPa),
R_s/R_{so} - relative shortwave radiation (less or equal to 1.0),
R_s - the calculated incoming solar radiation ($MJm^{-2}day^{-1}$),
R_{so} - the calculated clear-sky radiation ($MJm^{-2}day^{-1}$), was calculated by using

$$R_{so} = \left(0.75 + 2 * 10^{-5} * z_e\right) * R_a$$

where;
z_e - the station elevation above mean sea level (m) and R_a - the extraterrestrial radiation ($MJm^{-2}day^{-1}$), which was calculated by using equation below.
Actual vapour pressure (e_a);

$$e_a = \frac{e_{o(Tmin)} * \frac{RH_{max}}{100} + e_{o(Tmin)} * \frac{RH_{min}}{100}}{2}$$

where;
RH_{max} and RH_{min} - are the daily max and min relative humidity (%) and e_o - saturation vapour pressure (kPa) which was calculated by using;

$$e_{o(T)} = 0.6108 * \exp\left(\frac{17.27 * T}{T + 237.3}\right)$$

Saturation vapour pressure (e_s);

$$e_s = \frac{e_{o(Tmin)} + e_{o(Tmax)}}{2}$$

Psychrometric constant (γ)

$$\gamma = 0.665 * 10^{-3} * P$$

Atmospheric pressure (kPa);

$$P = 101.3 * \left(\frac{(293 - 0.0065 * z_e)}{293}\right)^{5.26}$$

Average daily wind speed (u_2) at a height of 2 m;

$$u_2 = u_z * \frac{487}{\ln(67.8 * z - 542)}$$

where;u_2 - average daily wind speed at a height of 2 m (ms^{-1}), u_z - average daily wind speed at a height of z (ms^{-1}) and z - height of original wind measurement (m).
G was set to zero for ETo calculation.
The total evapotranspration (ET) $ET = ET_{uz} + I + ET_g$ Total change in storage (ΔS) $\Delta S = \Delta S_g + \Delta S_{uz}$